The Regulation of Postsynaptic $GABA_A$ Receptor Signalling in Epilepsy

Andrei-Sorin Ilie

Thesis submitted for the degree of
Doctor of Philosophy



University College
University of Oxford
Hilary Term, 2013

Abstract

Fast postsynaptic inhibition in the brain is mediated by ionotropic $GABA_A$ receptors ($GABA_A$Rs), which are activated by the release of the neurotransmitter GABA from presynaptic interneurons. The $GABA_A$R is primarily permeable to chloride ions (Cl^-) and therefore the transmembrane gradient for Cl^- sets the reversal potential of the receptor (E_{GABA-A}). When intracellular Cl^- concentrations are relatively low, E_{GABA-A} is more negative than the membrane potential and $GABA_A$R responses will have a hyperpolarising and inhibitory effect upon the postsynaptic cell. In contrast, when intracellular Cl^- concentrations are relatively high, E_{GABA-A} will be more positive and $GABA_A$R activation will have a depolarising effect.

How a neuron controls its intracellular Cl^- concentrations is a fundamental question that has direct relevance to hyperexcitability conditions such as epilepsy. Recently, it has become clear that Cl^- homeostasis is altered in epileptic tissue such that postsynaptic inhibition via the $GABA_A$R is reduced and, under some conditions, $GABA_A$R signalling may even be excitatory. In my thesis I explore some of the mechanisms and factors that are responsible for regulating postsynaptic $GABA_A$R signalling in the context of epileptic seizure activity in the rat hippocampus.

In the first series of experiments I combined pharmacological approaches with electrophysiological recordings from pyramidal neurons in the CA3 region of the hippocampus to trigger seizure activity. My results show that intense neuronal activity during a seizure leads to a transient accumulation of intracellular Cl^-, which generates a pronounced depolarising shift in E_{GABA-A}. Under these conditions, GABAergic synapses become excitatory and contribute to ongoing neuronal activity rather than exerting their normal inhibitory role. I found that the same seizure activity also induces the release of a neuromodulator called adenosine, which serves to limit the deleterious effects of excitatory $GABA_A$R responses. Adenosine exerts these effects by activating downstream potassium channels, which increase the postsynaptic cell's membrane conductance and, in doing so, 'shunt' incoming $GABA_A$R responses.

In the second series of experiments I examined Cl^- homeostasis and E_{GABA-A} in the context of neonatal seizures. One of the main mechanisms by which neurons maintain their intracellular Cl^- levels is through the activity of ion transporter proteins that reside in the membrane and move Cl^- either into, or out of, the cell. I discovered that the intracellular trafficking of an important Cl^- transporter protein, NKCC1, correlates with changes in Cl^- homeostasis. Using a combination of biochemical and molecular techniques, I then identified a novel molecular association between NKCC1 and a motor protein, Myosin Va, which has been implicated in the intracellular trafficking of membrane proteins. Using electrophysiological recordings I found that Myosin Va is required for NKCC1's contribution to Cl^- homeostasis, which may be important for E_{GABA-A} changes in epilepsy.

In the final series of experiments I developed methods to study the temporal dynamics in E_{GABA-A} during a single seizure. These revealed a Cl^- unloading mechanism that emerges at the end of a seizure and which depends upon hyperpolarisation of the postsynaptic membrane potential. This mechanism aids E_{GABA-A} recovery after the seizure and moves E_{GABA-A} to more hyperpolarised values. This mechanism could boost postsynaptic inhibition after a seizure and thereby help to protect against further seizure episodes.

In conclusion, this work extends our understanding of postsynaptic GABAergic transmission in the context of epileptic seizure activity and suggests new mechanisms that could be relevant for the development of rational anti-epileptic treatments.

Acknowledgements

First and foremost, I would like to thank my supervisor Dr. Colin Akerman. He has been absolutely amazing! From spending time on the rig, to discussing concepts, ideas and designing experiments, Colin has been a permanent source of motivation and inspiration. I am grateful to him for making me both a better scientist and person.

A huge thank you goes to Dr. Sarah Newey, for introducing me to the fascinating world of molecular biology and for patiently answering my naive questions about cells, DNA and proteins. It has been great collaborating and working with Sarah and I thank her for sharing the data in Figure 4.1C-E and Figure 4.2.

All members of the Akerman Lab have been great colleagues and friends. They have made the time spent in the lab very enjoyable, and have greatly helped my scientific endeavours by offering invaluable advice and feed-back during lab meetings. In particular, I would like to thank Dr. Joseph Raimondo for sharing the secrets of the gramicidin-perforated patch clamp technique and for introducing me to data analysis in Matlab.

In addition, the members of the Emptage Lab have been great fun. Special thanks goes to Zahid Padamsey for sharing his tricks for making the rig a highly controlled and stable environment. Although they may have seemed unorthodox at times, these methods have proved highly efficient for achieving optimal recording conditions.

Furthermore, I have to thank all my friends in Oxford for providing some of the most exciting experiences in my life. From rock climbing and football, to salsa dancing and bopping, all contributed towards making these last few years unforgettable.

I thank the Wellcome Trust for the financial support through the Four-Year PhD in Neuroscience Fellowship, which allowed me to study at Oxford. Also I thank University College for financial support through the Junior Research Fellowship, which will allow me to continue my scientific pursuits in this amazing city.

The data presented in Chapter 3 has been published in the Journal of Neuroscience (Ilie et al., 2012).

Last but not least, I have to thank my parents. They have offered their unconditional love and support at every stage in my life.

Contents

1 Introduction 6

1.1 Synaptic transmission and excitatory-inhibitory balance in the brain 7

1.2 The synaptic organisation of the hippocampal formation 10

1.3 GABAergic inhibition at the level of single neurons 14

1.3.1 The $GABA_AR$ 14

1.3.2 Synaptic inhibition and GABAergic signalling via the $GABA_AR$ 15

1.3.3 Chloride homeostasis and the regulation of E_{GABA-A} 17

1.3.4 E_{GABA-A} switches from depolarising to hyperpolarising during development 19

1.4 Mechanisms regulating NKCC1, KCC2 and plasticity of E_{GABA-A} 23

1.5 Alterations in GABAergic signalling in epilepsy 26

1.5.1 GABAergic signalling in neonatal epilepsy 26

1.5.2 Cl^- homeostasis and postsynaptic GABAergic signalling in adult epilepsy 29

1.6 Aims of my thesis 34

2 Materials and Methods 37

2.1 Organotypic hippocampal slices 37

2.2 Electrophysiological recordings 38

2.2.1 Triggering seizure-like activity in organotypic slices 41

2.2.2 Measuring $GABA_AR$ response amplitude 43

2.2.3 Measuring E_{GABA-A} 44

2.3 Drug manipulations 45

2.4 Biotinylation and isolation of cell surface proteins in hippocampal slices 46

2.5 SDS-PAGE and western Blotting 47

2.6 Immunoprecipitation of NKCC1 and mass spectrometry 48

2.7 Co-immunoprecipitation of NKCC1 and Myosin Va from solubilised hippocampal slices and COS-7 cells. 49

2.8 Immunolabelling of cultured cells 50

2.9 Plasmids, plasmid preparation and transfections 51

2.10 Data analysis and statistics 52

3 The role of seizure-induced adenosine release in modulating postsynaptic GABAergic signalling 53

3.1 Developing a reliable seizure model that allows systematic pharmacological investigations 55

3.2 Endogenous adenosine release modulates seizure duration and the post-seizure recovery period 57

3.3 Adenosine receptor activation attenuates $GABA_A$ receptor-mediated depolarization during epileptiform activity 60

3.4 Adenosine attenuates postsynaptic $GABA_AR$ signalling by increasing membrane conductance via activation of K^+ channels, downstream of the A_1R 64

3.5 $GABA_AR$ reversal potential and conductance are not altered by AR activation 69

3.6 Discussion 73

4 Investigating the molecular regulation of the Cl^- transporter NKCC1 and its role in neonatal seizures 78

4.1 The developmental regulation of NKCC1 and KCC2 and their relation to Cl^- homeostasis 79

4.2 A potential association between NKCC1 and the motor protein Myosin Va 83

4.3 An electrophysiological assay to measure the contribution of NKCC1 to Cl^- homeostasis 86

4.4 Disrupting endogenous Myosin Va activity reduces the contribution of NKCC1 to Cl^- homeostasis 90

4.5 Investigating the activity-dependent regulation of NKCC1 in the context of neonatal seizures 95

4.6 Discussion 105

5 Exploring the dynamics of E_{GABA-A} during neonatal seizure activity 112

5.1 Repeated E_{GABA-A} measurements reveal interesting dynamics during neonatal seizure activity 112

5.2 Post-seizure hyperpolarisation of the cell's membrane potential is required for the transitory negative shift in E_{GABA-A} 117

5.3 Discussion 123

6 General Discussion 127

6.1 Experimental findings 127

6.2 Methodological considerations 130

6.2.1 Organotypic hippocampal slices 130
6.2.2 Measuring E_{GABA-A} with gramicidin-perforated patch clamp recordings 131
6.2.3 Seizure models 131
6.3 The role of adenosine in regulating postsynaptic GABAergic responses during seizures 134
6.4 Molecular regulation of NKCC1 in the normal and epileptic neonatal brain 139
6.5 A chloride unloading mechanism in the post-seizure period 142
6.6 The role of NKCC1 in neonatal seizure activity 144
6.7 Concluding remarks 146

7 Bibliography 147

List of Figures

Figure 1.1 Structural organisation of inhibitory circuits and the architecture of the hippocampus 11

Figure 1.2 Cl^- homeostasis in neonatal and mature neurons and the developmental switch in $GABA_AR$ signalling 21

Figure 1.3 Seizure activity renders GABAergic signalling excitatory in both the neonatal and the mature hippocampus 35

Figure 3.1 Removing Mg^{2+} from the perfusion media induces highly reproducible seizures in organotypic hippocampal brain slices. 56

Figure 3.2 Endogenous adenosine modulates seizure activity and post-seizure recovery. 58

Figure 3.3 Seizure activity induces depolarising and excitatory $GABA_AR$ signalling. 61

Figure 3.4 Adenosine receptor activity attenuates postsynaptic GABAergic potentials during seizures. 63

Figure 3.5 Exogenous adenosine application mimics the inhibitory effect on $GABA_AR$-mediated signalling. 65

Figure 3.6 Adenosine attenuates postsynaptic $GABA_AR$ potentials via A_1R activation of K^+ channels that increase membrane conductance. 68

Figure 3.7 Adenosine receptor activation does not alter Cl^- homeostasis. 71

Figure 3.8 Adenosine receptor activation has no effect on $GABA_AR$ conductance. 72

Figure 4.1 Developmental regulation of E_{GABA-A} and NKCC1 and KCC2 transporter expression in the rat hippocampus. 82

Figure 4.2 NKCC1 associates with Myosin Va in developing rat hippocampus. 85

Figure 4.3 NKCC1 is active in neonatal neurons and sets E_{GABA-A} to depolarising levels. 88

Figure 4.4 Assessing NKCC1 contribution to Cl^- homeostasis using a within-cell design. 89
Figure 4.5 Disrupting endogenous Myosin Va shifts resting E_{GABA-A} to more negative values. 92
Figure 4.6 Disrupting endogenous Myosin Va function reduces NKCC1 contribution to Cl^- homeostasis 94
Figure 4.7 Seizures in the neonatal hippocampus lead to excitatory effects of $GABA_AR$ activation. 97
Figure 4.8 NKCC1 is active in the post-seizure period and continues to contribute to Cl^- accumulation. 99
Figure 4.9 Neonatal seizure activity induces a bumetanide-dependent shift in $E_{GABA-A.}$ 101
Figure 4.10 Investigating the role of Myosin Va in the seizure-induced shift in $E_{GABA-A.}$ 103
Figure 5.1 Monitoring E_{GABA-A} throughout the seizure and post-seizure period. 114
Figure 5.2 E_{GABA-A} exhibits a positive shift during neonatal seizures, which is followed by a recovery and transitory negative shift during the post-seizure period. 116
Figure 5.3 Neonatal seizures induce a post-seizure hyperpolarisation of the membrane potential that correlates with the post-seizure negative shift in $E_{GABA-A.}$ 119
Figure 5.4 Post-seizure membrane potential hyperpolarisation correlates with the negative shift in $E_{GABA-A.}$ 120
Figure 5.5 Preventing the post-seizure hyperpolarisation of the membrane potential abolishes the negative shift in $E_{GABA-A.}$ 122

1 Introduction

Our brains are formed by billions of neurons that interact and communicate with each other via connections called synapses. These connections allow neurons to organise and perform as functional neuronal networks. Some of the synaptic connections are excitatory and promote neuronal activity, whilst others are inhibitory and reduce activity. Everything that our brains do, from perceiving a simple stimulus, to complex cognitive functions, requires a tight balance between synaptic excitation and inhibition. Alterations in this balance can give rise to pathological situations, such as occurs in epilepsy, when neuronal inhibition fails to restrain excitation and the result is abnormally elevated levels of activity. In the brain, synaptic inhibition is provided by γ-aminobutyric acidergic (GABAergic) neurons that influence their postsynaptic target cells by releasing the neurotransmitter GABA and signalling via postsynaptic GABA receptors. Recently, multiple lines of evidence have suggested that GABAergic signalling is altered in epileptic tissue such that the strength of inhibition is reduced, and under certain conditions, GABAergic signalling can even become excitatory and promote neuronal activity. In my thesis, I have explored some of the mechanisms responsible for regulating postsynaptic GABAergic signalling under both normal conditions and during the course of seizures. Exploring such mechanisms can advance our understanding of the pathophysiology of epilepsy and may lead to the development of rational antiepileptic therapies.

In this Chapter I will first introduce synaptic transmission and argue that synaptic excitation and inhibition are balanced within neuronal networks. I will present the basic synaptic organization of the hippocampus, a brain region frequently involved in the

generation of seizure activity, and I will discuss epilepsy as a severe neurological disorder associated with alterations in the excitatory-inhibitory balance. I will describe the functioning of GABAergic synapses and the mechanisms that regulate the postsynaptic response to GABA at the level of single neurons, and I will argue that alterations in these mechanisms could play a crucial role in the pathophysiology of epilepsy. Finally, I will outline the specific experimental aims and goals of my thesis with regard to understanding the mechanisms that regulate GABAergic signalling in epilepsy.

1.1 Synaptic transmission and excitatory-inhibitory balance in the brain

Broadly speaking, two main classes of neurons are responsible for excitation and inhibition in the brain: 1) principal projection neurons and 2) local circuit interneurons, respectively (Shepherd, 2004). Principal neurons send both short and long distance axonal projections and form excitatory synapses with the targeted neurons. These synapses function by releasing the excitatory neurotransmitter glutamate, which activates postsynaptic glutamate receptors. These receptors are ion channels, mainly permeable to sodium (Na^+), potassium (K^+) and calcium (Ca^{2+}; in some instances) and when activated, they give rise to an excitatory postsynaptic potential by depolarising the membrane potential towards the threshold for action potential generation. On the other hand, local circuit interneurons do not generally send long range axonal projections, but tend to form local synapses within the same brain region. These synapses typically release the inhibitory neurotransmitter GABA or glycine, which activates postsynaptic GABA or glycine receptors. These receptors are ion channels that are mainly permeable to chloride (Cl^-) and, when activated, typically give rise to inhibitory postsynaptic potentials by hyperpolarising the membrane potential. Numerically,

glutamatergic principal cells represent approximately 80% of the brain's neurons and local circuit GABAergic interneurons comprise the remaining 20% (Hendry et al., 1987).

The principal cells and local interneurons are highly interconnected and influence one another's activity in a reciprocal fashion. From a synaptic circuit perspective, two main organisational models and interactions have been described between principal cells and interneurons: 1) feed-back inhibitory connections and 2) feed-forward inhibitory connections (Figure 1.1A). In feed-back inhibitory circuits, principal cells excite local interneurons, which synapse back onto the same principal cells and inhibit their activity (Ali et al., 1998; Ali et al., 1999; Blasco-Ibanez and Freund, 1995; Buzsaki, 1984; Yoshimura and Callaway, 2005). Consistent with such an architecture, recent studies have revealed dense, non-specific connections between local interneurons and principal neurons (Packer and Yuste, 2011;Fino and Yuste, 2011) and the recruitment of local inhibitory interneurons by principal cell activity (Kapfer et al., 2007). This organisation allows local inhibitory neurons to be recruited as a function of local network activity, which then serves to limit principal cell activity. In feed-forward inhibitory circuits, long-range excitatory projections will simultaneously excite principal neurons and local interneurons (Alger and Nicoll, 1982;Empson and Heinemann, 1995;Turner, 1990;Buzsaki, 1984). When the interneurons fire action potentials they then inhibit the nearby principal neurons. This organisation leads to a tightly controlled temporal sequence of activity in which excitation of principal cells is quickly followed by inhibition (Pouille and Scanziani, 2001;Wilent and Contreras, 2005). Together, these feed-back and feed-forward inhibitory circuits form basic building blocks of neuronal networks that are found throughout the mammalian neocortex and hippocampus (Suzuki and Bekkers, 2012;Berezovskii et al., 2011;Torborg et al., 2010;Sloviter, 1991;Elfant et al., 2008;Gonchar and Burkhalter, 2003;Buzsaki, 1984).

Previous work in different brain areas has revealed that during normal sensory processing, feed-back and feed-forward inhibition serves to control the excitation of principal cells. For instance, the strengths of inhibition and excitation have been found to correlate and co-vary during both spontaneous neuronal activity and sensory-evoked activity (Haider et al., 2006;Okun and Lampl, 2008). In addition, an increase in stimulus intensity has been found to result in proportional increases in excitation and inhibition (Wilent and Contreras, 2004). Taken together, these studies suggest that neuronal circuits are constructed in such a way that a continuous balance is achieved between excitation and inhibition. This balance underlies normal brain function and is fundamental to the computational capabilities of neuronal networks (Kullmann, 2011;Isaacson and Scanziani, 2011).

In addition to the anatomical organisation of feed-back and feed-forward inhibitory circuits that allow concomitant recruitment of excitation and inhibition, the excitatory-inhibitory balance can be maintained via changes in the strength of synaptic connections and/or intrinsic neuronal excitability. Indeed, neurons have the ability to modulate the strength of their synapses such that the level of their activity is maintained within certain physiological boundaries (Turrigiano, 2008). For instance, manipulations that increase or reduce neuronal activity have been found to induce compensatory changes in the strength of excitatory synapses (Burrone et al., 2002;Turrigiano et al., 1998). In addition, neurons can regulate their intrinsic excitability to compensate for changes in their activity level (Desai et al., 1999;Grubb and Burrone, 2010;Pratt and Aizenman, 2007). Since these initial studies, multiple other mechanisms have been implicated in the homeostatic regulation of neuronal activity, which would encourage stability within a neuronal network (Thiagarajan et al., 2005;Lindskog et al., 2010;Goold and Nicoll, 2010;Gonzalez-Islas et al., 2010;Buckby et al., 2006). The existence of such homeostatic mechanisms further outlines the importance of maintaining a balance between excitation and inhibition.

The fundamental importance of maintaining excitatory-inhibitory balance for normal brain function is evident from the dramatic consequences that follow acute manipulations of synaptic excitation or inhibition. For instance, increased excitation or reduced inhibition can rapidly induce seizures and lead to the development of epilepsy (Trevelyan et al., 2006; Martin and Sloviter, 2001; Gruenthal et al., 1986; Chervin et al., 1988; Antonucci et al., 2012). On the other hand, reducing excitation or enhancing inhibition can induce comatose states (Brown et al., 2010). In between these two extreme situations (i.e. seizures and coma), more subtle alterations of the excitatory-inhibitory balance have been associated with several brain disorders including autism (Gogolla et al., 2009), schizophrenia (Marin, 2012) and Alzheimer's disease (Verret et al., 2012).

In summary, the architecture of neuronal circuits and the functional changes in synaptic strength allow neuronal networks to establish a balance between excitation and inhibition, which stabilises network activity and prevents the occurrence of abnormal events like seizures.

1.2 The synaptic organisation of the hippocampal formation

Most of the work in my thesis was conducted in brain slices from the rat hippocampal formation. The hippocampal formation (i.e. the hippocampus) is a brain structure situated in the medial temporal lobe, which has been the focus of intense research into cognitive processes and diseases such as epilepsy. In the 1950s, it was found that several patients (including the famous H.M.) were unable to form new memories as a result of bilateral resection of the hippocampus (Scoville and Milner, 1957). These findings linked the hippocampus to memory and learning and, since then, numerous studies in animals and

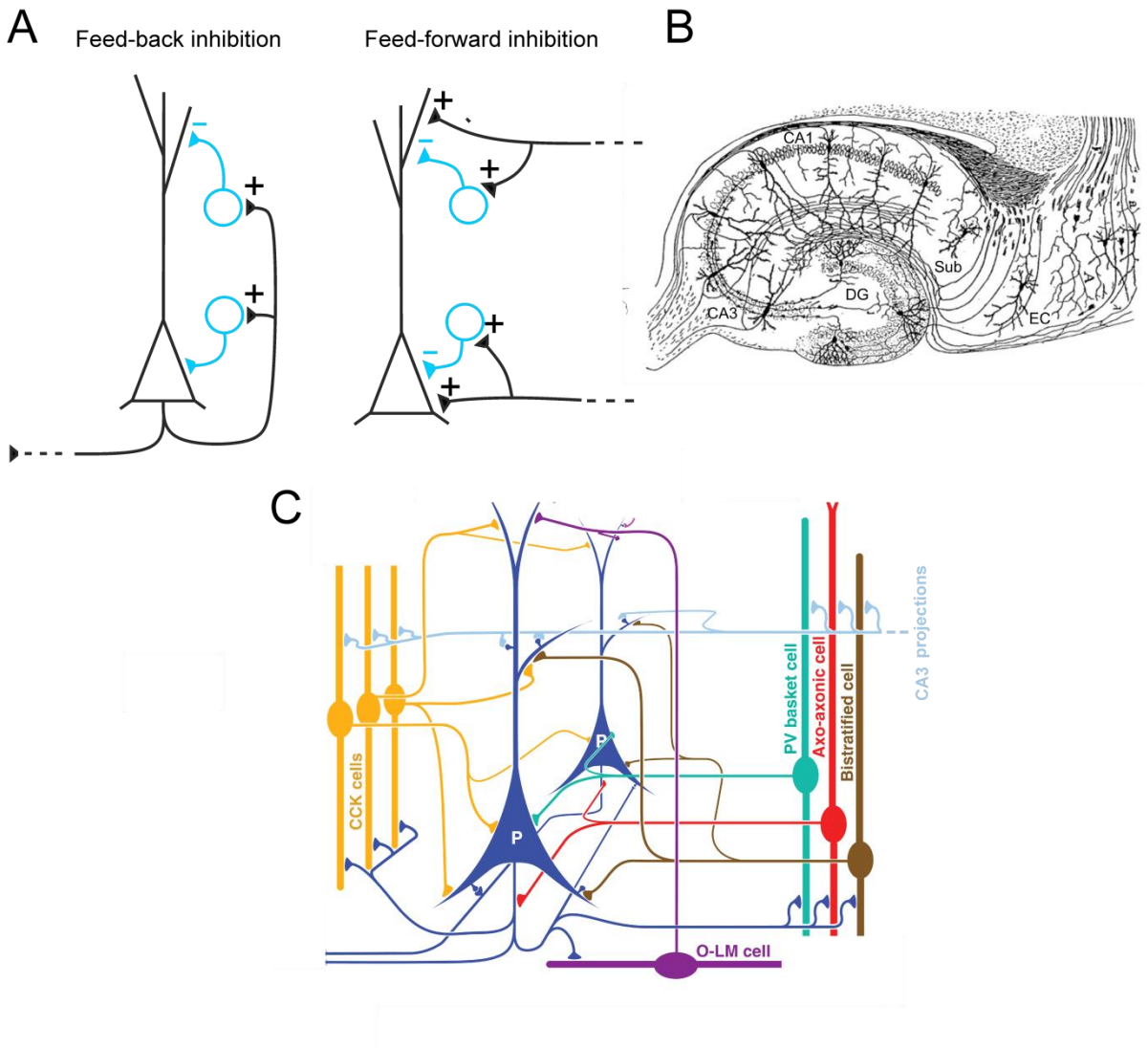


Figure 1.1 Structural organisation of inhibitory circuits and the architecture of the hippocampus.

A, Schematic representation of feed-back and feed-forward inhibitory circuits. In feed-back inhibition, pyramidal neurons (black) excite local interneurons (blue), which in turn synapse back onto the pyramidal neurons. In feed-forward inhibition, long-range excitatory inputs simultaneously activate both pyramidal neurons and local interneurons. The interneurons then synapse onto nearby pyramidal neurons and provide inhibition with a synaptic delay. ***B,*** The architecture of a hippocampal slice, adapted from (Ramon y Cajal 2002). DG - dentate gyrus, CA3 - cornu amonis area 3, CA1 - cornu amonis area 1, Sub - subiculum, EC - entorhinal cortex. ***C,*** Schematic representation of different interneuron subtypes targeting specific subcellular domains of the pyramidal neurons, adapted from (Klausberger and Somogyi, 2008). P - pyramidal neurons, CCK - cholecystokinin, PV - parvalbumin, O-LM - oriens lacunosum-moleculare.

humans have investigated the role of the hippocampus in memory formation, spatial navigation and learning (Burgess et al., 2002; Moser et al., 2008; Buzsaki, 2005).

In addition to its physiological functions, the hippocampus is one of the most susceptible brain regions to the induction of seizure activity (Abdelmalik et al., 2005; Racine, 1975). In line with this high seizure susceptibility, more than 50% of partial seizures have their origin in the temporal lobe (Luciano, 1993). In addition, hippocampal sclerosis is the most common histopathological finding in drug-resistant human temporal lobe epilepsy, although it remains unclear whether this is a cause or a consequence of epilepsy (Malmgren and Thom, 2012). For these reasons, the hippocampus has been an important brain region for studying mechanisms related to seizure activity and epilepsy.

Structurally, the hippocampal formation includes: the dentate gyrus, the hippocampus proper (i.e. cornus ammonis; CA), the subiculum and the entorhinal cortex (Figure 1.1B). The hippocampus receives inputs from and projects to several brain areas including the cortex, amygdala and thalamus (Shepherd, 2004). The principal glutamatergic neurons are represented by the granule cells in the dentate gyrus and the pyramidal neurons in the CA areas, the subiculum and the entorhinal cortex. At a synaptic level, the information can flow from the entorhinal cortex to the hippocampus via two main excitatory pathways called the trisynaptic and monosynaptic pathways (Yeckel and Berger, 1990; Nakashiba et al., 2008; Andersen et al., 1971; Amaral and Witter, 1989). In the trisynaptic pathway, neurons in layer two of the entorhinal cortex send projections to the dentate gyrus and CA3 via the perforant path, the granule cells of the dentate gyrus then contact pyramidal neurons in the CA3 area via the mossy fibres pathway, and CA3 pyramidal neurons synapse on to pyramidal neurons in the CA1 area via the Schaffer collaterals pathway. In the monsynaptic pathway, neurons in layer three of the entorhinal cortex synapse directly onto CA1 pyramidal neurons. These

pathways have been involved in controlling different aspects of learning and memory formation (Nakashiba et al., 2009; Suh et al., 2011; Nakashiba et al., 2008).

The flow of activity through these pathways is highly controlled and regulated by a variety of different types of local GABAergic interneurons. Indeed, more than 20 different types of interneuron have been described in the CA1 area (Klausberger and Somogyi, 2008). These interneurons express different molecular markers, have distinct morphologies and firing patterns, and innervate different subcellular domains of the pyramidal neurons (Figure 1.C). For instance, axo-axonic cells target the axon initial segment of pyramidal neurons (Szabadics et al., 2006; Buhl et al., 1994; Somogyi et al., 1982). Parvalbumin-expressing basket cells synapse onto the soma of pyramidal neurons and cholecystokinin-expressing basket cells synapse onto both the soma and the apical dendrites (Foldy et al., 2010; Freund and Katona, 2007; Glickfeld and Scanziani, 2006). Bistratified and Ivy interneurons target both the apical and basal dendrites of pyramidal neurons and O-LM interneurons synapse mainly onto the apical dendrites (Maccaferri et al., 2000; Klausberger et al., 2004; Fuentealba et al., 2008; Halasy et al., 1996). In addition, neurogliaform cells target mainly the apical dendrites and are capable of releasing large amounts of GABA, which leads to a form of volume transmission (Karayannis et al., 2010; Olah et al., 2009; Price et al., 2008). As mentioned earlier, these different types of interneurons are interconnected with the pyramidal neurons via feed-back and feed-forward circuits. In addition, interneurons can be connected with each other via both synaptic (Elfant et al., 2008; Lovett-Barron et al., 2012) and gap junction connections (Zsiros et al., 2007). This can regulate the synchronisation of populations of interneurons activity and may have important consequences both for normal brain activity and pathological activity such as seizures (Zsiros et al., 2007; Lovett-Barron et al., 2012; Elfant et al., 2008). This highly diverse population of interneurons organises and shapes the spatial and temporal activity profile of the excitatory principal neurons, while

maintaining the excitatory-inhibitory balance in hippocampal circuits (Klausberger and Somogyi, 2008; Kullmann, 2011).

In spite of their diversity, a common feature of all of these interneurons is that they exert their effects by activating postsynaptic GABA receptors. Therefore, in the next section I will describe GABAergic transmission at the level of a single neuron and the factors that regulate GABA receptor signalling.

1.3 GABAergic inhibition at the level of single neurons

GABA exerts its actions by activating two types of receptors: the ionotropic $GABA_A$ receptor ($GABA_AR$) and the metabotropic $GABA_B$ receptor ($GABA_BR$). The ionotropic $GABA_A$Rs are responsible for the fast synaptic inhibition (Farrant and Nusser, 2005), while the metabotropic $GABA_B$Rs modulate neuronal activity over a slower time course via G-protein and second messenger signalling pathways (Gassmann and Bettler, 2012).

1.3.1 The $GABA_AR$

$GABA_A$Rs are pentameric ionotropic receptors formed by the assembly of five subunits, from a potential of at least 18 different subunits (Farrant and Nusser, 2005). The specific subunit composition is responsible for some of the $GABA_AR$ properties, such as open channel kinetics, sensitivity to modulators (Glykys et al., 2007; Benkwitz et al., 2004), and subcellular localization of the receptor (e.g. synaptic versus extra-synaptic; (Glykys et al., 2008; Nusser et al., 1996). Synaptic $GABA_A$Rs are activated in a phasic manner by the release of GABA from a presynaptic neuron, while extrasynaptic $GABA_A$Rs are activated in

a tonic manner by ambient GABA levels (Farrant and Nusser, 2005). These two different locations and types of $GABA_ARs$ form the basis for phasic and tonic inhibition.

1.3.2 Synaptic inhibition and GABAergic signalling via the $GABA_AR$

Once released from the presynaptic terminal, GABA binds to the postsynaptic $GABA_AR$ and induces a conformational change that results in the opening of the ion channel. The $GABA_AR$ is mainly permeable to Cl^- and, to a lesser extent, bicarbonate (HCO_3^-; Bormann et al., 1987; Kaila et al., 1993). When the $GABA_ARs$ are open, Cl^- and HCO_3^- ions will flow down their electro-chemical gradient, such that they tend to move the membrane potential towards their reversal potential (i.e. the membrane potential at which the electro-chemical driving force is zero, meaning there is no net flow of ions through the opened channel). In the majority of mature neurons in the adult brain, the intracellular Cl^- concentration ($[Cl^-]_i$) is maintained at relatively low levels (Kahle et al., 2008; Blaesse et al., 2009). This low $[Cl^-]_i$ typically sets the reversal potential for Cl^- (E_{Cl}-) at more negative values than the resting membrane potential. This means that once the $GABA_AR$ is open, Cl^- will flow into the neurons and will hyperpolarise the membrane potential. The reversal potential for HCO_3^- is significantly more depolarised than E_{Cl}- (E_{HCO3}-is approximately -10 mV), meaning that when $GABA_ARs$ are open, HCO_3^- will typically flow out of the neuron and will depolarise the membrane potential (Kaila et al., 1993). However, as the $GABA_AR$ is approximately four to five times more permeable to Cl^- than to HCO_3^- (Bormann et al., 1987), the reversal potential of the $GABA_AR$ receptor (E_{GABA-A}) is dominated by E_{Cl}-. In pyramidal neurons in the adult rat hippocampus, E_{GABA-A} has been found to be around -75 to -80 mV (Lamsa and Taira, 2003; Tyzio et al., 2007), which is more hyperpolarised than the resting membrane potential and thus hyperpolarising responses are typically seen upon $GABA_AR$ activation.

Activation of $GABA_AR$s inhibits neuronal activity via two mechanisms. Firstly, as described above, Cl^- influx hyperpolarises the membrane potential and therefore moves it further away from the threshold for inducing action potentials. Secondly, activation of $GABA_AR$s can inhibit neuronal activity via a mechanism called shunting inhibition (Lamsa et al., 2000; Staley and Mody, 1992). Opening of the $GABA_AR$ increases the conductance of the neuronal membrane and, in doing so, 'short-circuits' or 'shunts' concurrent incoming excitatory currents and thus reduces their effect on the membrane potential. This shunting mechanism is independent of the hyperpolarisation of the membrane potential and accounts for the inhibitory actions of $GABA_AR$s that are observed when $E_{GABA\text{-}A}$ is very close to the membrane potential (Lamsa et al., 2000; Staley and Mody, 1992).

At this point, several important conclusions can be made about signalling via the $GABA_AR$. Firstly, the strength of hyperpolarising inhibition depends on the difference between $E_{GABA\text{-}A}$ and the resting membrane potential (i.e. the more hyperpolarised $E_{GABA\text{-}A}$, the stronger the hyperpolarising inhibition). Secondly, if $E_{GABA\text{-}A}$ is more depolarised than the membrane potential, then activation of $GABA_AR$s would result in a depolarising response that would move the membrane potential closer to the action potential threshold. Since activation of $GABA_AR$s causes shunting inhibition, irrespective of the effect upon membrane potential, a depolarising $GABA_AR$ response is not always excitatory. Indeed, a depolarising $GABA_AR$ response promotes excitation only under certain conditions, such as when $E_{GABA\text{-}A}$ is more depolarised than the threshold for action potential, or when the depolarising response summates with incoming excitatory responses to trigger action potentials (Valeeva et al., 2010; Gulledge and Stuart, 2003).

In summary, $E_{GABA\text{-}A}$ is a crucial parameter for determining the functional consequences of $GABA_AR$ activation. Since $E_{GABA\text{-}A}$ is mainly set by the $[Cl^-]_i$, it becomes clear that the regulation and homeostasis of $[Cl^-]_i$ are key for determining the effects of

$GABA_AR$ activation. Therefore, in the next section, I will discuss the mechanisms responsible for regulating intracellular Cl^- and how these impact GABAergic signalling.

1.3.3 Chloride homeostasis and regulation of E_{GABA-A}

In many cell types including neurons, Cl^- homeostasis is regulated by a family of protein ion-transporters called cation-chloride co-transporters (CCCs; Blaesse et al., 2009; Kahle et al., 2008). These transporters function at the level of the plasma membrane and use the energy from the ionic gradients for K^+ and Na^+ to co-transport Cl^- in or out of the cell (Blaesse et al., 2009). The gradients for K^+ and Na^+ are primarily maintained by the activity of the Na^+-K^+-ATPase pump, therefore changes in the activity of this pump can indirectly influence CCCs activity (Brumback and Staley, 2008a). Transport via CCCs is electroneutral (i.e. the same amount of positive and negative charges are transported in the same direction) therefore the activity of CCCs does not directly influence the membrane potential (Mercado et al., 2004).

In neurons within the central nervous system, two of the most important transporters responsible for regulating intracellular Cl^- are the K^+ - Cl^- - co-transporter, KCC2, and the Na^+ - K^+ - Cl^- - co-transporter, NKCC1 (Woo et al., 2002; Rivera et al., 1999; Pfeffer et al., 2009; Payne et al., 1996; Hubner et al., 2001a; Hubner et al., 2001b; Clayton et al., 1998a). These two transporters move Cl^- in opposite directions. For instance, Cl^- extrusion is mediated via KCC2, which uses the K^+ gradient to co-transport Cl^- out of neurons (Rivera et al., 1999; Payne, 1997; Kakazu et al., 2000; Acton et al., 2012). Meanwhile, Cl^- uptake is mediated via NKCC1, which uses the Na^+ gradient to transport Cl^- into neurons (Rohrbough and Spitzer, 1996; Achilles et al., 2007; Yamada et al., 2004). The interplay between the activity and expression levels of KCC2 and NKCC1 is responsible for setting the baseline $[Cl^-]_i$ (Blaesse et al., 2009). The function and expression of these two transporters can be

modulated via multiple mechanisms (Woodin et al., 2003; Shimizu-Okabe et al., 2007; Rinehart et al., 2011; Puskarjov et al., 2012; Lee et al., 2010; Fiumelli et al., 2005), which will impact E_{GABA-A} and the effect that $GABA_AR$ activation has under both physiological and pathological conditions (see Section 1.4).

In addition to CCCs, other transporters and channels can contribute to Cl^- homeostasis. For instance, the anion-exchanger AE3, which exchanges Cl^- for HCO_3^-, has been reported to contribute to Cl^- accumulation in immature hippocampal neurons (Pfeffer et al., 2009). Besides the activity of ion transporters, Cl^- homeostasis can also be mediated via voltage-gated Cl^- channels. One such example is the CLC-2 voltage-gated channel, which is activated by hyperpolarisation and high levels of $[Cl^-]_i$, and which can aid Cl^- extrusion during periods of intense neuronal activity (Rinke et al., 2010; Foldy et al., 2010).

Finally, The $GABA_AR$ itself represents a key component in the regulation of $[Cl^-]_i$. This is because the activation of $GABA_ARs$ can lead to significant Cl^- fluxes across the plasma membrane (Staley et al., 1995; Staley and Proctor, 1999; Isomura et al., 2003b). Once $GABA_ARs$ are activated, Cl^- will flow either in or out of the cell, depending on the driving force between E_{GABA-A} and the membrane potential. This means that the level of network activity, by controlling the amount of $GABA_AR$ activation and the membrane potential, will influence the direction and extent of Cl^- fluxes. The implications of these Cl^- fluxes are discussed further bellow (see Section 1.4).

In summary, neurons possess a variety of mechanisms that are responsible for the tight regulation of $[Cl^-]_i$. In the next section I will discuss how changes to these mechanisms contribute to setting E_{GABA-A} and how this can impact GABAergic signalling.

1.3.4 E_{GABA-A} switches from depolarising to hyperpolarising during development

As described above, $GABA_AR$ responses are typically hyperpolarising and inhibitory in mature neurons (Farrant and Kaila, 2007; Fishell and Rudy, 2011). In contrast, in immature neurons during early development, GABA has been shown to generate depolarising responses that are excitatory under some conditions (Valeeva et al., 2010; Owens et al., 1996; Luhmann and Prince, 1991; Ben-Ari et al., 1989; Ben-Ari et al., 2007; Figure 1.2). This difference between immature and mature neurons, and a gradual developmental shift in GABAergic signalling from depolarising to hyperpolarising (Figure 1.2), has been documented in various species and different neuronal structures (Akerman and Cline, 2006; Lu and Trussell, 2001; Stil et al., 2009; Tyzio et al., 2007; Yamada et al., 2004).

In pyramidal neurons in rat hippocampus and neocortex, GABAergic signalling switches from depolarising to hyperpolarising during the first two postnatal weeks (Tyzio et al., 2007; Yamada et al., 2004). This switch correlates with the upregulation of the expression of the Cl^--extruding transporter KCC2, which is at low levels early after birth but increases dramatically in the first two postnatal weeks (Lu et al., 1999; Rivera et al., 1999; Stein et al., 2004). In rat hippocampus, at postnatal day 1 (P1), KKC2 mRNA has been found to barely be detectable but it increased substantially at P5 and continued to increase by P9 when it had reached levels comparable with adult P47 hippocampus (Rivera et al., 1999). Consistent with a crucial role for KCC2 in normal development, KCC2 knockout mice fail to generate inhibitory $GABA_AR$ responses and, as a consequence, develop generalized seizures and die prematurely (Woo et al., 2002; Hubner et al., 2001b). NKCC1 expression meanwhile has been reported to significantly decrease from high levels early after birth, to low levels in the mature brain (Yamada et al., 2004; Dzhala et al., 2005). Interestingly, the developmental changes in NKCC1 and KCC2 expression do not seem to occur synchronously across the whole nervous system. For instance, KCC2 expression has been found to follow a caudal-

rostral gradient with spinal cord and subcortical neurons producing KCC2 mRNA early during embryogenesis, while in cortical neurons, KCC2 expression increased after birth (Wang et al., 2002; Stein et al., 2004). Furthermore, within the same brain area, individual neurons can show differences in their $[Cl^-]_i$ levels, which correlated with differences in Cl^- transporters expression (Yamada et al., 2004). During the first three postnatal days, in the rat neocortex, cortical plate neurons have been reported to show higher Cl^- levels than layer V-VI neurons, which are born earlier (Yamada et al., 2004). This difference correlated with higher levels of NKCC1 mRNA levels in the cortical plate neurons compared to earlier born layer V/VI neurons, while KKC2 mRNA was not different between the two neuronal populations (Yamada et al., 2004). By P5-P7, the difference in NKCC1 mRNA between cortical plate neurons and layer V/VI neurons was no longer present, consistent with a role for NKCC1 in accumulating Cl^- at early stages of development (Yamada et al., 2004). Overall, these studies suggest that the relative expression of NKCC1 and KCC2 is dependent on the birth age of neurons, with a gradual reduction in NKCC1 and an upregulation of KCC2 during development. Nevertheless, other studies have found that NKCC1 mRNA actually increases during the first few postnatal weeks and persists into adult life (Clayton et al., 1998a; Wang et al., 2002). It therefore seems likely that developmental changes in E_{GABA-A} reflect relative changes in the expression, localisation and/or activity of the two transporters, rather than a simple upregulation of KCC2 and downregulation of NKCC1 expression. In Chapter 4, I have further explored the developmental shift in E_{GABA-A} in relation to the expression of KCC2 and NKCC1 at the surface of the plasma membrane.

The differences between GABAergic signalling in immature and mature neurons can have important consequences both for normal brain development and pathological conditions such as epilepsy. During early development, depolarising $GABA_AR$ responses have been

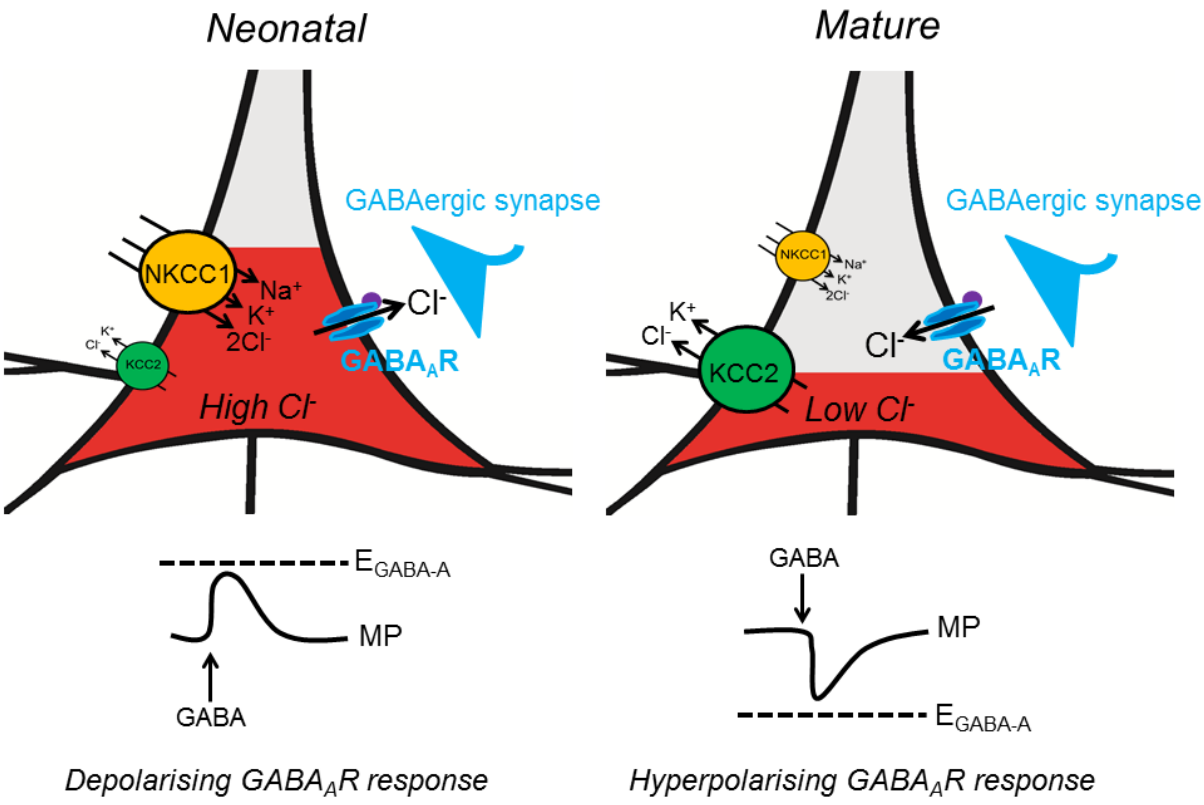


Figure 1.2 Cl^- homeostasis in neonatal and mature neurons and the developmental switch in $GABA_AR$ signalling

Cartoons of an immature (left) and mature (right) pyramidal neuron illustrating the impact of Cl^- homeostasis mechanisms upon $GABA_AR$ transmission. In immature neurons (left), high expression and activity of NKCC1, and low expression of KCC2, lead to relatively high intracellular Cl^- concentration. This sets E_{GABA-A} to relatively depolarised values compared to the membrane potential (MP), such that $GABA_AR$ activation results in depolarising responses (bottom). In mature neurons (right), KCC2 expression increases significantly and generates a lower intracellular Cl^- concentration. This moves E_{GABA-A} to more hyperpolarising values relative to MP, such that $GABA_AR$ activation typically generates hyperpolarising responses (bottom).

suggested to orchestrate early network activity and maturational processes (Ben-Ari, 2002; Ben-Ari et al., 2007; Cossart, 2011). In the hippocampus, GABAergic synapses have been found to form and mature before glutamatergic synapses (Hennou et al., 2002; Khazipov et al., 2001; Tyzio et al., 1999) and it has been argued that early network activity is driven by depolarising GABA signalling (Ben-Ari et al., 1989; Ben-Ari et al., 2007). However, this view has been challenged by two recent studies, which argued that the depolarising effect of GABA is due to inadequate energy supply in in vitro preparations and can be overcome by the addition of ketone bodies (Holmgren et al., 2010; Rheims et al., 2009). However, subsequent studies using various techniques to evaluate the depolarising and excitatory actions of GABA, have failed to reproduce the effect of ketone bodies on depolarising GABA when physiologically relevant concentrations are used (Ruusuvuori et al., 2010; Waddell et al., 2011; Kirmse et al., 2010; Khakhalin and Aizenman, 2012; Bos and Vinay, 2012; Ben-Ari et al., 2011). Consistent with the developmental shift, early depolarising GABA is required for the normal maturation of glutamatergic synapses, because interfering with the activity of NKCC1, which sets the high $[Cl^-]_i$ required for depolarising GABA actions, results in alterations in glutamatergic synaptic transmission that persist into adulthood (Wang and Kriegstein, 2008; Wang and Kriegstein, 2011; Pfeffer et al., 2009). Glutamatergic synapses become operational over the same period that GABAergic signalling assumes an inhibitory role, which is consistent with the idea that excitation and inhibition are balanced during development. This sequence, whereby GABAergic synapses form before glutamatergic synapses, has been suggested to allow permissive activity-dependent maturation of neuronal networks, while preventing the risk of overexcitation (Ben-Ari et al., 2007). Nevertheless, depolarising GABA signalling and the immaturity of Cl^- homeostatic mechanisms might render developing networks more susceptible to seizure activity and may account for some of the particularities of neonatal epilepsy (see Section 1.5.1).

1.4 Mechanisms regulating NKCC1, KCC2 and plasticity of E_{GABA-A}

In addition to the developmental changes described above, the Cl^- transporters can be modulated by a variety of activity-dependent mechanisms. For example, either prolonged postsynaptic spiking (Fiumelli et al., 2005), or pairing of pre- and postsynaptic spiking (Woodin et al., 2003), has been found to result in reduced KCC2 function, which shifted E_{GABA-A} to more positive values and reduced the strength of inhibition. Similarly, protocols that induce long-term potentiation (LTP), such as theta-burst stimulation, have been reported to downregulate KCC2 expression in an NMDAR-dependent manner (Wang et al., 2006). Furthermore, direct application of glutamate can also downregulate KCC2 via an NMDAR and Ca^{2+}-dependent mechanism (Lee et al., 2011b; Kitamura et al., 2008). Such changes have been suggested to play important roles during pathological conditions, such as cerebral ischemia and seizures, which are associated with high levels of glutamate release (Lee et al., 2011b; Kitamura et al., 2008).

Regarding the molecular mechanisms that underlie changes in KCC2 function, it has been found that phosphorylation/dephosphorylation is responsible for controlling the stability of KCC2 at the surface of the cell. For instance, phosphorylation of serine 940 by protein kinase C (PKC) has been found to increase the stability of KCC2 (Lee et al., 2007), while dephosphorylation of the same amino acid by protein phosphatase 1 has the opposite effect (Lee et al., 2011b). Moreover, phosphorylation of tyrosine 903 and 1087 has been shown to decrease the surface expression of KCC2 by enhancing its degradation via the lysosomal pathway (Lee et al., 2010). In addition, it has recently been reported that KCC2 can be degraded as a result of cleavage via the Ca^{2+}-activated protease calpain (Puskarjov et al., 2012). Such mechanisms have been proposed to contribute to an activity-dependent downregulation of KCC2, which has been reported during periods of intense network activity, such as occurs during seizures (see Section 1.5.2).

Relatively less is known about NKCC1 regulation. In immature neurons, coincident pre- and postsynaptic spiking activity has been found to downregulate NKCC1 activity and hyperpolarise E_{GABA-A} (Balena and Woodin, 2008). In epileptic tissue from patients with drug-resistant epilepsy, NKCC1 protein levels are increased (Sen et al., 2007) and this may contribute to altered GABAergic signalling (see below). Similar to KCC2, NKCC1 function has been found to be regulated as a result of the phosphorylation state of the transporter (Kahle et al., 2010; Russell, 2000). A signalling cascade involving WNK (with no K (lysine) kinases) and SPAK (Ste20-related proline-alanine-rich kinase) and OSR1 (oxidative stress response 1) kinase has been found to upregulate NKCC1 activity (Vitari et al., 2006; Kahle et al., 2005; Kahle et al., 2010). However, these studies have been mainly performed in non-neuronal cells, so the exact relevance of these mechanisms for central nervous system neurons remains to be determined.

In addition to setting the basal E_{GABA-A} level, Cl^- homeostasis mechanisms become relevant under conditions of intense neuronal activity. For instance, prolonged activation of $GABA_A$Rs, by high frequency electrical stimulation can result in a switch in $GABA_A$R response from hyperpolarising to depolarising (Raimondo et al., 2012; Alger and Nicoll, 1979; Staley et al., 1995; Thompson and Gahwiler, 1989). Such depolarising shifts are relatively short lived as hyperpolarising $GABA_A$R responses recover within tens of seconds once the stimulation has ended. Regarding the mechanisms underlying such changes, it has been argued that Cl^- influx through activated $GABA_A$Rs can exceed the capacity of Cl^- extrusion mechanisms, such that there is a transient increase in $[Cl^-]_i$ and a collapse in the Cl^- gradient across the membrane (Kaila et al., 1989; Staley and Proctor, 1999; Staley et al., 1995). At the same time, the transmembrane gradient for HCO_3^- is maintained by the efficient activity of carbonic anhydrases, which continue to generate HCO_3^- (Rivera et al., 2005).

Therefore, prolonged $GABA_AR$ activation can lead to a relative shift in E_{GABA-A} towards depolarising levels (Staley et al., 1995; Staley and Proctor, 1999).

The plasticity of ionic shifts in Cl^- seems to be somewhat specific compared to other ions. Several factors may explain why neurons have such increased capacity for experiencing changes in $[Cl^-]_i$ levels. Early during development, high $[Cl^-]_i$ and depolarising GABA responses may be necessary for the assembly of functional networks, allowing for permissive depolarisation while preventing overexcitation and potential excitotoxicity (Ben-Ari et al., 2007). Similar mechanisms may be important for the integration of newly born neurons in the adult brain into a preexisting neuronal network (Chancey et al., 2013; Overstreet et al., 2005). Compared to other ions, such as Ca^{2+}, Cl^- does not function as a second messenger and Cl^- levels are not controlled by any known intracellular Cl^- buffers. Rather, Cl^- transporters, Cl^- channels and diffusion seem to be the main players for regulating Cl^-. Such mechanisms may have a permissive role for Cl^- changes under normal physiological processes such as LTP induction (Fiumelli et al., 2005; Wang et al., 2006; Woodin et al., 2003). Such functional processes may be 'hijacked' under pathological conditions of intense neuronal activity such as seizures, when $[Cl^-]_i$ increases dramatically. Nevertheless, even under these conditions, neurons seem to be able to tolerate high levels of $[Cl^-]_i$.

In summary, neurons possess a variety of mechanisms for regulating their $[Cl^-]_i$. The interplay between these mechanisms dictates the level of E_{GABA-A} and therefore the polarity of the response following $GABA_AR$ activation. Alterations in Cl^- homeostasis have now been documented in various neurological disorders such as epilepsy, cerebral ischemia and neuropathic pain (Ben-Ari et al., 2012; Kahle et al., 2008; Miles et al., 2012). In the next section I will discuss such alterations and their relevance for GABAergic signalling in the context of neonatal and adult epilepsy.

1.5 Alterations in GABAergic signalling in epilepsy

Epilepsy is a severe neurological disorder, which is characterised by recurrent seizures that result from an inability of inhibitory mechanisms to restrain neuronal activity. Around 50 million people suffer with epilepsy worldwide (World Health Organisation, 2013). Generally, epilepsy has been viewed as an imbalance between excitation and inhibition, and consequently, most treatments are aimed either at enhancing GABAergic signalling or reducing excitation. However, current medication is ineffective in more than 30% of patients, whom continue to have uncontrolled seizures (Vajda, 2007). Over the last 10 years it has become increasingly clear that viewing epilepsy as an imbalance between inhibition and excitation is an oversimplification, and that the particularities of GABAergic signalling and alterations in Cl^- homeostasis play an important role in the pathophysiology of both neonatal and adult epilepsy.

1.5.1 GABAergic signalling in neonatal epilepsy

In humans, the risk for seizures is highest in the first postnatal month (Lanska and Lanska, 1996) and seizures in this period have been associated with the development of epilepsy later in life (Ronen et al., 2007). The depolarising and excitatory actions of GABAergic signalling in early development have been suggested to contribute to the high seizure susceptibility of the neonatal brain (Holmes et al., 2002). Consistent with this idea, studies using high K^+ application to trigger seizure-like events in neonatal rat hippocampal slices have found that GABA antagonists can reduce seizure duration (Dzhala and Staley, 2003). Furthermore, it has been found that high K^+ was able to induce seizure-like events only during a restricted developmental window between postnatal days 6 and 16, with a peak around 11 days

(Khazipov et al., 2004). During this developmental time window GABA still exerted depolarising effects (Khazipov et al., 2004). However, other studies using repetitive application of high K^+/low Mg^{2+} to trigger seizure activity in the neonatal rat hippocampus have found that concomitant application of GABA antagonists can actually increase seizure susceptibility and duration (Isaev et al., 2005; Isaev et al., 2007). Taken together, these studies suggest that GABA can exert both pro- and anti-convulsive actions in neonatal seizures. This may depend upon the exact developmental stage, the model used to trigger seizures and importantly, the prior seizure history (e.g. continuous seizure-like activity versus a single seizure episode).

In addition to seizure activity itself, GABAergic signalling has been implicated in the process by which a naive neuronal network becomes epileptic and capable of initiating seizures (Khalilov et al., 2003; Khalilov et al., 2005). To study how a naive network is converted into an epileptic one, Khalilov et al. (2003) have used an ingenious preparation comprising the two interconnected hippocampi and their commissural fibres in three separate perfusion chambers (Khalilov et al., 2003). Application of kainate to one hippocampus triggered seizures that propagated to the naive contralateral hippocampus via the commissural fibres. After 10-15 such seizure episodes, the naive hippocampus had become epileptogenic in its own right, and generated spontaneous seizure activity when the commissural connections were blocked. Interestingly, the formation of this secondary epileptic focus was associated with chronic depolarising shifts in $E_{GABA\text{-}A}$, which established the conditions for excitatory GABAergic signalling (Khalilov et al., 2003). These findings suggested that when seizure activity propagates into a naive network it could induce long-term changes to Cl^- homeostasis mechanisms. A subsequent study using the same preparation has found that both NMDAR and $GABA_AR$ antagonists were able to block the formation of the secondary

epileptic focus, further suggesting a role of depolarising GABA during repeated seizure activity and epileptogenesis (Khalilov et al., 2005).

The depolarising responses to $GABA_AR$ activation during the neonatal period are a result of high $[Cl^-]_i$, which is maintained by the Cl^--intruding transporter NKCC1 (Yamada et al., 2004). In keeping with a role for depolarising GABAergic signalling in promoting seizures, blocking NKCC1 in the neonatal hippocampus with the loop diuretic bumetanide has been reported to attenuate ongoing seizure activity (Dzhala et al., 2005). And NKCC1 has been found to contribute to a progressive Cl^- accumulation during repeated seizures (Dzhala et al., 2010). These studies are consistent with the idea that seizure activity induces alterations in Cl^- homeostasis and that $[Cl^-]_i$ accumulation can shift GABAergic signalling from inhibitory to excitatory. Furthermore, phenobarbital, a positive modulator of $GABA_ARs$, was able to block seizure activity after a single seizure episode in the interconnected hippocampi model (Nardou et al., 2011) but it had the opposite effect once the epileptogenic foci had been established (Nardou et al., 2011). Consistent with a role for NKCC1 in promoting Cl^- accumulation, bumetanide has been found to enhance the efficacy of phenobarbital in stopping seizure activity (Dzhala et al., 2008; Nardou et al., 2011). In addition to the role of NKCC1, it has been reported that Cl^- accumulation in the immature hippocampus can be exacerbated by a downregulation of the Cl^--extruding transporter KCC2 (Nardou et al., 2011).

In agreement with the animal studies that have revealed a pro-excitatory role for GABA during neonatal seizures, GABA enhancing drugs such as phenobarbital and diazepam are relatively inefficient at stopping neonatal seizures in humans. In some cases, these agents may even aggravate seizure activity (Booth and Evans, 2004). Therefore, new therapies should be developed and a promising avenue is the modulation of the NKCC1 transporter. Recently, the NKCC1 blocker bumetanide has been found to reduce seizure

activity in a neonatal patient with drug-resistant status epilepticus (Kahle et al., 2009). Larger clinical trials, testing bumetanide as a treatment for neonatal seizures, are currently ongoing. Nevertheless, the mechanisms by which seizures induce changes in NKCC1 function and the temporal dynamics of such changes have been largely unexplored. In Chapter 4 I investigate a novel molecular mechanism for regulating NKCC1 function under both normal conditions and during seizure activity. And in Chapter 5, I explore the temporal dynamics of E_{GABA-A} in relation to seizure activity and the post-seizure period.

1.5.2 Cl^- homeostasis and postsynaptic GABAergic signalling in adult epilepsy

In the normal adult brain, activation of $GABA_A$Rs typically results in hyperpolarising and inhibitory effects upon neurons and blocking GABAergic signalling leads to seizure activity (Trevelyan et al., 2007b; Treiman, 2001; Gruenthal et al., 1986; Davidson and Barbeau, 1975; Chervin et al., 1988). Consistent with this view, multiple lines of evidence point towards a reduction in the strength of GABAergic synaptic inhibition in epilepsy, which can be manifest in multiple ways. This includes the downregulation of $GABA_A$Rs (Terunuma et al., 2008), a reduction in presynaptic GABA release (Hirsch et al., 1999) and a loss of GABAergic interneurons (Dinocourt et al., 2003). In addition to these processes, it has recently become clear that epileptic seizure activity in the adult brain can also involve alterations in Cl^- homeostasis mechanisms. These alterations not only reduce the strength of inhibition, but can even switch GABAergic signalling from inhibitory to excitatory (Palma et al., 2006; Huberfeld et al., 2007; Fujiwara-Tsukamoto et al., 2003; Cohen et al., 2002; Barmashenko et al., 2011). Such changes include both transitory, short-term alterations that are associated with ongoing seizure activity, and persistent, long-term changes that are found in chronic epilepsy (Barmashenko et al., 2011; Isomura et al., 2003b; Pathak et al., 2007; Sen et al., 2007).

1.5.2.1 Transitory short term alterations in postsynaptic GABAergic signalling

As mentioned above, intense activation of $GABA_A$Rs in the adult hippocampus has been associated with intracellular Cl^- accumulation, a collapse in the transmembrane Cl^- gradient and a depolarising shift in $GABA_A$R signalling (Raimondo et al., 2012; Alger and Nicoll, 1979; Staley et al., 1995; Thompson and Gahwiler, 1989). A similar depolarising shift in $GABA_A$R signalling has been found to occur in the adult hippocampus during the course of seizure-like activity that was triggered either by high frequency stimulation or exposure to low Mg^{2+} (Fujiwara-Tsukamoto et al., 2003; Fujiwara-Tsukamoto et al., 2006; Isomura et al., 2008). This shift has been shown to be mediated by intracellular Cl^- accumulation that results from large Cl^- fluxes via activated $GABA_A$Rs (Isomura et al., 2003b). One report has suggested that intracellular Cl^- accumulation may begin just before the onset of the full seizure (Lillis et al., 2012). It is during the seizure however, that the most significant Cl^- accumulation occurs (Isomura et al., 2003b; Lillis et al., 2012). This shifts E_{GABA-A} to more depolarising values and leads to excitatory $GABA_A$R responses that can excite and promote the activity of hippocampal pyramidal neurons, which could promote further seizure activity into adjacent brain areas (Isomura et al., 2003a). In addition, the synchronization of interneuronal activity via gap junctions has been suggested to play an important role in the propagation of such seizure activity (Fujiwara-Tsukamoto et al., 2003). Consistent with this idea, it has recently been shown that electrical stimulation can induce prototypic seizure-like activity that is dependent solely on GABAergic transmission, and can occur when glutamatergic transmission is entirely blocked (Fujiwara-Tsukamoto et al., 2010). Taken together, these studies show that seizures can lead to an acute increase in $[Cl^-]_i$, which induces an excitatory shift in GABAergic signalling that in turn promotes ongoing seizure activity. Such changes are usually transitory and normal hyperpolarising $GABA_A$R responses

are reinstated shortly after the end of the seizure (Fujiwara-Tsukamoto et al., 2003). Although such changes in GABAergic signalling could be extremely important for the pathophysiology of seizures, the underlying mechanisms responsible and the factors that control the effects of depolarising GABAergic responses have not been fully explored. For instance, a variety of neuromodulatory factors are released during seizures and it is not known how these influence excitatory GABAergic signalling during seizures. One of the earliest and most ubiquitous responses to seizure activity is the production and release of a neuromodulator called adenosine (Berman et al., 2000; Boison, 2006; Dunwiddie, 1999; During and Spencer, 1992; Etherington et al., 2009; Lopatar et al., 2011; Lovatt et al., 2012). Extracellular adenosine concentration can rapidly increase during periods of intense neuronal activity, and adenosine can then modulate synaptic transmission by acting via four known adenosine receptors coupled with G-proteins (Fredholm et al., 2005; Boison, 2006; Dale and Frenguelli, 2009). Several mechanisms have been reported to contribute to the increase in extracellular adenosine in response to neuronal activity. Firstly, adenosine can be released from neuronal cells directly into the extracellular space via transporters such as equilibrative nucleoside transporters (Wall and Dale, 2013; White and MacDonald, 1990; Jonzon and Fredholm, 1985; Lovatt et al., 2012). This occurs when intracellular ATP is metabolised at high rates to ADP, AMP and adenosine, leading to an increase in adenosine outward concentration gradient and release of adenosine from cells into the extracellular space. Secondly, extracellular adenosine concentration can increase following release of ATP by exocytosis from glial cells and extracellular metabolism of ATP to adenosine by ecto-5'-nucleotidase (Zhang et al., 2003; Wall and Dale, 2013; Pascual et al., 2005). In addition, adenosine levels are regulated by enzymes that metabolise adenosine such as adenosine kinase and adenosine deaminase (Boison, 2006; Boison, 2013). In the hippocampus, direct adenosine release from neurons and glial ATP release followed by extracellular conversion to adenosine have been

recently reported to have roughly equal contributions to increases in extracellular adenosine levels following pulses of electrical stimulation (Wall and Dale, 2013). Nevertheless, in the context of seizure activity, it has been suggested that direct adenosine release may be the primary source for increased extracellular adenosine levels (Lovatt et al., 2012). Regardless of the exact mechanisms of adenosine release, adenosine concentration rapidly increases during seizure activity and numerous studies have reported that adenosine acts as an endogenous anti-epileptic mechanism, which can reduce seizure activity probably by inhibiting glutamate release via the A1 receptor (Boison, 2006; Dunwiddie, 1999; During and Spencer, 1992; Etherington and Frenguelli, 2004; Etherington et al., 2009; Fedele et al., 2006; Li et al., 2007). Nevertheless, relatively less is known about adenosine's effects upon GABAergic signalling, particularly in the context of seizure activity where GABA can induce depolarising responses. In Chapter 3 I have explored the role of adenosine release in modulating postsynaptic GABAergic signalling during seizure activity.

1.5.2.2 Persistent, long term alterations in postsynaptic GABAergic signalling

In addition to short-term transient changes in Cl^- gradients, epilepsy has been associated with persistent alterations to Cl^- homeostasis mechanisms that can compromise inhibitory GABAergic signalling. In a pioneering study, in hippocampal slices generated from tissue surgically excised from human epileptic patients, Cohen et al. (2002) showed that approximately 25 % of pyramidal neurons in the subiculum exhibit depolarising GABAergic responses during inter-ictal network events (Cohen et al., 2002). These depolarising GABA responses correlated with a reduction in the expression of the Cl^--extruding transporter KCC2 (Huberfeld et al., 2007). Furthermore, the NKCC1 blocker bumetanide induced a hyperpolarising shift in E_{GABA-A} and reduced inter-ictal activity, suggesting that NKCC1 is active in human epileptic tissue and contributes to Cl^- accumulation (Huberfeld et al., 2007).

Consistent with these findings, several other studies have reported an upregulation in NKCC1 and a downregulation in KCC2 expression in tissue surgically excised from human patients with drug-refractory epilepsy (Palma et al., 2006; Sen et al., 2007). And in keeping with a key role for Cl^- homeostasis in the pathophysiology of epilepsy in the mature brain, a recent study has found that the NKCC1 blocker bumetanide can reduce seizure frequency in adult patients with temporal lobe epilepsy (Eftekhari et al., 2012).

In addition to the findings in human epileptic patients, a series of studies using different animal models of epilepsy have found persistent alterations in Cl^- homeostasis (Pathak et al., 2007; Okabe et al., 2002; Barmashenko et al., 2011; Bragin et al., 2009; Jin et al., 2005). For instance, amygdala kindling has been reported to increase NKCC1 expression in the piriform cortex (Okabe et al., 2002). Lesions that generate cortical epilepsy have been associated with a decreased ability of neurons to deal with Cl^- influxes (Jin et al., 2005). And pilocarpine-induced status epilepticus has been shown to result in a depolarising shift in $E_{GABA\text{-}A}$, a downregulation of KCC2, and an upregulation of NKCC1, all of which are evident during the 2-3 week period that follows the initial insult (Pathak et al., 2007; Barmashenko et al., 2011; Bragin et al., 2009). In addition to changes in the expression levels of Cl^- transporter proteins, seizure activity could modulate the activity of these transporters via post-translational processes. For instance, in the case of KCC2, its stability at the plasma membrane has been reported to be controlled by phosphorylation mechanisms (Lee et al., 2007; Lee et al., 2010; Lee et al., 2011b) and by the activity of proteases such as calpain (Puskarjov et al., 2012). However, we do not yet know the relevance of these mechanisms for epileptic tissue or how other Cl^- regulating proteins may be modulated. Understanding the exact mechanisms by which seizure activity leads to persistent changes in Cl^- homeostasis therefore requires future study.

1.6 Aims of my thesis

Consistent with a pro-excitatory role for GABAergic signalling during seizures, experiments in my thesis show that seizure activity induces an acute depolarising shift in GABAergic signalling, which becomes excitatory and promotes ongoing seizure activity (Figure 1.3). Such a shift occurs both in the neonatal and adult rat hippocampus, suggesting that intracellular Cl^- accumulation and the resulting excitatory GABAergic signalling are a fundamental feature of seizure activity and epilepsy (Figure 1.3). Therefore investigating the mechanisms that underlie these changes is crucial for understanding the pathophysiology of epilepsy and this has been the main focus of my thesis.

The **first aim** of my thesis was to explore the role of the neuromodulator adenosine in regulating postsynaptic responses to $GABA_AR$ activation during seizures. Adenosine is known to be released by heightened network activity but adenosine's interactions with the GABAergic system have not been examined during a seizure. I used pharmacological manipulations and gramicidin-perforated patch clamp recordings to determine the effect of adenosine on $GABA_AR$ responses in an in vitro seizure model in the mature rat hippocampus **(Chapter 3)**.

My **second aim** was to investigate the molecular mechanisms involved in the regulation of the Cl^- transporter NKCC1. Biotinylation experiments were used in combination with electrophysiological recordings to investigate the expression and surface delivery of NKCC1, and how this relates to Cl^- regulation. Co-immunoprecipitation and mass spectrometry experiments were then used to identify proteins that associate with NKCC1 and could regulate the function of the transporter. I explored one such association between NKCC1 and a molecular motor protein, Myosin Va, in regulating NKCC1 function under normal conditions and during seizure activity in the neonatal rat hippocampus **(Chapter 4)**.

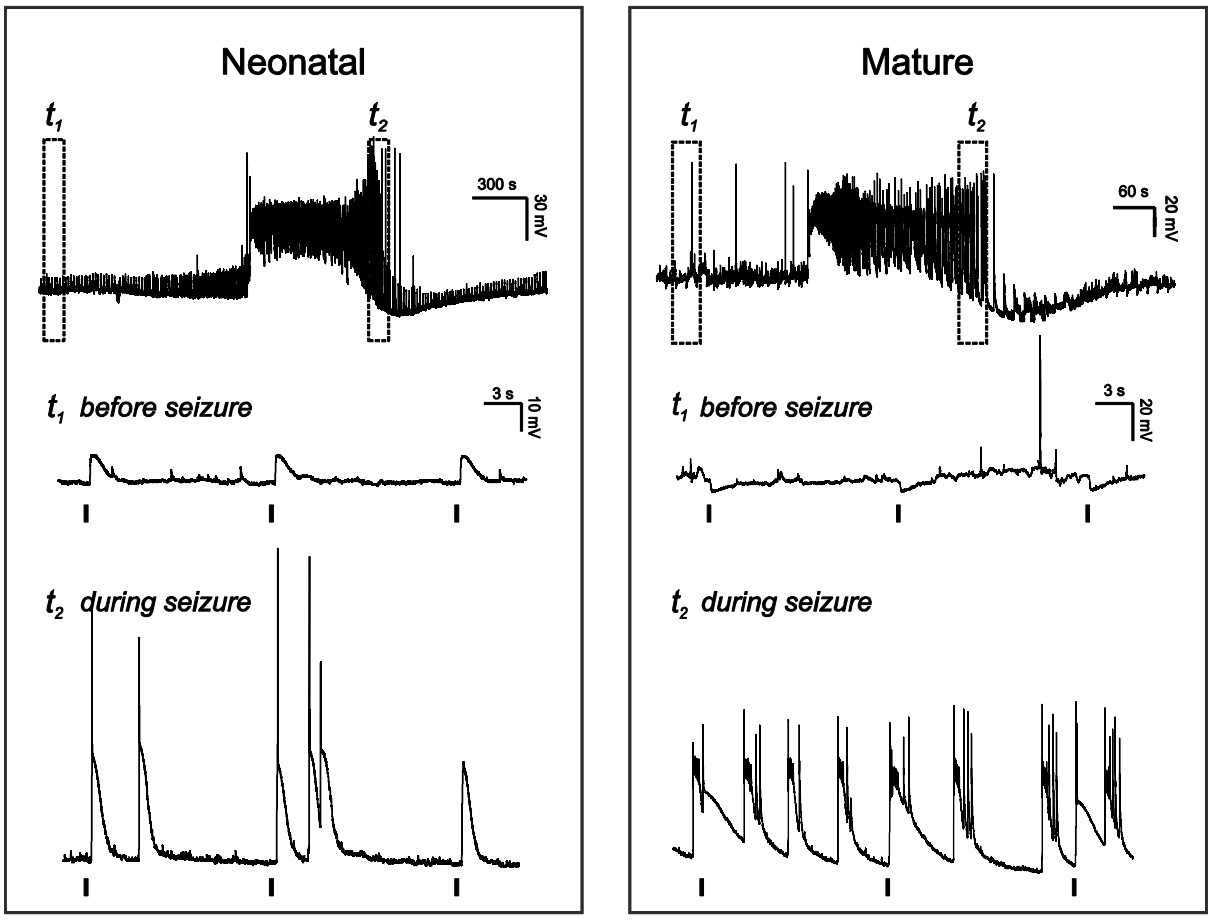


Figure 1.3 Seizure activity renders GABAergic signalling excitatory in both the neonatal and the mature hippocampus

Current clamp recordings illustrating seizure activity (top) and $GABA_AR$ responses to local agonist application in CA3 pyramidal neurons (bottom) from neonatal (left) and mature hippocampal brain slices (right). Dashed rectangles represent two time points: t_1 - before the seizure, and t_2 – during the seizure; vertical bars represent the time of $GABA_AR$ agonist application. Before the seizure $GABA_AR$ responses are depolarising in the neonatal neuron and hyperpolarising in the mature neuron. During the seizure $GABA_ARs$ become depolarising and excitatory (i.e. able to trigger action potentials) in both the neonatal and mature tissue.

My **third aim** was to systematically investigate the temporal dynamics of E_{GABA-A} with respect to neonatal seizure activity. To achieve this I developed a protocol that allows repeated E_{GABA-A} measurements, concomitant with monitoring seizure activity. Using this protocol I revealed a novel Cl^- extrusion mechanism in the post-seizure period, which may facilitate the recovery of GABAergic signalling from excitatory back to inhibitory **(Chapter 5)**.

2 Materials and Methods

2.1 Organotypic hippocampal slices

Rat organotypic hippocampal slice cultures were prepared using a method similar to that described by Stoppini and colleagues (Stoppini et al., 1991). Briefly, male Wistar rats were killed by cervical dislocation in accordance with Schedule 1 methods of the UK Animals Scientific Procedures Act 1986. The brains were extracted and placed in cold (4 °C) Geys Balanced Salt Solution (GBSS), supplemented with D-glucose (34.7 mM). All reagents were purchased from Sigma-Aldrich, unless stated. The hemispheres were separated and individual hippocampi were removed and immediately sectioned into 350 µm thick slices on a McIlwain tissue chopper. Slices were rinsed in cold dissection media, placed onto Millicell-CM membranes (Millipore) and maintained in culture media containing 25 % EBSS, 50 % MEM, 25 % heat-inactivated horse serum, glucose, and B27 (Invitrogen), and incubated at 36 °C in a 5 % CO_2 humidified incubator.

Previous studies using acute slice recordings from rat hippocampus have established that GABAergic signalling is immature during the first postnatal week and that $E_{GABA\text{-}A}$ in pyramidal neurons is more depolarised than the resting membrane potential (Pfeffer et al., 2009; Sipila et al., 2005; Tyzio et al., 2007). By the end of the second postnatal week GABAergic signalling exhibits more mature properties and $E_{GABA\text{-}A}$ is typically more hyperpolarised than the resting membrane potential (Tyzio et al., 2007; Rivera et al., 1999). Work in rat organotypic hippocampal slices found that postsynaptic $GABA_AR$ responses in pyramidal neurons are also hyperpolarising at an equivalent age (postnatal day 5-7 + 8-13

days in vitro; Streit et al., 1989). In order to study the neonatal and mature stages of GABAergic synaptic transmission I generated slices from two different ages of rat. For the 'neonatal' stage, slices were prepared from rats that were 1-2 postnatal days old (P1-2) and these slices were maintained in culture for 2-4 days (equivalent to 3-6 days in vivo). Meanwhile for the 'mature' stage, slices were prepared from rats that were 7 postnatal days old (P7) and kept in culture for 7-14 days (equivalent to 14-21 days in vivo). Consistent with previous work (Yamada et al., 2004; Tyzio et al., 2007; Rivera et al., 1999), I found that the resting E_{GABA-A} was significantly more depolarised in the neonatal slices (-66.8 ± 2.0 mV, n = 26) than in the mature slices (-84.5 ± 0.9 mV, n = 13, $p < 0.001$, unpaired t-test). Although GABAergic signalling has been found to reach mature levels by the end of the second postnatal week (Tyzio et al., 2007), other developmental changes might occur after this period in slices kept in culture between 7-14 days. For instance, the number of connections between neurons is likely to increase with time in culture. This could result in increased variability with regard to seizure activity, time to seizure initiation and seizure duration. To account for such factors, experiments in Chapter 3 were performed using a within-cell design, in which different parameters were compared before and after drug manipulations in the same cell. This design reduces the effect of variability across slices and increases the statistical power to detect changes specific to the pharmacological manipulations.

2.2 Electrophysiological recordings

To preserve the intracellular mileu of the cell and particularly the $[Cl^-]_i$, I performed gramicidin-perforated patch-clamp recordings (Akerman and Cline, 2006; Ebihara et al., 1995; Kyrozis and Reichling, 1995). Patch pipettes of 3-5 MOhm tip resistance were pulled from filamental borosilicate glass capillaries (1.2 mm outer diameter, 0.69 mm inner

diameter; Harvard Apparatus Ltd), using a horizontal puller (Sutter P-97). The pipettes were filled with a high KCl internal solution containing gramicidin. The composition of internal solution was (in mM): KCl (135), Na_2ATP (4), Na_3GTP (0.3), $MgCl_2$ (2), and HEPES (10). Osmolarity was adjusted to 290 mOsM and the pH was adjusted to 7.35 with KOH. Gramicidin (Calbiochem) was dissolved in dimethylsulfoxide (DMSO) to achieve a stock solution of 10 mg/ml. This was then diluted in internal solution on the day of experimentation to achieve a final concentration of 80 μg / ml. The resulting solution was vortexed for 1 min, sonicated for 30 s and then filtered with a 0.45 μm pore cellulose acetate membrane filter (Nalgene).

Hippocampal slices were transferred to a recording chamber and continuously superfused with 95 % O_2/ 5 % CO_2 oxygenated artificial cerebro-spinal fluid (aCSF), warmed to 30-32 °C. The composition of aCSF was (in mM): NaCl (120), KCl (3), $MgCl_2$ (2), $CaCl_2$ (1.5), NaH_2PO_4 (1.2), $NaHCO_3$ (23), D-Glucose (11). The pH was adjusted to be between 7.35 and 7.40 using NaOH. Neurons were visualized under a 60x, water-immersion objective (Olympus BX51WI, Japan) and pyramidal neurons from the CA3 region were identified based upon their location within the hippocampus and their triangular somatic morphology. Following formation of a tight seal between the pipette and the underlying plasma membrane (> 1 GOhm), the perforation progress was evaluated by continuously monitoring the decrease in the access resistance. Recordings were started once the access resistance had stabilized between 30-100 MOhm (mean R_a ~ 65 MOhm), which usually occurred at around 20-50 min from the time of gigaseal formation. During off-line analysis, all membrane potentials were subsequently corrected for the voltage drop across the access resistance. Access resistance was calculated from -10 mV steps applied in voltage clamp from a holding voltage of -70 mV. Subsequently, 70% access resistance correction was applied for voltage drop and the corrected holding voltage was calculated using the following formula $V_{Corrected} = V_{Command}$ -

I_{Hold} * R_a * 0.7). For example, for a R_a of 68.5 MOhm, command holding voltages of -40 mV, -50 mV, -60 mV, -70 mV, -80 mV and -90 mV were corrected during off-line analysis to -41.9 mV, -50.7 mV, -60.3 mV, -69.8 mV, -79.6 mV, and -89.3 mV respectively under baseline conditions. Nevertheless, since the voltage drop also depends on the amount of current that needs to be injected (i.e. I_{Hold}), the voltage error will be higher for instances when the cell's membrane conduction is increased, such as occurs for example during the activation of GABA-A receptors by local agonist application. $V_{Corrected}$ at the peak of the GABA-A R response, for the example mentioned above, becomes -54.8 mV, -58.2 mV, -62.2 mV, -66.8 mV, -72.9 mV and -80.9 mV respectively. Therefore, correction for access resistance is an important step for reducing errors in E_{GABA-A} measurements. Recordings were made using an Axopatch 1D amplifier (Axon Instruments) and data acquired using WinWCP Strathclyde Whole Cell Analysis software (V.3.9.7; University of Strathclyde) and stored for off-line analysis. At the end of the experiment the integrity of the perforated patch was confirmed by applying suction in order to rupture the underlying membrane and achieve whole cell recording mode. This led to a rapid decrease in the access resistance and a shift in E_{GABAA} due to diffusion of Cl^- from the pipette into the cell's cytoplasm. In some cases spontaneous ruptures of the perforated patch occurred. The hallmark of these spontaneous ruptures is a sudden and rapidly increasing depolarising shift in E_{GABA-A} and/or high amplitude depolarising GABA-A R responses due to Cl^- diffusion from the high-Cl^- pipette solution into the cell. Data from these cells was excluded from any further analysis. For experiments in which perforated-patch clamp was performed in cells expressing fluorescent proteins, the membrane of the cell can be visualised at the tip of the pipette. Nevertheless, in my experience this is not a reliable marker for the integrity of the perforated-patch since small ruptures that cannot be detected by visual inspection can lead to Cl^- diffusion inside the cell.

Therefore the use of high-Cl^- solution in the pipette is crucial for having a sensitive method to assess the integrity of the patch and detect any spontaneous ruptures.

2.2.1 Triggering seizure-like activity in organotypic slices

In the mature slices, seizures were induced by perfusion with nominally Mg^{2+}-free aCSF. Removing of extracellular Mg^{2+} can increase network excitability and promote seizure activity via several mechanisms including: reduced surface charge screening, increased neurotransmitter release, and increased activation of NMDA receptor by removal of the Mg^{2+} block (Isaev et al., 2012; Mody et al., 1987; Stanton et al., 1987). The precise contribution of each of these mechanisms to triggering seizure activity is not fully established, but both NMDA receptors antagonists and increasing extracellular divalent cations concentration had been found to block low-Mg^{2+} seizures (Traub et al., 1994; Isaev et al., 2012; Mody et al., 1987).

Once a seizure event has been triggered, the perfusion media was switched back to normal aCSF. This transient exposure to 0 Mg^{2+} allowed me to induce reproducible seizure episodes and prevented continuous seizure activity that can occur with prolonged exposure to 0 Mg^{2+}. Using this model I was able to trigger two consecutive seizure episodes and use pharmacological manipulations in a within-cell design.

In the neonatal slices, exposure to Mg^{2+}-free aCSF was not sufficient to trigger seizures and this was probably due to relatively low levels of synaptic connectivity within the first post-natal week (Hsia et al., 1998). In order to trigger seizures at this stage, the K^+ channel blocker 4-AP (100 µM) was used in combination with 0 Mg^{2+} aCSF. Exposing the slices to 4-AP and 0 Mg^{2+} reliably induced seizures in all slices. In order to induce long-

lasting (over 10 min) single seizure episodes, perfusion with the 4-AP and 0 Mg^{2+} aCSF was maintained for 10 min from the start of the seizure, before returning to normal aCSF.

In both the mature and the neonatal slices, seizure onset was characterized by a pronounced depolarising shift in the membrane potential, which was maintained and upon which high frequency, low amplitude discharges occurred. In accordance with previous work, I could distinguish two phases of the seizure episodes: (1) the initial ictal-like phase (also referred to as the 'tonic' phase) and (2) the after-discharge phase (also referred to as the 'clonic' phase; Trevelyan et al., 2007a; Isomura et al., 2008; Higashima et al., 1996). For analysis purposes the onset of the seizure was defined as the time at which the membrane potential depolarized beyond a 'threshold' set at 40 mV above the cell's resting membrane potential ('baseline'). The end of the ictal-like phase and start of the after-discharge phase was defined as the point at which the membrane potential returned to baseline for the first time after the start of the seizure. The after-discharge phase was composed of rhythmic bursts of activity occurring from a relatively hyperpolarized membrane potential. An individual after-discharge event was defined as a burst of activity in which the membrane potential depolarized above the threshold for seizure onset, and then returned to below the baseline value. The end of the after-discharge phase was defined as the end of the last after-discharge event. Post-seizure hyperpolarization was measured from the end of the after-discharge phase and expressed relative to the baseline membrane potential. All seizure experiments in Chapter 3 and 4 were performed using uncompensated current clamp recordings, without any DC injection in the 'I=0' mode. Seizure experiments in Chapter 5 were performed by alternating between current clamp recordings and voltage clamp recordings. All experiments comparing seizure activity, $GABA_AR$ responses, resting E_{GABA-A}, $GABA_AR$ conductance and membrane conductance were conducted with a within-cell design, so that each parameter was compared before and after a treatment.

2.2.2 Measuring $GABA_AR$ response amplitude

$GABA_ARs$ were activated by delivering short 'puffs' of the $GABA_AR$ selective agonist, muscimol (45 μM), through a patch pipette placed in the vicinity of the cell and connected to a picospritzer (5-10 psi for 20-500 ms; General Valve, Fairfax, NJ). Puffs were delivered at 15 second intervals in order to allow recovery of chloride homeostasis (Jin et al., 2005; Staley and Proctor, 1999). To measure the amplitude of individual $GABA_AR$ potentials in current clamp, the membrane potential immediately prior to the muscimol puff (measured over a 20 ms window) was subtracted from the membrane potential at the peak of the muscimol response (measured over a 5 ms window). To measure hyperpolarising $GABA_AR$ responses under seizure-free conditions the resting membrane potential was held at -70 mV by somatic DC current injection. Depolarising $GABA_AR$ responses were recorded from a resting membrane potential of -110 mV, established by injecting DC current through the recording pipette in the presence of 200 μM furosemide to block the activity of Cl^- transporter proteins. For the seizure-free experiments presented in Chapter 3 and 4, slices were perfused with normal aCSF containing tetrodotoxin (TTX; 1 μM) to prevent spiking activity. For the seizure experiments $GABA_AR$ potentials were found to be depolarising early during the post-seizure period and then gradually decreased in amplitude and reversed polarity to become hyperpolarising. To estimate the kinetics of this recovery we fitted an exponential to the amplitudes of depolarising $GABA_AR$ responses during a one-minute time window prior to their reversal to hyperpolarising. The recovery rate was calculated as the time constant of the exponential fit.

2.2.3 Measuring E_{GABA-A}

In order to measure resting E_{GABA-A}, $GABA_AR$ currents were evoked by local application of either muscimol (45 µM; Chapter 3) or GABA (100 µM; Chapter 4) and recorded in the voltage clamp configuration at six different holding potentials (between -50 mV and -100 mV). Muscimol application (45 µM) gave rise to large responses, which were long lasting (up to several seconds). Such large responses can influence intracellular Cl^- concentration and therefore longer recovery times are required between consecutive applications. To avoid muscimol-induced alterations in Cl^- concentration, at least 15 seconds were allowed between two consecutive muscimol applications. On the other hand, application of GABA (100 µM) resulted in shorter responses (lasting up to 1.5-2 sec) with faster kinetics. Such responses require shorter recovery times and therefore GABA application was preferred for measuring E_{GABA-A} in Chapters 4 and 5. For each cell, I-V curves were constructed for the 'holding current' and the peak of the 'total current' (reflecting the holding current plus the current through the activated $GABA_ARs$). E_{GABA-A} was defined as the intersection of these two I-V curves, which indicated the voltage at which there was no net current through the $GABA_AR$ (see Figure 3.7 in Chapter 3). To estimate peak $GABA_AR$ conductance (see Figure 3.8 in Chapter 3), a voltage ramp (1 s duration, ramping from -100 to -30 mV) was applied to the membrane to provide a more accurate estimate of the holding current at every membrane potential. 'Pure' $GABA_AR$ currents were then calculated by subtracting this holding current from the peak of the total current (in response to muscimol or GABA) for specific membrane potentials. In this manner I-V plots of the peak $GABA_AR$ current were constructed and the peak $GABA_AR$ conductance was calculated as the slope of the linear fit. Membrane conductance was calculated from the membrane current generated by 1 s hyperpolarising voltage steps (-10 mV), delivered under voltage clamp conditions. Experiments in Chapter 4 were performed in the presence of the $GABA_B$ receptor blocker CGP55845 (5 µM) to prevent

activation of $GABA_BRs$ by local GABA application. In some of the seizure-free experiments used to measure resting E_{GABA-A}, TTX (1 µM) was added to the aCSF to prevent spiking activity.

To measure E_{GABA-A} during seizure activity (Chapter 5), recordings were rapidly alternated between current clamp and voltage clamp modes. The current clamp recordings allowed the monitoring of seizure activity, whilst the periods in voltage clamp (2.5 s duration) were used to measure E_{GABA-A} with voltage ramp protocols (see Figure 5.1 in Chapter 5). Each period in voltage clamp consisted of 2 consecutive voltage ramps (500 ms duration, ramping from -100 to -50 mV). The 1st ramp was applied under baseline conditions and the 2nd ramp was applied during activation of $GABA_ARs$ by local application of GABA (100 µM), in the presence of the $GABA_B$ receptor blocker CGP55845 (5 µM). This made it possible to construct I-V plots of the 'holding current' generated by the 1st ramp and the 'total current' generated by the 2nd ramp (reflecting the holding current plus the current through the activated $GABA_ARs$. E_{GABA-A} was defined as the voltage at which the 'holding current' and the 'total current' intersected (see Figure 5.1 in Chapter 5).

2.3 Drug manipulations

Pharmacological manipulations were performed by bath application of drugs using a perfusion system. Adenosine was dissolved directly into the aCSF on the day of experiment, whereas all other drugs were prepared in stock solutions, stored at -20 °C and added to the aCSF on the day of experiment to reach the required concentration. Tolbutamide, CGS 15943, 8-cyclopentyl-1,3-dipropylxanthine (DPCPX) and bumetanide were dissolved in DMSO. All other drugs were dissolved in normal aCSF. Adenosine, $BaCl_2$, furosemide and

tolbutamide were purchased from Sigma-Aldrich. Muscimol, TTX, tertiapin, apamine, CGS 15943, CGP55845, DPCPX, and bumetanide were purchased from Tocris.

2.4 Biotinylation and isolation of cell surface proteins in hippocampal slices

The aim of the biotinylation experiments was to calculate the ratio of 'surface' proteins (captured by biotin) to 'total' protein (membrane bound plus intracellular). Each experimental data point was derived from 3 organotypic hippocampal slices cultured on the same Millicell insert. Neonatal and mature hippocampal slices (3 slices per Millicell inset), were placed on ice and washed twice with ice-cold aCSF. Slices were then incubated in ice-cold aCSF containing 100 μM cleavable biotin (EZ-Link Sulfo-NHS-SS-Biotin, Thermo Scientific) with O_2/CO_2 bubbling for 45 min to label surface proteins with biotin. Then the slices were washed twice with 100 μM lysine in ice-cold ACSF to remove any un-bound biotin and lysed with 0.5ml ice-cold lysis buffer (20 mM Tris pH 7.5, 50 mM NaCl, 1 mM EDTA, 0.1 % w/v sodium dodecyl sulphate (SDS), 1 % v/v Triton X-100 protease inhibitors (Roche)). The lysate was centrifuged at 14,000 rpm at 4 ^{o}C for 10 min. 50 μl of the resultant supernatant was removed as the "Total" protein lysate sample and stored in 50 μl 2 x sample buffer. Biotinylated proteins were captured by incubation with 60 μl washed NeutrAvidin Ultralink Resin beads (Thermo Scientific) on a turning wheel overnight at 4 ^{o}C. The beads were washed three times with ice-cold lysis buffer and the "Captured" sample eluted at 37 ^{o}C for 30 min in 60 μl 2 x sample buffer to cleave captured proteins from the NeutrAvidin beads. Samples were stored at -20 ˚C.

2.5 SDS-PAGE and western Blotting

Prepared protein samples were separated on 6 % or 8 % SDS polyacrylamide gels (SDS-PAGE) in running buffer (25 mM Tris, 192 mM glycine, 0.1 % w/v SDS) at 140 V for 1.5 h. Separated proteins were transferred onto Protran nitrocellulose membranes (Sigma) at 85 V for 1 h in transfer buffer (25 mM Tris-Base, 192 mM glycine, 20 % v/v methanol, 0.1 % w/v SDS). After blocking the membrane for 1 h in Tris-buffered saline (50 mM Tris, pH 7.5, 150 mM NaCl) containing 0.1 % v/v Tween-20 (TBS-T) with 5 % w/v skimmed milk powder (blocking buffer), blots were incubated overnight at 4 ^{o}C with the following primary antibodies: mouse anti-NKCC1 (1:2000), rabbit anti-KCC2 (Millipore, 1:500), rabbit anti-Myosin Va (1:1000), mouse anti-β-tubulin (Cambridge Bioscience, 1:2000) or mouse anti-Flag (Sigma, 1:1000). Blots were washed in TBS-T and incubated with the following horseradish-peroxidase (HRP) conjugated secondary antibodies for 2 h at room temperature (RT): donkey anti-mouse (1:3000) and/or donkey anti-rabbit (1:3000; Jackson Immunoresearch). After four washes in TBS-T, western blots were developed with Enhanced Chemiluminescence (ECL) western blotting substrate (Pierce) according to the manufacturer's instructions. The ECL signal was captured digitally using a Fluor-S MultiImager (Bio-Rad) and also on X-ray film. Quantification of western blots of biotinylation samples was performed, using Quantify One software (Biorad), by measuring band volume pixel intensities and subtracting background intensity levels. To compare across the two developmental stages, total protein levels of P3 and P13 slices were normalised by performing a protein assay using the Bio-Rad Dc Protein Assay kit. Equal loading of total protein samples on gels for western blotting with KCC2 and NKCC1 antibodies was confirmed by staining identically loaded gels with the Gelcode Blue stain to visualize all proteins. The neonatal values were normalised to 100 % and the values of the mature tissue were expressed as a percentage of the neonatal. To compare the total protein expression and

surface/total protein ratio across development, neonatal and mature samples were always run in parallel and quantified from the same blots.

2.6 Immunoprecipitation of NKCC1 and mass spectrometry

To perform the affinity purification of NKCC1, neonatal rat brain homogenate was mixed with recombinant Protein G sepharose beads (Invitrogen), to which the T4 monoclonal NKCC1 antibody (DHSB) had been coupled. Beads were first washed 5 x with PBS at RT and then incubated with the T4 antibody (3 mg per mL of beads) by rotating the mixture for 1 h at RT. The beads were then washed with PBS to remove unbound antibody, washed with borate buffer (0.1 M), spun down and resuspended in borate buffer containing dimethyl pimelimidate (DMP; 20 mM), and the mixture rotated for 30 min at RT. The reaction was then stopped and unreacted DMP quenched by spinning down the beads, resuspending in 0.1 M ethanolamine (pH 8.0) and then rotating for 2 h at RT. The antibody-coupled beads were then washed and stored in PBS. The homogenate was prepared from dissected neonatal rat brain (P3-5) and solubilised in RIPA buffer (150 mM NaCl, 50 mM Tris-HCl (pH 8.0), 1 mM EGTA, 1 % Triton X-100, 0.5 % deoxycholate) containing protease inhibitors (Roche). After incubation on ice for 30 min, the homogenate was centrifuged at 100,000 g for 30 min at 4 °C and pre-cleared with fresh Protein G sepharose beads for 3 h at 4 °C. The homogenate was then mixed with the T4 antibody-coupled beads and the mixture rotated O/N at 4 °C. The following day the mixture was spun at 2,000 rpm for 5 min and washed 2 x with RIPA buffer containing protease inhibitors. Samples were eluted from the beads into 80 µl of 2 x SDS sample buffer with 5 % beta-mercaptoethanol by heating at 96 °C for 5 min. The resulting samples were analysed by electrophoresis on 8 % Bis-Tris NuPAGE® Novex gels with MOPs running buffer (Invitrogen). Gels were rinsed for 10 min in distilled H_2O and incubated with

GelCode Blue Stain Reagent (Pierce) by gentle rocking for 1 h at RT. Protein bands were enhanced by repeatedly washing the gel in distilled H_2O and selected by comparison to control lanes using non-crosslinked beads. Selected bands were excised for in gel trypsinisation and identified using fourier transform ion cyclotron (FT-ICR) mass spectrometry at the School of Biosciences, University of Birmingham. For protein identification, data from the mass spectrometer were searched against the SwissProt database using the Mascot search algorithm (Matrix Science). Mascot searches were restricted to the Rattus taxonomy allowing up to 3 missed trypsin cleave sites, with carbamidomethyl cysteine as a fixed modification and oxidised methionine, N-terminus acetylation, tyrosine, serine and threoine phosphorylation and deamidation of asparagines and glutamine included as potential variable modifications. The peptide tolerance was set to 20 ppm and the fragment mass tolerance was set at 0.5 Da. Positive identifications were accepted with a confidence interval of 95 % or greater, 7 or more unique peptides and a coverage of 10 % or more.

2.7 Co-immunoprecipitation of NKCC1 and Myosin Va from solubilised hippocampal slices and COS-7 cells.

Hippocampal slices were washed in ice-cold ACSF and harvested in tubes containing 0.5 ml lysis buffer (50 mM Tris pH 7.4, 150 mM NaCl, 0.5 % Chaps, plus protease inhibitors (Roche)). Slices were homogenised in tissue homogenisation buffer (TB; 75 mM Tris pH 6.8, 3.8 % SDS, 4 M Urea, 40 % Glycerol). 50 µl of solubilised protein lysate was removed to serve as the "Input" sample to which 50 µL of 2 x SB++ was added. To pre-clear the lysates of proteins that bind non-specifically to Pierce Protein A/G Plus beads (Thermo Scientific), 30 µl of washed agarose beads were added to the lysates and rotated for 2 h at 4 °C. Upon discarding the beads, 1-2 µg of the following antibodies were added to the lysates: mouse

anti-NKCC1 (T4 clone, Developmental Studies Hybridoma Bank, University of Iowa), rabbit anti-Myosin Va (Cell Signalling Technologies), rodent IgG (Thermo Scientific). Samples were rotated at 4 °C overnight. 50 µl of washed agarose Pierce Protein A/G Plus beads were added to each tube and rotated for 2 h at 4 °C. The captured complexes were washed three times before being eluted in 50 µl of 2 x SB++ at 60 °C for 10 min.

COS-7 cells were washed in 1x phosphate buffered saline (PBS) and harvested in 500µl of lysis buffer (50mM Tris pH 7.5, 150 mM NaCl, 0.5 % Triton X-100 plus protease inhibitors) and centrifuged as described above. The following antibodies were added to the solubilised lysates overnight: 1µg anti-NKCC1 T4 antibody and 2µg anti-Flag antibody, with resulting complexes captured by adding 50µL of washed agarose beads and rotating for 3 h at 4 °C. Agarose beads were washed in lysis buffer and eluted in 50 µL of 2 x SB++ at 60°C for 10 min.

2.8 Immunolabelling of cultured cells

Dissociated hippocampal neurons and transfected COS-7 cells were washed in 1x PBS, fixed in 4 % paraformaldehyde, permeabilised in 0.25 % v/v Triton X-100 for 5 min, and blocked in 10 % w/v BSA for 30 min. For neuronal staining 100 µl of antibodies in PBS containing 2 % w/v BSA were added to each coverslip for 2 h at RT: anti-NKCC1 (mouse IgG, 1:50) and Myosin Va (rabbit IgG, 1:50). Neurons were washed in 3x PBS and secondary antibodies Alexa Fluor 555 goat anti-mouse IgG and/or Alexa Fluor 488 goat anti-rabbit IgG (1:1000) were added in PBS containing 2 % w/v BSA for 1 h at RT. Coverslips were washed in 3x PBS and mounted in Prolong Gold. The fixed COS-7 cells were incubated with anti-Flag antibody (mouse IgG, 1:1000) overnight and then incubated with Alexa Fluor 555 goat anti-mouse (1:1000) for 1 h at RT. Cells were imaged on a Leica DM 5000B fluorescence

microscope equipped with a Hamamatsu cooled CCD camera and Open Lab Image Capture software.

2.9 Plasmids, plasmid preparation and transfections

All plasmids were amplified in XL1-Blue competent cells (Stratagene) and extracted using QIAGEN maxiprep kits (Qiagen, USA). Sequencing, diagnostic restriction digests and gel electrophoresis were used to confirm plasmid identity.

The pEGFP-MyoVa-DN construct encoding the rat Myosin Va globular tail (amino acids 1396-1830) fused to EGFP under the CMV promoter was used to disrupt endogenous Myosin Va function in organotypic hippocampal slices (see Chapter 4). This construct was a generous gift from Dr Jose Esteban, Centro de Biología Molecular Severo Ochoa, Consejo Superior de Investigaciones Científicas, Madrid, Spain (Correia et al., 2008). The pEGFP-N3 construct encoding EGFP under the CMV promoter was used as a control (see Chapter 4). These constructs were delivered using biolistic gene-delivery and slices were transfected on the day of preparation, after 30 min in culture using a protocol described by (Woods and Zito, 2008). Briefly, 50 µg of DNA were precipitated onto 15 mg of 1.6 µm gold particales (Bio-Rad, UK). These coated gold particles were propelled into neurons from hippocampal slices using a Helios Gene Gun (Bio-Rad, UK) at 140 psi of helium pressure. Recordings were performed 2-4 days post-transfection.

For the co-immunoprecipitation and co-localisation experiments in Chapter 4, the p3xFlag-CMV-7-1 construct encoding the C-terminal globular tail of chick Myosin Va fused to a Flag tag, and the pEGFP-NKCC1 construct encoding full length NKCC1 fused to EGFP, were transfected into COS-7 cells using Lipofectamine 2000 (Invitrogen). The C-terminal globular tail of chick Myosin Va was a kind gift from Dr Britta Eickholt, MRC Centre for

Developmental Neurobiology, King's College London, London (van Diepen et al., 2009). Full length NKCC1 was a kind gift from Dr Yoshinori Marunaka, Department of Molecular Cell Physiology, Graduate School of Medical Science, Kyoto Prefectural University of Medicine, Kyoto (Nakajima et al., 2007).

2.10 Data analysis and statistics

Digital signal processing, data analysis and presentation were performed using custom-made programs in the MATLAB environment (MathWorks, Natick, MA). All electrophysiological signals were acquired using WinWCP software (Strathclyde Whole Cell Analysis software; V.3.9.7; University of Strathclyde). Signals were digitised and recorded at a sampling interval of 682 points per second. From WinWCP, the data were exported as '.txt' files and then imported into MATLAB using import function. All analysis and measurements of $E_{GABA\text{-}A}$, GABA-A R responses amplitude and seizure duration were performed using custom-made scripts written in MATLAB. Data presentation and plotting was performed using custom-made scripts in MATLAB. The graphs were the exported from MATLAB as '.eps' files and imported into Corel Draw software where figure assembly and presentation was further performed.

For statistical analysis, population data are presented as mean ± SEM. Statistical comparisons were performed using SPSS, In-stat and Prism software. The statistical test and p value are presented for each comparison in the results Chapter.

3 The role of seizure-induced adenosine release in modulating postsynaptic GABAergic signalling

One of the earliest and most ubiquitous responses to seizure activity is the production and release of the neuromodulator adenosine. Adenosine comes from the breakdown of ATP under conditions when metabolic demands are not matched by energy supply, such as happens during seizures and cerebral ischemia (Dale and Frenguelli, 2009). Indeed, in vitro and in vivo studies, both in animal models of epilepsy and in human epileptic patients, have reported increased concentrations of adenosine during seizures activity (Berman et al., 2000; During and Spencer, 1992; Etherington et al., 2009; Lopatar et al., 2011). Once released into the extracellular space, adenosine can modulate synaptic transmission by activating four types of G-protein coupled adenosine receptors (ARs): A_1R, $A_{2A}R$, $A_{2B}A$ and A_3 (Fredholm et al., 2005). In particular, activation of A_1Rs has been shown to inhibit network excitability, limit the extension of seizures and mediate seizure arrest (Etherington and Frenguelli, 2004; Fedele et al., 2006; Li et al., 2007). Therefore adenosine has been considered an endogenous, antiepileptic factor.

The coupling of A_1Rs to G_i/G_o-proteins underlies several mechanisms by which adenosine can modulate synaptic transmission (Dunwiddie and Masino, 2001). In the case of glutamatergic transmission, presynaptic activation of A_1Rs causes a reduction in release probability by inhibiting calcium (Ca^{2+}) influx through voltage-gated channels (Yawo and Chuhma, 1993; Wu and Saggau, 1994; Gundlfinger et al., 2007), or by interfering directly with the release process (Scanziani et al., 1992; Thompson et al., 1993). At the same time, adenosine has been shown to function postsynaptically where it activates a series of

downstream potassium (K^+) channels, including G-protein coupled inward rectifying K^+ channels (GIRKs), that can modulate the excitatory effects of postsynaptic glutamate receptors (Takigawa and Alzheimer, 2002).

Relatively less is known about how adenosine modulates GABAergic transmission. This could be particularly crucial in the context of seizures where, as described in Chapter 1, Cl^- accumulation can lead to positive shifts in $E_{GABA\text{-}A}$ that generate depolarising and excitatory responses to $GABA_AR$ activation. Under baseline conditions, exogenous adenosine does not affect the presynaptic release of GABA in hippocampal neurons (Thompson et al., 1992; Yoon and Rothman, 1991). Whether adenosine contributes to the modulation of $GABA_AR$ signalling in the acute setting of a seizure remains unexplored. For instance, adenosine is known to regulate the activity of several protein kinases (including protein kinase A and protein kinase C; Fredholm et al., 2001), which have been implicated in the regulation of Cl^- transporter proteins that set the driving force for $GABA_ARs$ (Fiumelli et al., 2005; Lee et al., 2007). Therefore in this Chapter I set out to investigate whether seizure-induced adenosine release modulates the response to postsynaptic $GABA_AR$ activation. My specific aims were:

1. To develop a seizure model that allows systematic pharmacological investigations.
2. To test the effect of adenosine release in modulating postsynaptic $GABA_AR$ signalling during seizures.
3. To investigate the mechanisms underlying adenosine's modulation of $GABA_AR$ signalling during seizures.

3.1 Developing a reliable seizure model that allows systematic pharmacological investigations

A commonly used model of seizure activity is the removal of extracellular Mg^{2+}, which predisposes hippocampal slices to periods of synchronised hyperexcitability (Anderson et al., 1986; Gutierrez et al., 1999; Mody et al., 1987; Avoli et al., 2002). In order to establish a robust model for studying GABAergic signalling, gramicidin-perforated patch clamp recordings were made from CA3 pyramidal neurons in organotypic hippocampal slices from rats. Switching the perfusion media form normal aCSF to 0 Mg^{2+} aCSF readily induced seizure activity in all slices tested. Once a seizure was started, the perfusion media was switched back to normal aCSF. This transient exposure to 0 Mg^{2+} allowed the induction of reproducible single seizure episodes and prevented repeated seizure activity that can occur with continuous exposure to 0 Mg^{2+} (Figure 3.1). Seizures were readily induced in all tested slices with a latency of 318.8 s ± 54.4 s, n = 6, from 0 Mg^{2+} application to seizure initiation of . Comparing two consecutive seizures within the same recordings confirmed that the seizures were highly reproducible (Figure 3.1A and B). There was no difference between the first and second seizure in terms of seizure length (1^{st} seizure mean was 246.6 ± 45.9 s, 2^{nd} seizure mean was 267.1 ± 46.7 s; n = 6, p = 0.44, paired t-test; Figure 3.1C) or the extent of membrane hyperpolarization post-seizure (1^{st} seizure showed a maximum hyperpolarization relative to baseline of -17.1 ± 2.5 mV, 2^{nd} seizure hyperpolarisation was -18.2 ± 1.9 mV; n = 6, p = 0.25, paired t-test; Figure 3.1D). These data show that using the repeated 0 Mg^{2+} exposure is a reliable model for triggering reproducible seizure activity. This allowed the use of pharmacological manipulations in a 'within-cell' design in which a control seizure is recorded first and then the effects of drugs are examined on a second seizure episode in the same slice.

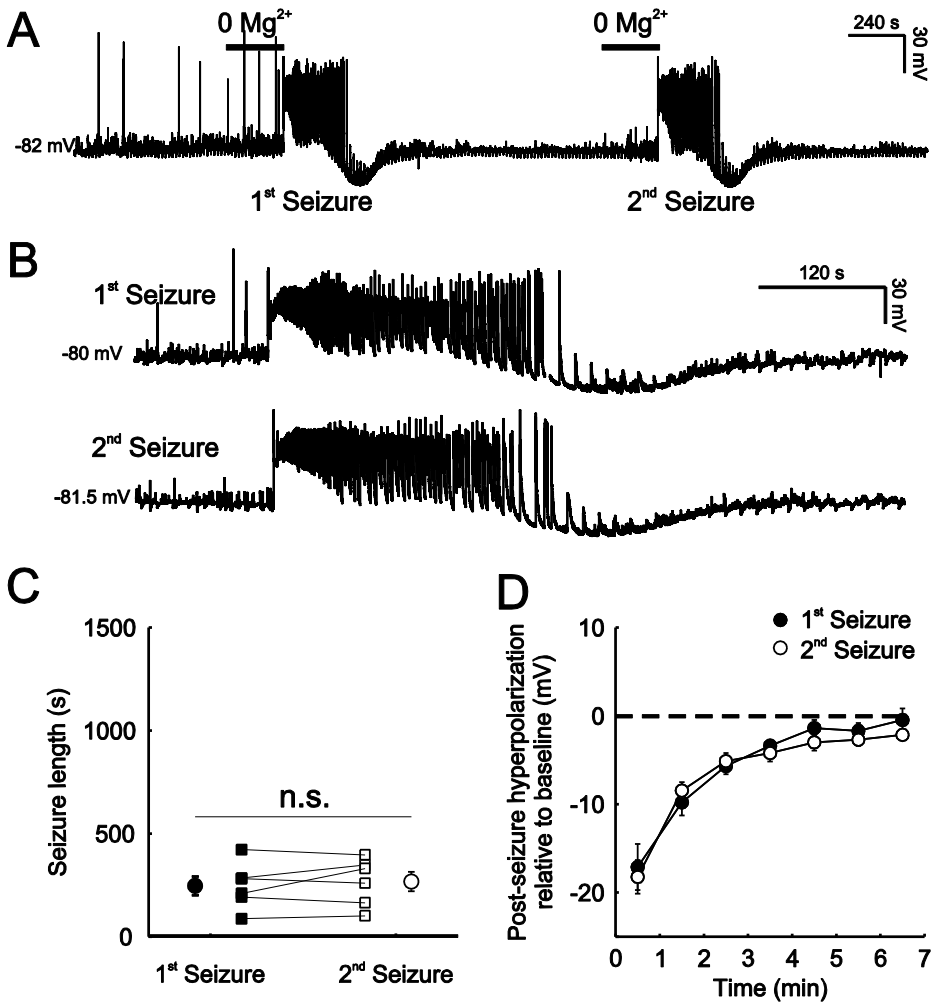


Figure 3.1 Removing Mg^{2+} from the perfusion media induces highly reproducible seizures in organotypic hippocampal brain slices.

A, Example recording in a CA3 pyramidal neuron in current clamp mode showing two seizures in the same slice. Recordings were performed using gramicidin-perforated patch clamp in current clamp mode, without DC current injection. ***B,*** Expanded version of the two seizures presented in 'A'. ***C, D,*** Population data from 6 cells showing no difference in seizure duration (***C***) or post seizure-hyperpolarisation (***D***) between the two consecutive seizures. Square symbols indicate individual experiments; circles indicate population means. Error bars - S.E.M., n.s. - $p > 0.05$, paired t-test.

In accordance with previous work, I could distinguish two phases of the seizure episodes: (1) the initial ictal-like phase (also referred to as the 'tonic' phase) and (2) the after-discharge phase (also referred to as the 'clonic' phase; Trevelyan et al., 2007a; Isomura et al., 2008; Higashima et al., 1996). The ictal phase was characterized by a >40 mV membrane potential depolarization upon which occurred high frequency, low amplitude discharges (Figure 3.2A). As the seizure progressed, the membrane potential slowly repolarized, reached pre-seizure resting membrane potential values and then entered the after-discharge phase. The after-discharge phase was composed of rhythmic bursts of activity that emerged from a relatively hyperpolarized membrane potential background. Beyond the after-discharge phase, the membrane potential remained at relatively hyperpolarized values for several min and slowly recovered to pre-seizure values (Figure 3.2A).

3.2 Endogenous adenosine release modulates seizure duration and the post-seizure recovery period

Having established a robust seizure model, I set out to investigate the contribution of AR signalling during seizures. To test whether endogenous adenosine is released at levels that modulate a seizure episode, I investigated the effect of 1 µM CGS 15943 - an antagonist of the four-known ARs. Blockade of ARs had a significant effect on the seizures (Figure 3.2). Firstly, it increased total seizure duration from 272.8 ± 43.8 s to 666.4 ± 121.8 s ($n = 10$, $p < 0.01$, paired t-test; Figure 3.2B). This effect was primarily due to an increase in the after-discharge period from 185.7 ± 43.8 s to 565.7 ± 129.7 s ($n = 10$, $p < 0.01$, paired t-test). Meanwhile the ictal phase was not significantly affected by AR antagonism, as it had a duration of 87.0 ± 19.6 s under control conditions and 100.6 ± 27.3 s following application of CGS 15943 ($n = 10$, $p = 0.61$, paired t-test). Secondly, blockade of ARs reduced the post-

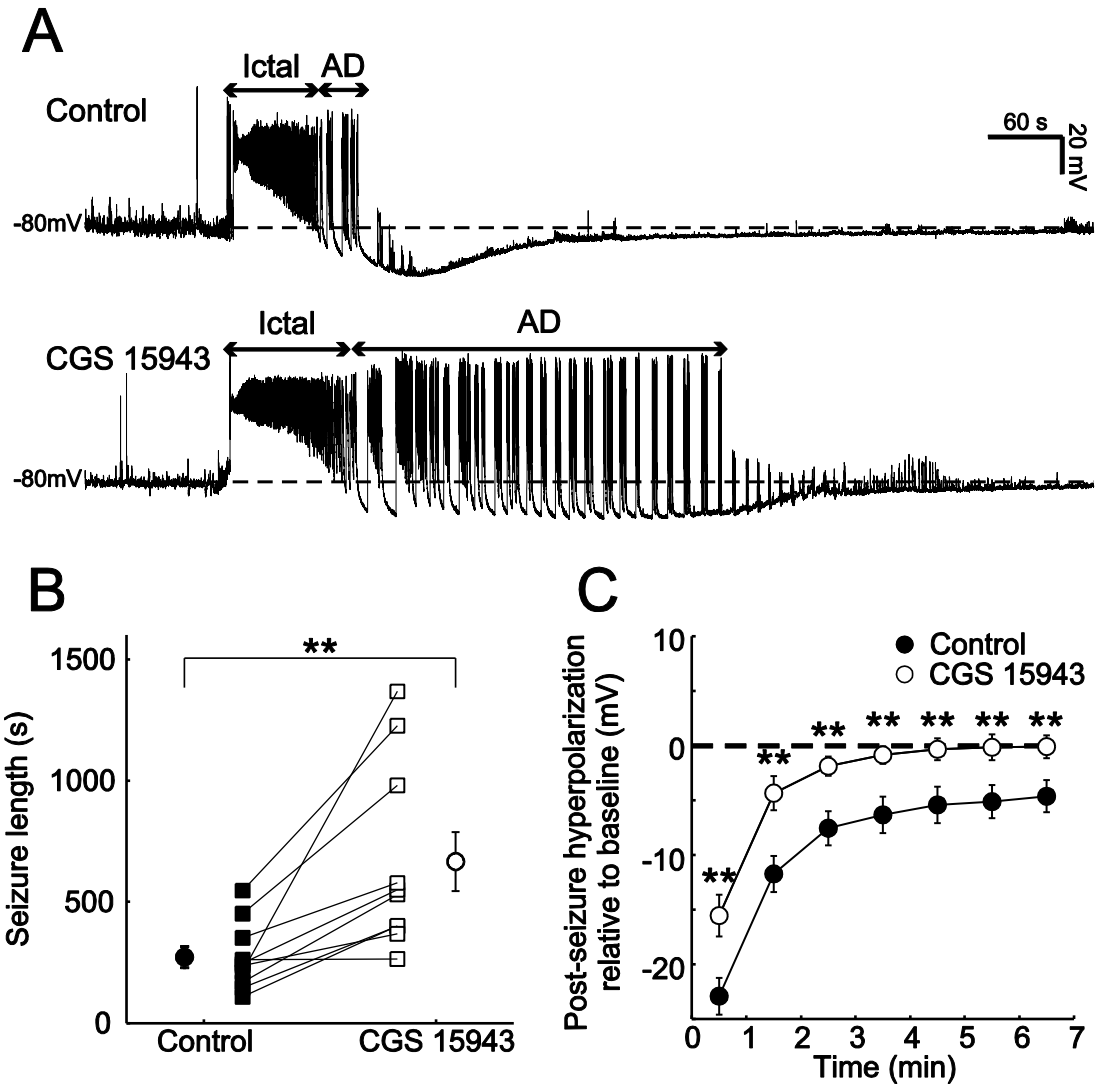


Figure 3.2 Endogenous adenosine modulates seizure activity and post-seizure recovery.

A, Example seizures recorded from a CA3 pyramidal neuron under control conditions (upper trace) and during blockade of ARs with 1 μM CGS 15943 (lower trace). Arrows indicate the ictal-like ('Ictal') and after-discharge ('AD') phases of the seizure. Horizontal dashed lines indicate pre-seizure resting membrane potential. Note that AR blockade results in an increase in total seizure duration and a faster recovery of the membrane potential to baseline levels following the end of the after-discharge phase. ***B,*** Population data (n = 10 cells) for seizure length under control conditions (black symbols) and in the presence of the AR antagonist (open symbols). Square symbols indicate individual experiments; circles indicate population means. ***C,*** Population data (n = 10 cells) for post-seizure membrane potential recovery under control conditions (black circles) and in the presence of the AR antagonist (open circles). Values indicate the degree of hyperpolarization compared to pre-seizure baseline, where zero min represents the point of maximum hyperpolarization following the end of the after-discharge phase. Error bars - S.E.M., ** - $p < 0.01$, paired t-test.

seizure membrane hyperpolarization. For instance, the maximum post-seizure hyperpolarization under control conditions was -22.9 ± 1.6 mV relative to baseline, and this was reduced to -15.5 ± 1.9 mV when ARs were blocked ($n = 10$, $p < 0.01$, paired t-test; Figure 3.2C). The adenosine-induced effects persisted for several min into the post-seizure period - a time course that matches with previous reports of AR antagonism on evoked field potentials (Etherington and Frenguelli, 2004; Etherington et al., 2009).

Before the start of seizure activity, AR antagonism had no effect on the neuron's membrane potential. Under control conditions, membrane potential was -74.8 ± 2.4 mV and remained unchanged in the presence of 1 μM CGS 15943 when membrane potential was -75.5 ± 2.3 mV, $n = 8$, $p = 0.45$, paired t-test. These results are consistent with a low level of adenosine under normal conditions in the absence of seizure activity. However, once a seizure episode had started, adenosine levels are likely to increase rapidly. Consistent with this idea, I found that over the course of the seizure the membrane potential became more depolarised under AR antagonism, than in control conditions, and this was first evident 25 s from the start of the seizure (absolute membrane potential -37.9 ± 1.0 mV vs -42.2 ± 1.6 mV, $n = 10$, $p < 0.05$, paired t test, membrane potential averaged over 5 s bins).

These results demonstrate that ARs are strongly activated during seizures and function to attenuate seizure activity. This is consistent with earlier evidence that adenosine acts mainly as a seizure-suppressing substance (Boison, 2006; Dunwiddie, 1999; During and Spencer, 1992).

3.3 Adenosine receptor activation attenuates $GABA_A$ receptor-mediated depolarization during epileptiform activity

Previous work has demonstrated that $GABA_A$Rs are strongly activated during periods of hyper-synchronous activity, such as ictal-like episodes (Fujiwara-Tsukamoto et al., 2006). Furthermore, it has been reported that intense activation of $GABA_A$Rs leads to a pronounced influx and accumulation of intracellular Cl^-, which generates a transient positive shift in E_{GABA-A} (Isomura et al., 2008; Wright et al., 2011). This rapid depolarising shift in E_{GABA-A} can create a situation where $GABA_A$R activation excites pyramidal cells and thus actually promotes their activity (Fujiwara-Tsukamoto et al., 2010; Kohling et al., 2000). Using gramicidin-perforated patch recordings I was able to record $GABA_A$R-mediated responses from CA3 pyramidal neuron, during seizure episodes, without disturbing $[Cl^-]_i$ dynamics. As shown in Figure 3.3, local somatic application of the selective $GABA_A$R agonist, muscimol (45 μM), hyperpolarized the membrane potential of CA3 pyramidal neurons in the period before the seizure. However, during the after-discharge phase of the seizure and immediately following the seizure, $GABA_A$R activation strongly depolarized the neurons (Figure 3.3B). Importantly, $GABA_A$R responses during the after-discharge phase were sufficient to trigger action potentials, meaning that GABAergic signalling had actually become excitatory and could contribute to the promotion of ongoing seizure activity. In the post-seizure period, the amplitude of the depolarising $GABA_A$R responses gradually decreased, $GABA_A$R responses were no longer able to trigger action potentials and eventually reversed polarity and reverted back to hyperpolarising (Figure 3.3B).

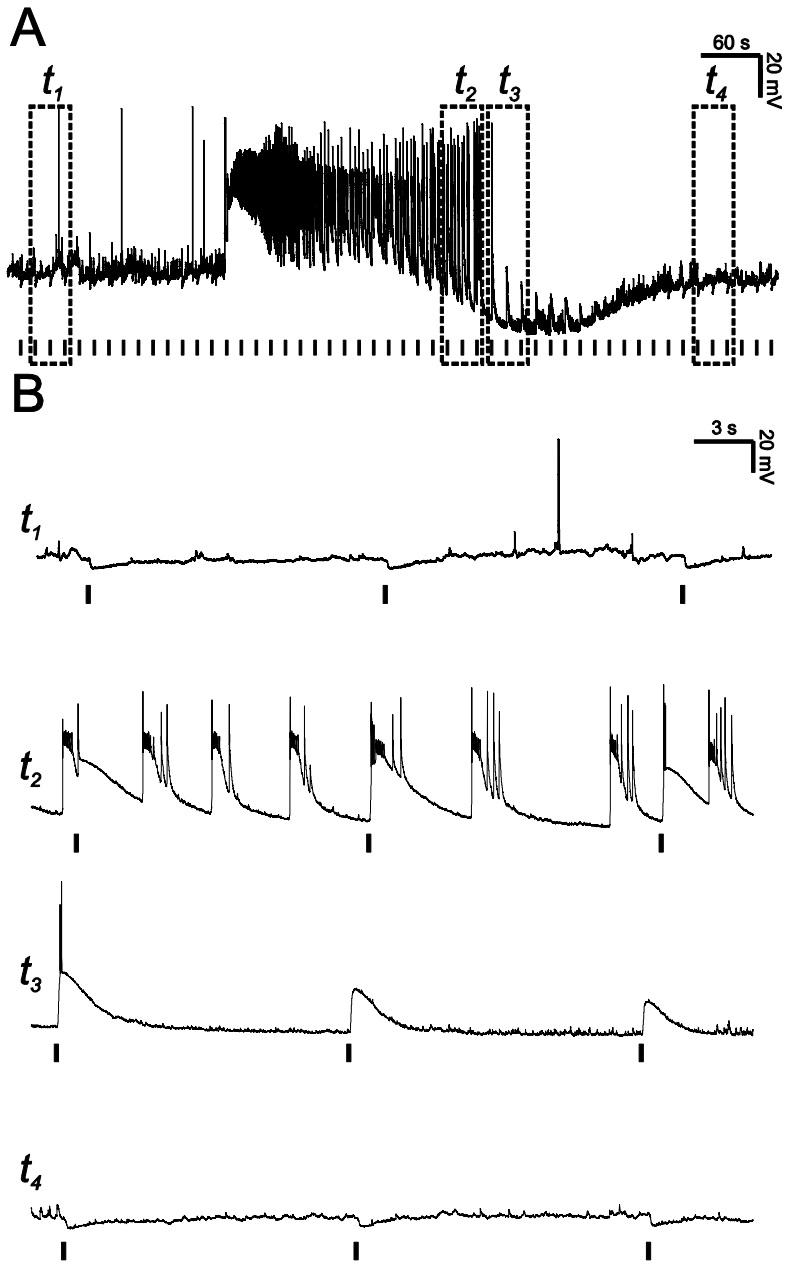


Figure 3.3 Seizure activity induces depolarising and excitatory $GABA_AR$ signalling.

A, Example seizure recorded from a CA3 pyramidal neuron. Postsynaptic $GABA_AR$ responses were elicited with a muscimol puff every 15 seconds (vertical bars) during the seizure episode. Dashed boxes indicate time windows before the seizure ('t_1'), during the after-discharge phase ('t_2'), immediately after the seizure ('t_3') and during the post-seizure recovery period ('t_4'). ***B,*** Expanded traces from the time windows represented by the boxes in 'A'. $GABA_AR$ responses before the onset of the seizure are hyperpolarising ('t_1'). During the after-discharge period $GABA_AR$ responses become depolarising and can trigger spikes ('t_2'). Immediately after the seizure, $GABA_AR$ responses are still depolarising but show decreased amplitude and are less likely to trigger spikes ('t_3'). During the post-seizure recovery period $GABA_AR$ responses return to being hyperpolarising ('t_4').

To test whether endogenous adenosine modulates these seizure-induced changes in $GABA_AR$ transmission, I used a within-cell design to measure $GABA_AR$-mediated potentials during control seizures and during seizures in which ARs were blocked with CGS 15943 (1 μM; Figure 3.4). The amplitude of depolarising $GABA_AR$ potentials was measured during the two minute period before the muscimol response reversed polarity (Figure 3.4A and B). AR blockade had a strong and consistent effect on depolarising $GABA_AR$ responses recorded during the seizure episode. Blockade of ARs increased the amplitude of depolarising $GABA_AR$ responses to 155.5 ± 20.9 % of control values ($n = 10$, $p < 0.05$, paired t-test; Figure 3.4C and D), indicating that seizure-induced adenosine release could attenuate depolarising GABAergic potentials during seizures. Consistent with this hypothesis, when I examined the number of after-discharge events per seizure, I found that AR blockade increased their mean number from 45.8 ± 9.22 under control conditions to 87.30 ± 11.31 ($n = 10$, paired t-test, $p < 0.05$). As depolarising $GABA_AR$ responses can contribute to prolongation of seizures and the generation of after-discharges (Fujiwara-Tsukamoto et al., 2003; Higashima et al., 1996; Higashima et al., 2000; Isomura et al., 2003a; Isomura et al., 2008; Velazquez and Carlen, 1999), the attenuation of depolarising $GABA_AR$ activity by adenosine may be an important aspect of adenosine's anti-convulsant action. I also examined the modulatory effect of AR activation after $GABA_AR$ responses had reverted to hyperpolarising. Hyperpolarising $GABA_AR$ responses were measured during a two minute period after the muscimol response reversed polarity (Figure 3.4A and B). Similar to the effects on depolarising $GABA_AR$ responses, antagonism of ARs increased the amplitude of the hyperpolarising $GABA_AR$ response amplitude to 150 ± 13.7 % of control values ($n = 10$, $p < 0.05$, paired t-test, Figure 3.4C and D). These results demonstrate that seizure-induced adenosine release attenuates not only the excitatory GABAergic potentials, but can also persist and modulate inhibitory $GABA_AR$-mediated signalling.

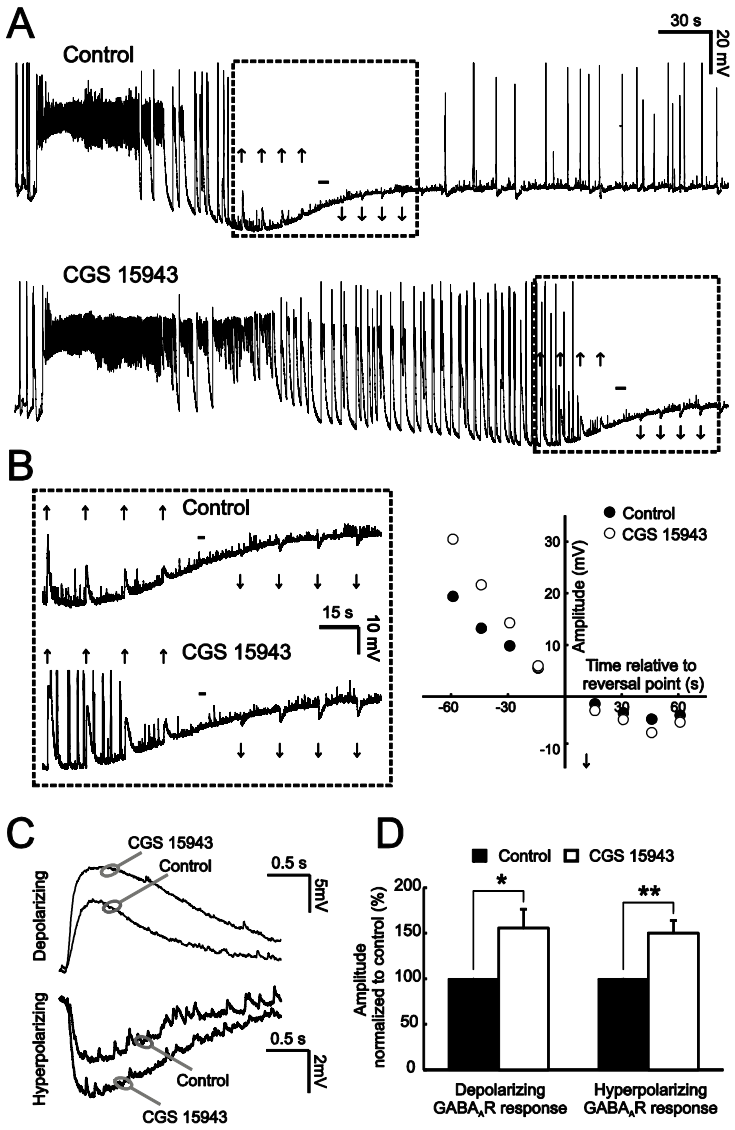


Figure 3.4 Adenosine receptor activity attenuates postsynaptic GABAergic potentials during seizures.

A, Example seizures recorded under control conditions (upper trace) and in the presence of the AR antagonist CGS 15943 (1 μM; lower trace). Upward arrows indicate depolarising postsynaptic $GABA_AR$ responses, downward arrows indicate hyperpolarising $GABA_AR$ responses and the hyphen indicates the reversal point, when there is no net response to a muscimol puff. Rectangles indicate a 2 minute time window, centered about the reversal for the $GABA_AR$ response. ***B,*** Traces (left) are expanded versions of the recording in 'A' and illustrate the amplitude and direction of $GABA_AR$ responses. The plot (right) shows the amplitude of $GABA_AR$ responses in this recording (y-axis), in relation to the time when the $GABA_AR$ response switched back from depolarising to hyperpolarising (at 0 s on the x-axis). ***C,*** Averaged traces for the cell shown in 'A' confirm that blocking ARs augments both the depolarising and hyperpolarising $GABA_AR$ responses. ***D,*** Population data (n = 10 cells) for the amplitude of depolarising and hyperpolarising postsynaptic $GABA_AR$ responses. Data are shown for the AR antagonist (open bars), normalized to control values (black bars). Error bars - S.E.M., * - $p < 0.05$, ** - $p < 0.01$, paired t-test.

3.4 Adenosine attenuates postsynaptic $GABA_AR$ signalling by increasing membrane conductance via activation of K^+ channels, downstream of the A_1R

The fact that AR activation during a seizure can attenuate both depolarising and hyperpolarising $GABA_AR$ responses could be explained via an adenosine-induced change in the postsynaptic cell's membrane conductance, which would generate a 'shunting' effect (Takigawa and Alzheimer, 2002).

First, to establish if AR activation is sufficient to generate the observed effects, I tested whether exogenously applied adenosine (100 µM) can attenuate the $GABA_AR$-mediated responses in seizure-free slices (see Materials and Methods; Figure 3.5). Bath application of adenosine induced a hyperpolarization of the membrane potential of CA3 pyramidal neurons from -76.5 ± 0.9 mV to -89.7 ± 0.9 mV ($n = 6$, $p < 0.001$, paired t-test), consistent with the downstream activation of K^+ channels (Fredholm et al., 2005; Clark et al., 2009). To maintain the same driving force for the $GABA_AR$, I compensated for the adenosine-induced hyperpolarization by current injection through the patch pipette. The baseline membrane potential was maintained at either -110 mV to compare depolarising $GABA_AR$ responses, or at -70 mV to compare hyperpolarising $GABA_AR$ responses (Figure 3.5A and C). Depolarising and hyperpolarising $GABA_AR$ responses were elicited by local application of muscimol under control conditions and in the presence of 100 µM adenosine. In the presence of adenosine, depolarising $GABA_AR$ responses were significantly smaller. The amplitude was reduced to 68.1 ± 4.7 % of control values ($n = 5$, $p < 0.01$, paired t-test), which was reversed following washout of the adenosine (97.7 ± 5.9 % of control, $p < 0.01$, paired t-test compared to adenosine; Figure 3.5B). Under conditions that generated

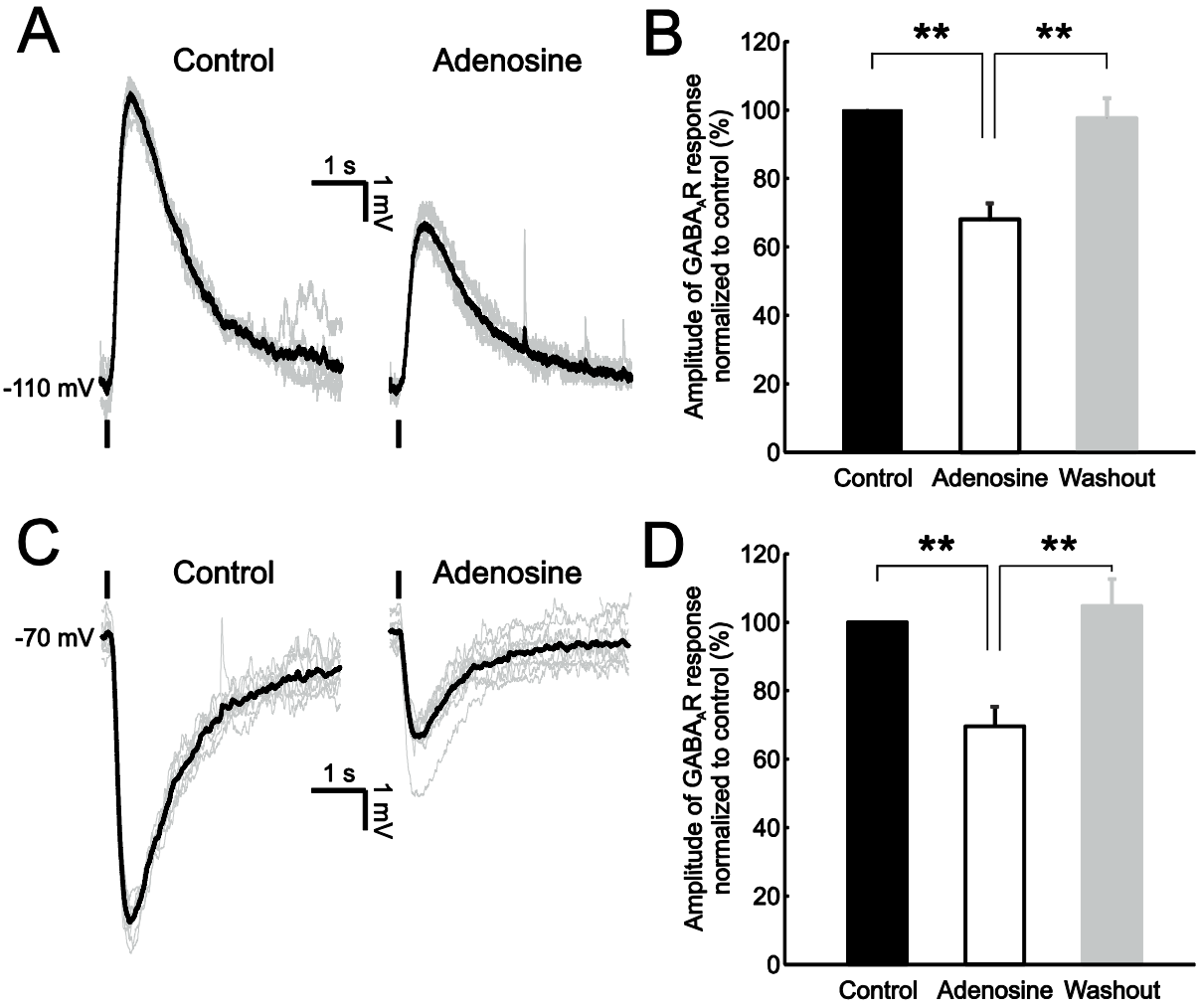


Figure 3.5 Exogenous adenosine application mimics the inhibitory effect on $GABA_AR$-mediated signalling.

A, Depolarising $GABA_AR$ responses recorded from a CA3 pyramidal neuron under control conditions (left) and in the presence of adenosine (right). Cells were maintained at a resting membrane potential of -110 mV by somatic DC current injection (see Materials and Methods). Individual (grey traces) and mean (black traces) $GABA_AR$ potentials are shown; vertical black bars represent the time of muscimol application. ***B,*** Population data (n = 5 cells) for the amplitude of depolarising postsynaptic $GABA_AR$ responses in the presence of adenosine (open bars) and after adenosine washout (grey bars), normalized to control values (black bars). Error bars - S.E.M., ** - $p < 0.01$, Paired t-test. ***C,*** Hyperpolarising $GABA_AR$ responses recorded from a CA3 pyramidal neuron under control conditions (left) and in the presence of adenosine (right); vertical black bars represent the time of muscimol application. Cells were maintained at a resting membrane potential of -70 mV by somatic DC current injection. ***D,*** Population data (n = 6 cells) for the amplitude of hyperpolarising postsynaptic $GABA_AR$ responses, using the same conventions as above. Error bars - S.E.M., ** - $p < 0.01$, paired t-test.

hyperpolarising $GABA_AR$ responses, a similar reduction in GABAergic signalling was observed. Adenosine caused a reduction in the amplitude of $GABA_AR$ responses to 69.5 ± 5.7 % of control values (n = 6, $p < 0.01$, paired t-test) and this effect was also reversed following washout of the adenosine (104.7 ± 7.8 % of control, $p < 0.01$, paired t-test compared to adenosine; Figure 3.5D). These results demonstrate that activation of ARs is sufficient to attenuate postsynaptic $GABA_AR$ signalling when it is either depolarising or hyperpolarising.

To test whether a shunting mechanism can account for the effect of adenosine upon $GABA_AR$ responses, I used voltage and current clamp recordings to measure the effect of adenosine on membrane conductance and the role of various downstream K^+ channels. Adenosine has been reported to activate several K^+ channels via A_1R signalling (Kawamura, Jr. et al., 2010; Hosseinzadeh and Stone, 1998; Fredholm et al., 2005; Clark et al., 2009) including: G-protein coupled inward rectifying K^+ channels (GIRKs; Clark et al., 2009; Fredholm et al., 2005), ATP-sensitive K^+ channels (KATPs; Hosseinzadeh and Stone, 1998; Kawamura, Jr. et al., 2010), and small conductance Ca^{2+}-activated K^+ channels (SKs; Clark et al., 2009). Membrane conductance was calculated from the membrane current generated by 1 s hyperpolarising voltage steps (-10 mV), delivered under voltage clamp conditions (Figure 3.6 A). As predicted, the application of adenosine resulted in a significant shift in the membrane conductance of CA3 pyramidal neurons from 4.5 ± 0.4 nS to 9.9 ± 1.0 nS. This represented an increase to 225.6 ± 14.9 % of control values (n = 23, $p < 0.001$, paired t-test; Figure 3.6B). Furthermore, the effect of adenosine on membrane conductance was substantially reduced by co-administration of the A_1R antagonist DPCPX (5 µM; 118.4 ± 8.3 % of control, n = 6, $p < 0.01$), by co-administration of the non-selective K^+ channel blocker Ba^{2+} (1.5mM; 113.1 ± 5.4 % of control, n = 6, $p < 0.01$), or by co-administration of a cocktail of K^+ channel blockers designed to block the major downstream targets of A_1Rs (GIRKs - 400nM tertiapin, KATPs - 1mM tolbutamide, and the SKs - 400nM apamine; 141.2 ± 8.7 %

of control, n = 10, $p < 0.01$; Figure 3.6B). Importantly, the same pharmacological manipulations abolished the effect of adenosine on $GABA_AR$ responses. The effects of $GABA_AR$ activation upon the membrane potential were measured in current clamp, with the baseline membrane potential maintained at -70 mV. As before, adenosine alone significantly reduced $GABA_AR$ response amplitude to antagonist, DPCPX (94.2 ± 3.1 % of control; n = 5, $p < 0.01$, ANOVA with post-hoc Bonferroni correction). The effect of adenosine upon $GABA_AR$ responses was also abolished 59.3 ± 3.2 % of control (n = 25, $p < 0.001$, paired t-test compared to control). However, this effect of adenosine was prevented by co-administration of the A_1R by co-administration of the non-selective K^+ channel blocker Ba^{2+} (88.2 ± 11.5 % of control; n = 6, $p < 0.01$, ANOVA with post-hoc Bonferroni correction), or by co-administration of the cocktail of K^+ channel blockers designed to block the major downstream targets of A_1Rs (84.9 ± 4.5 % of control; n = 5, $p < 0.05$, ANOVA with post-hoc Bonferroni correction; Figure 3.6C and D). There was no significant difference between the DPCPX, Ba^{2+} and the cocktail of K^+ channel blockers for membrane conductance or $GABA_AR$-mediated response amplitude ($p > 0.05$ in all cases, ANOVA with post-hoc Bonferroni correction). These results suggest that adenosine suppresses postsynaptic $GABA_AR$-mediated responses by increasing the cell's membrane conductance via activation of K^+ channels that are downstream of A_1R-signaling.

In order to better understand how the changes in membrane conductance and $GABA_AR$ response relate to extracellular adenosine concentration I tested the effects of 1 µM, 10 µM and 100 µM adenosine (Figure 3.6D and E). Exogenous application of 1 µM adenosine had no statistically significant effect on either the membrane conductance (106.4 ± 6.4 % of control, $p = 0.37$, n = 5, paired t-test) or on the amplitude of $GABA_AR$ potentials (96.7 ± 3.4 % of control, $p = 0.44$, n = 3, paired t-test).

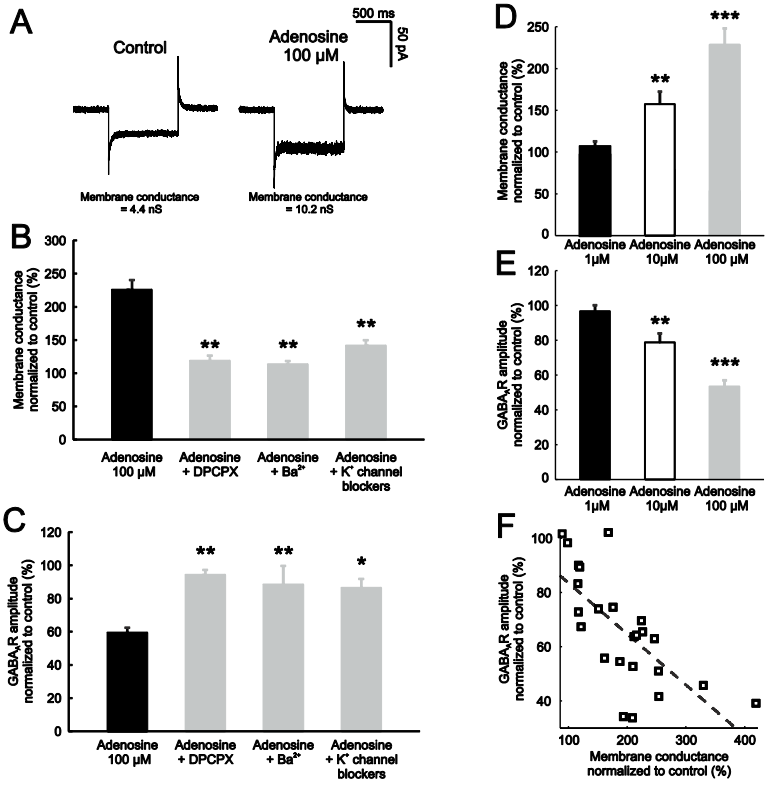


Figure 3.6 Adenosine attenuates postsynaptic $GABA_AR$ potentials via A_1R activation of K^+ channels that increase membrane conductance.

A, Example voltage-clamp recordings, showing the membrane current response to a -10 mV voltage step from a holding voltage of -70 mV, under control conditions and in the presence of adenosine; note the increase in membrane conductance during adenosine application. ***B,*** Adenosine (100 µM; black bar, n = 23) increased the membrane conductance to ~220 % of control values. Co-administration of adenosine with the selective A_1R antagonist DPCPX (5 µM; n = 6) prevented the adenosine-induced increase in membrane conductance. Similar results were obtained when adenosine was co-administered with either a non-specific blocker of K^+ channels (Ba^{2+} 1.5 mM; n = 6), or with a cocktail of K^+ channel blockers containing the K-ATP channel blocker (tolbutamide 1 mM), a G-protein coupled inward rectifying K^+ channel blocker (tertiapin 400nM) and a small conductance Ca^{2+}-activated K^+ channel blocker (apamine 400nM; n = 10). *C,* Population data for the amplitude of postsynaptic $GABA_AR$ responses for each of the groups in 'A'. When adenosine was delivered alone it reduced the amplitude of $GABA_AR$ responses by ~40%. This effect was blocked when adenosine was applied in the presence of DPCPX, Ba^{2+} or the K^+ channel blocker cocktail. All measurements were normalized to control values in the absence of any drugs. Statistical tests reflect comparisons with the adenosine-only group. Error bars - S.E.M., * - $p < 0.05$, ** - $p < 0.01$, ANOVA with post-hoc Bonferroni correction. ***D, E,*** The effect of 1, 10 and 100 µM adenosine on membrane conductance (***D***) and $GABA_AR$ response amplitude (***E***). Results from statistical tests indicate within-cell comparisons before and after adenosine administration. Error bars - S.E.M., ** - $p < 0.01$, *** - $p < 0.001$, paired t-test. ***F,*** The increase in membrane conductance showed a significant negative correlation with the $GABA_AR$ response amplitude (Pearson correlation, $r^2 = 0.49$, $p < 0.001$, n = 24). Dashed line indicates linear fit of the data.

In contrast, application of 10 µM adenosine increased the membrane conductance to 157.4 ± 15.0 % of control ($p < 0.01$, $n = 8$, paired t-test) and decreased the amplitude of $GABA_AR$ potentials to 78.7 ± 5.2 % of control ($p < 0.01$, $n = 7$, paired t-test). Finally, application of 100 µM adenosine increased the membrane conductance to 228.4 ± 19.7 % of control ($p < 0.001$, $n = 14$, paired t-test, Figure 3.6D) and decreased the $GABA_AR$ response amplitude to 53.4 ± 3.5 % of control ($p < 0.001$, $n = 14$, paired t-test, Figure 3.6E). The importance of extracellular adenosine concentration was also evident from the correlation between the adenosine-induced increase in membrane conductance and the decrease in $GABA_AR$ response amplitude (Pearson correlation, $r^2 = 0.49$, $p < 0.001$, $n = 24$; Figure 3.6F).

3.5 $GABA_AR$ reversal potential and conductance are not altered by AR activation

Other mechanisms that could contribute to the adenosine-induced effect upon postsynaptic $GABA_AR$-mediated responses include alterations in Cl^- homeostasis mechanisms (Dzhala et al., 2005; Dzhala et al., 2010; Huberfeld et al., 2007; Jin et al., 2005; Kaila et al., 1997) and/or changes in the conductance of the $GABA_AR$ (Roseti et al., 2008; Roseti et al., 2009). To investigate whether AR activation affects Cl^- homeostasis I measured E_{GABA-A} under control conditions and following bath application of adenosine. Muscimol-evoked $GABA_AR$ currents were recorded at six different holding voltages (from -50 mV to -100 mV) and E_{GABA-A} was calculated from the resulting I-V plots (see Materials and Methods; Figure 3.7A). Under control conditions the mean E_{GABA-A} was -82.7 ± 1.2 mV and this remained unchanged following activation of ARs, when the mean E_{GABA-A} was -82.2 ± 1.0 mV ($n = 17$, $p = 0.48$, paired t-test; Figure 3.7B). These results suggest that adenosine signalling does not directly modulate the Cl^--regulating mechanisms that set E_{GABA-A}.

In order to further explore a potential role for adenosine in modulating Cl^- homeostasis mechanisms during seizure activity, I analysed the seizure data from Figure 3.4 to assess the rate at which $GABA_AR$ responses recovered from depolarising back to hyperpolarising during the post-seizure period. In agreement with previous studies that have studied chloride homeostasis, I found that the recovery of depolarising $GABA_AR$ responses could be estimated using an exponential fit (Brumback and Staley, 2008b; Nardou et al., 2011). Under control conditions I found that the recovery rate had a time constant of 34.7 ± 2.8 s and that this was not affected by AR blockade with CGS 15943, when the mean time constant was 31.6 ± 3.0 ($p = 0.22$, $n = 8$, paired t-test). Taken together, these results show that changes in Cl^- homeostasis mechanisms are unlikely to contribute to the attenuation of the $GABA_AR$-mediated potentials.

Reducing either the postsynaptic density of $GABA_AR$ receptors and/or their permeability would result in a decreased $GABA_AR$ conductance, which could also potentially contribute to the adenosine-induced attenuation of $GABA_AR$-mediated responses. To test this possibility I used voltage clamp recordings and measured the $GABA_AR$ conductance across a range of membrane potentials (see Materials and Methods). I-V plots of the $GABA_AR$-mediated currents were constructed and conductance was calculated as the slope of linear fits of the data (Figure 3.8A). Under control conditions the peak $GABA_AR$ conductance was 14.- ± 1.8 nS on average and remained unchanged following 10 min activation of ARs when the mean was 14.9 ± 1.8 nS ($n = 9$, $p = 0.23$, paired t-test; Figure 3.8B). These results show that changes in the $GABA_AR$ conductance are unlikely to contribute to the adenosine-induced attenuation of the $GABA_AR$-mediated potentials.

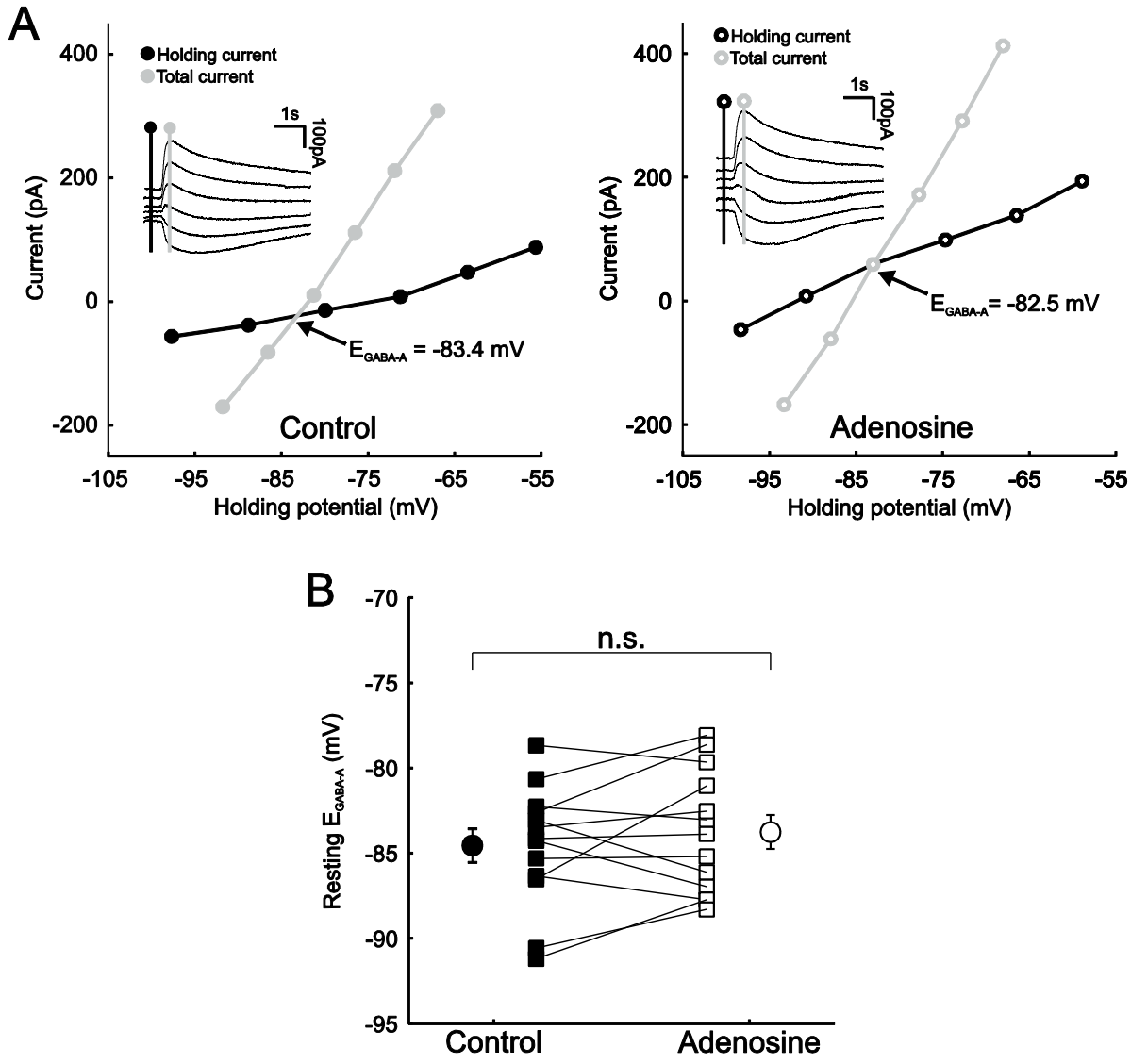


Figure 3.7 Adenosine receptor activation does not alter Cl^- homeostasis.

A, Data from a representative CA3 pyramidal neuron in which resting E_{GABA-A} was measured under control conditions (left) and in the presence of 100 µM adenosine (right). Inserts show example $GABA_AR$ currents evoked by muscimol puffs at different holding potentials. Holding current (reflecting membrane current) and total current (reflecting membrane current plus the muscimol-evoked current) were measured at the points indicated by the vertical black and grey lines, respectively. I-V plots were constructed and E_{GABA-A} was calculated as the potential at which the total current was equal to the holding current. ***B,*** Resting E_{GABA-A} values for individual cells (n = 17) under control conditions (black squares) and in the presence of adenosine (open squares). Population averages are also shown (black circles, control; open circles, adenosine). Error bars - S.E.M., n.s. - non-significant, paired t-test.

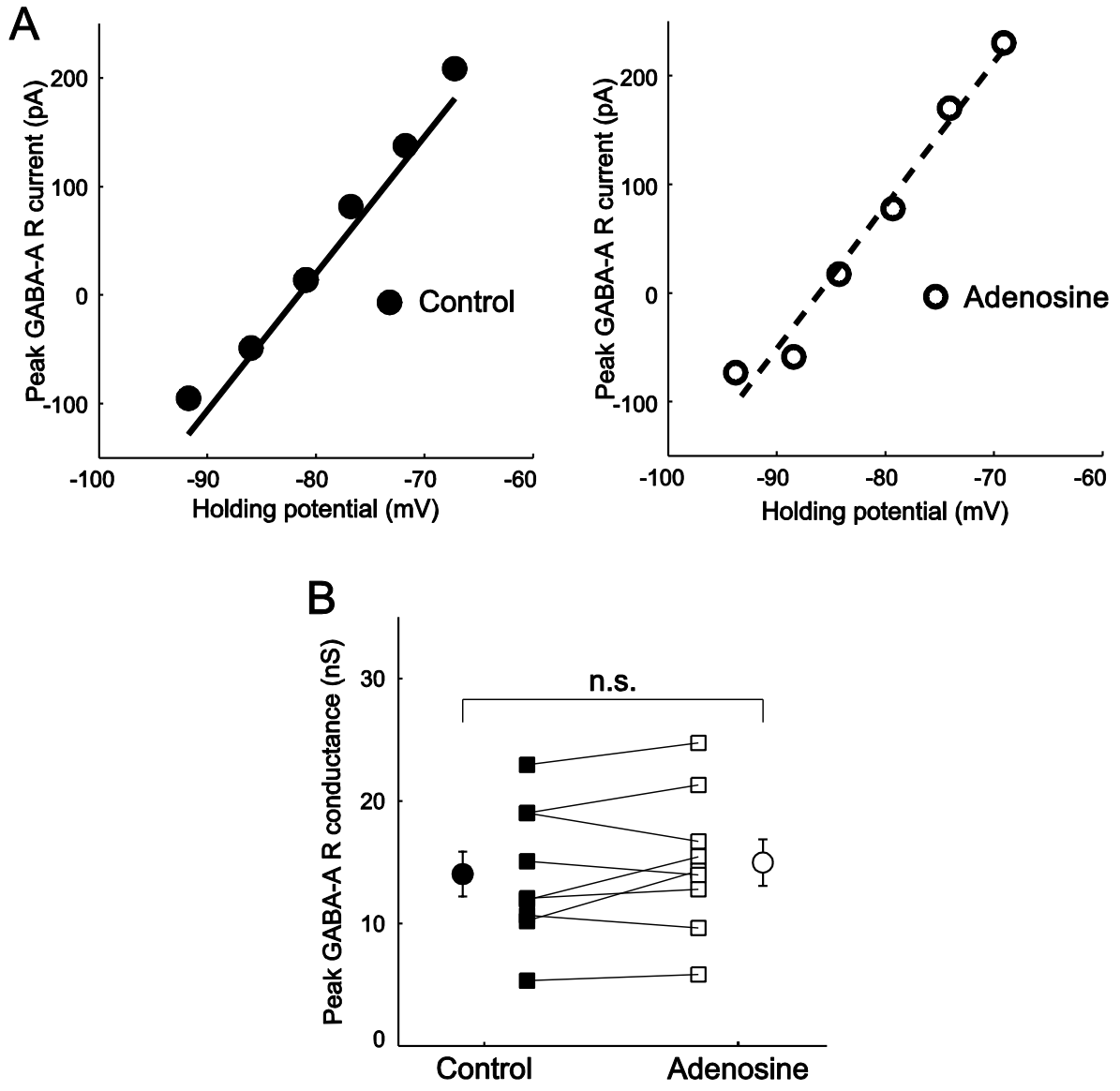


Figure 3.8 Adenosine receptor activation has no effect on $GABA_AR$ conductance.

A, Data from a representative CA3 pyramidal neuron in which the $GABA_AR$ conductance was measured under control conditions (left) and in the presence of 100 μM adenosine (right). The peak $GABA_AR$ current was calculated as described in the text and the peak $GABA_AR$ conductance was calculated as the slope of the linear fit. ***B,*** Peak $GABA_AR$ conductance for individual cells (n = 9) under control conditions (black squares) and in the presence of adenosine (open squares). Population averages are also shown (black circles, control; open circles, adenosine). Error bars - S.E.M., n.s. - non-significant, paired t-test.

3.6 Discussion

In this Chapter I investigated the role of the endogenous anti-convulsant neuromodulator, adenosine in regulating GABAergic signalling during epileptiform activity. Intense activation of the GABAergic system during seizure activity leads to a transient switch in the action of $GABA_AR$'s from inhibitory to excitatory. Seizure activity also raises the levels of extracellular adenosine. I found that the resulting AR activation reduced the amplitude of excitatory GABAergic potentials during seizures and that the suppression of GABAergic potentials lasted beyond the period in which the E_{GABA-A} was shifted positively. These effects of endogenously released adenosine were mimicked by exogenous adenosine administration. In examining the mechanism of adenosine's effects, I established that adenosine does not change chloride homeostasis mechanisms that set $E_{GABA-A,}$ or the conductance of $GABA_ARs$. Rather, A_1R-dependent activation of K^+ channels can account for the suppression of depolarising and hyperpolarising GABAergic potentials via an increase in postsynaptic membrane conductance and a resulting shunting effect. As depolarising $GABA_AR$-mediated signalling has been implicated in seizure initiation and progression, the adenosine-induced attenuation of depolarising $GABA_AR$ potentials may represent an important mechanism by which adenosine can limit seizure activity.

Studies using microdialysis probes implanted in the hippocampus of epileptic patients have estimated that seizures lasting 40-200 s trigger substantial (up to 65 µM) increases in extracellular adenosine levels (During and Spencer, 1992). This adenosine surge correlates with seizure arrest and adenosine levels remain elevated during the post-seizure period. In rat hippocampal slices, short seizures are sufficient to elevate mean extracellular levels of adenosine to up to ~5 µM and blocking A_1Rs increases seizure duration and intensity (Etherington et al., 2009; Lopatar et al., 2011). Seizures in my study had a mean duration of

~250 s, which would be predicted to trigger adenosine release. Consistent with this prediction, blockade of the four known ARs doubled seizure duration. These results confirm that adenosine has a net antiepileptic effect and they are consistent with in vivo studies in which focal augmentation of adenosine in the hippocampus of epileptic rats can reduce seizure frequency and duration, and even prevent epileptogenesis (Guttinger et al., 2005b; Guttinger et al., 2005a; Li et al., 2009; Boison, 2009; Li et al., 2007; Szybala et al., 2009).

Adenosine had its principal effects during the after-discharge phase of the seizures. Synchronized after-discharge activity is characteristic of epileptiform activity and it has been shown that a transient change in E_{GABA-A} is central to this process (Fujiwara-Tsukamoto et al., 2003; Fujiwara-Tsukamoto et al., 2006; Isomura et al., 2003b). During the ictal phase of seizures, intense activation of $GABA_A$Rs in combination with membrane depolarization results in a substantial Cl^- influx into principal neurons, which overwhelms Cl^- homeostasis mechanisms. The resulting positive shift in E_{Cl} (and therefore E_{GABA-A}) sets the conditions for networks of GABAergic interneurons to generate the synchronized excitation that underlies an after-discharge (Zsiros et al., 2007; Isomura et al., 2003b). Consistent with this scenario, my gramicidin recordings showed that activation of $GABA_A$Rs during the after-discharge period is able to generate depolarising excitatory responses and trigger action potentials. Using pharmacological manipulations I showed that blocking ARs during seizures increased the excitatory actions of GABAergic signalling. Consistent with the role of excitatory GABAergic signalling in triggering after-discharges, I found that when ARs were active under control conditions, seizures had less after-discharge events and a shorter after-discharge period.

The acute effect of adenosine upon $GABA_A$R-mediated signalling could involve changes to Cl^- homeostasis mechanisms or changes to the expression and/or properties of $GABA_A$Rs. Indeed, previous studies have reported seizure-induced alterations in E_{GABA-A} that

are mediated by changes in the activity of Cl^- transporter proteins, including NKCC1 and KCC2 (Dzhala et al., 2010; Jin et al., 2005; Khirug et al., 2010; Rivera et al., 2004). However, I found that adenosine had no direct effect on steady-state E_{GABA-A} or the rate of recovery of depolarising $GABA_AR$ responses back to hyperpolarising. AR activation also did not alter the conductance of the $GABA_AR$, indicating that adenosine release over the timescale relevant to a seizure does not have an acute effect upon the properties of the $GABA_AR$. These observations are consistent with previous recordings following short-term activation of ARs (Kruglikov and Rudy, 2008; Thompson et al., 1992; Yoon and Rothman, 1991) and with the conclusion that adenosine's effects upon $GABA_AR$ responses during seizure activity must be via an alternative mechanism.

The parsimonious explanation for adenosine's effects upon $GABA_AR$ responses is that they are mediated by a postsynaptic shunting effect that develops under conditions where GABAergic transmission transiently changes from inhibitory to excitatory. In support of such a shunting mechanism, as E_{GABA-A} and the postsynaptic membrane potential shifted throughout the seizure period, AR activation consistently reduced the amplitude of $GABA_AR$-mediated potentials. In addition, AR antagonism reduced the post-seizure membrane potential hyperpolarisation, which could reduce the driving force for depolarising GABA-A R responses by moving the membrane potential closer to E_{GABA-A}, while increasing the driving force for the hyperpolarising responses by moving the membrane potential further away from $E_{GABA-A.}$ This suggests that if the effect of adenosine on GABA-A R driving force had been accounted for, the shunting effect of adenosine might actually be larger for the depolarising GABA-A R responses than for the hyperpolarising responses during the post-seizure period. This idea is consistent with a larger adenosine-induced increase in membrane conductance during the seizure activity itself and early in the post-seizure period, when GABA-A R responses are still depolarising.

I found that adenosine reduced $GABA_AR$ responses via an A_1R-dependent activation of K^+ channels that hyperpolarize the membrane potential and increase membrane conductance. Adenosine has been reported to activate 3 types of K^+ channels that are downstream of A_1R signaling: GIRKs, KATPs and SK channels, all of which would be expected to increase membrane conductance (Clark et al., 2009; Fredholm et al., 2005; Hosseinzadeh and Stone, 1998; Kawamura, Jr. et al., 2010). The relative contribution of each of these channels to modulating membrane conductance and $GABA_AR$ responses is not currently known, but is likely to depend on both their relative number and location along the somatodendritic axis.

GIRK channel activation has also been implicated in the effective shunting of postsynaptic glutamatergic responses in hippocampal pyramidal neurons (Takigawa and Alzheimer, 2002) and the size of the GIRK channel response in the postsynaptic cell is likely to be important in setting the scale of the shunting effects. In the context of seizure activity, it is likely that glutamatergic inputs will also be shunted by the adenosine-induced activation of K^+ channels. This could contribute to the inhibitory actions of adenosine by reducing the activity of excitatory neurons and interneurons that receive excitatory inputs. In addition, K^+ channel activation hyperpolarises the membrane potential, moving it away from action potential threshold and thereby further reducing excitability. On the other hand, hyperpolarisation may reduce the inactivation of voltage-gated Na^+ and Ca^{2+} channels, which may have pro-excitatory effects, allowing incoming inputs to activate these channels. Nevertheless, the net overall effect of adenosine at a network level in the context of seizure activity is inhibitory, and this is clearly evident from the fact that AR blockade dramatically increased seizure duration and the number of after-discharges.

Using different adenosine concentrations I was able to show a direct relationship between adenosine concentration and response, such that higher levels of adenosine resulted

in both a higher membrane conductance and greater attenuation of $GABA_AR$ responses. These results are consistent with the idea that the level of adenosine released during the course of a seizure has to reach a certain threshold before activation of ARs becomes effective in suppressing $GABA_AR$ potentials. Previous studies using direct measurement of adenosine release had reported that adenosine levels are directly related to seizure intensity and duration (During and Spencer, 1992; Etherington et al., 2009; Lopatar et al., 2011). In my study $GABA_ARs$ were attenuated when adenosine was applied at concentrations between 10-100 μM, which are within the range of adenosine levels reported by previous studies during seizures and other pathological conditions such as ischemia (Pearson et al., 2006; During and Spencer, 1992). Previous studies have also suggested that elevated adenosine levels persist well into the post-seizure period, until the adenosine has been cleared from the extracellular space (During and Spencer, 1992; Etherington et al., 2009; Lopatar et al., 2011). Consistent with this, I found that adenosine signalling in the post-seizure period continued to attenuate $GABA_AR$ signalling once it had returned to hyperpolarising. The exact mechanisms of adenosine release and accumulation in the extracellular space are still a subject for debate. Both direct adenosine release by neurons and exocytosis of ATP form glial cells can contribute to activity-dependent increases in extracellular adenosine levels in the hippocampus (Zhang et al., 2003; Wall and Dale, 2013). However, in the context of seizure activity it has been suggested that direct adenosine release may be the primary source for increased adenosine levels (Lovatt et al., 2012).

In summary, this Chapter shows that as GABAergic signalling switches from inhibitory to excitatory during the course of a seizure, activation of ARs acts to attenuate the depolarising postsynaptic $GABA_AR$ responses, thereby reducing their excitatory contribution to ongoing seizure activity. This may be a novel mechanism by which adenosine exerts antiepileptic effects and limits seizure activity.

4 Investigating the molecular regulation of the Cl^- transporter NKCC1 and its role in neonatal seizures

In the previous Chapter I investigated the role of seizure-induced adenosine release in modulating the postsynaptic response to $GABA_AR$ activation. My results showed that during seizure activity, $GABA_AR$ signalling switches from hyperpolarising to depolarising, and under these conditions activation of $GABA_ARs$ has excitatory effects that promote ongoing seizure activity. At the same time, seizures trigger the release of adenosine, which acts to reduce the impact of depolarising $GABA_AR$ responses by increasing the cell's membrane conductance and thus creating a shunting effect. This effect could underlie some of the important antiepileptic properties of adenosine (Boison and Stewart, 2009; Fedele et al., 2006).

Nevertheless, adenosine did not directly modulate Cl^- accumulation, which represents the initial process that leads to the excitatory shift in GABAergic signalling during seizures. To better understand how Cl^- is regulated during the course of a seizure, in the remainder of my thesis I investigated mechanisms that are directly involved in Cl^- regulation. Specifically, I focused upon the regulation of Cl^- transporter proteins. As described in Chapter 1, the altered functioning of these transporter proteins has been related to abnormal Cl^- homeostasis and GABAergic transmission in epilepsy. For instance, the activity of the Cl^--intruding transporter NKCC1 has been linked to progressive Cl^- accumulation during repeated seizures (Dzhala et al., 2010). Moreover, the expression of NKCC1 has been found to increase in the epileptogenic period that follows a brain insult such as status epilepticus (Bragin et al., 2009). These studies suggest that NKCC1 regulation could play a central role in Cl^- homeostasis alterations in epilepsy. Understanding the mechanisms that regulate NKCC1 might therefore

offer new insights into the pathophysiology of seizures. In this Chapter my specific aims were:

1. To explore the expression and surface delivery of NKCC1 and how this relates to Cl^- regulation under normal conditions.
2. To investigate the molecular mechanisms responsible for NKCC1 regulation by exploring a potential interaction between NKCC1 and a motor protein, Myosin Va, which can transport protein cargos to the surface of cells.
3. To develop an electrophysiological protocol for assessing NKCC1 contribution to Cl^- homeostasis and to test the effects of disrupting Myosin Va activity.
4. To develop a neonatal model for inducing prolonged seizure activity (equivalent to status epilepticus) and to use this model to explore the contribution of NKCC1 and the potential association with Myosin Va in regulating Cl^- homeostasis in the post seizure-period.

4.1 The developmental regulation of NKCC1 and KCC2 and their relation to Cl^- homeostasis

As outlined in Chapter 1, the expression of NKCC1 and KCC2 transporters has been reported to be regulated in a developmental manner. The expression of the Cl^--extruding transporter, KCC2, has been found to increase significantly during the first two postnatal weeks from low levels at birth to high levels of expression that persist into the adult life (Rivera et al., 1999). On the other hand, the expression of NKCC1 has been suggested to decrease in the postnatal period (Yamada et al., 2004; Dzhala et al., 2005). However, this view has been challenged by other studies, which have found that NKCC1 mRNA actually increases during the first two postnatal weeks and that NKCC1 expression can persist into adult life (Clayton et al., 1998a;

Wang et al., 2002). Changes in the expression of NKCC1 and KCC2 have been suggested to underlie the observed shift in E_{GABA-A} from depolarising to hyperpolarising, which occurs during the first two postnatal weeks in rat hippocampus (Tyzio et al., 2008).

To further investigate these aspects in hippocampal organotypic slices, I explored the developmental changes in E_{GABA-A} in relation to developmental changes in NKCC1 and KCC2 expression. Two developmental stages were assessed: 1) neonatal (equivalent to P3-4), and 2) mature (equivalent to P13-14; see Materials and Methods). I used gramicidin-perforated patch clamp recordings and a voltage-step protocol (see Materials and Methods) to measure resting E_{GABA-A} in CA3 pyramidal neurons from neonatal and mature slices. Typical examples of responses to $GABA_AR$ activation and E_{GABA-A} measurements are shown in Figure 4.1A. E_{GABA-A} was significantly more depolarised in the neonatal slices compared to the mature stage. At P3-4 the mean E_{GABA-A} was -66.8 ± 2.0 mV, whereas by P13-14 it had shifted negatively to -84.5 ± 0.9 mV ($p < 0.001$, unpaired t-test). These results are consistent with previous work in acute hippocampal slices (Tyzio et al., 2007) and suggest that between P3-4 and P13-14 there is a change in the mechanisms responsible for Cl^- homeostasis, such that the relative rate of Cl^- extrusion versus Cl^- influx is increased.

To explore the role of NKCC1 and KCC2 in regulating Cl^- levels over this period of development, I examined the expression and surface delivery of these proteins in collaboration with Dr. Sarah Newey (Figure 4.1C, D and E). As with other transporters, in order to be functional, NKCC1 and KCC2 must be delivered to the surface of the cell. Therefore, to assess both the total expression and the surface delivery of NKCC1 and KCC2, biotinylation experiments were performed. These made it possible to quantify the amount of surface protein as a proportion of the total protein expressed by cells (see Materials and Methods). Total NKCC1 protein levels were found to increase by approximately two-fold between P3-4 and P13-14 ($p < 0.01$, $n = 8$, unpaired t-test; Figure 4.1D). Interestingly

however, the surface/total NKCC1 protein ratio decreased by approximately 50% ($p < 0.01$, $n = 8$, unpaired t-test; Figure 4.1D). Over the same period, total KCC2 protein levels increased by approximately six-fold between P3-4 and P13-14 ($p < 0.05$, $n = 6$, unpaired t-test), while the KCC2 surface/total protein ratio remained unchanged ($p = 0.84$, $n = 6$, unpaired t-test; Figure 4.1E).

With regards to KCC2, these results are consistent with previous studies that have shown increased expression of KCC2 (Rivera et al., 1999; Wang et al., 2002) and indicate that the proportion of KCC2 that is delivered to the membrane is relatively stable. Such an increase in total KCC2 expression would predict an increase in Cl^- extrusion capacity with development, consistent with the observed negative shift in E_{GABA-A} between P3-4 and P13-14. With regards to NKCC1, even though this transporter's expression was increased, the proportion at the cell surface was significantly reduced over development. This suggests that in addition to transcriptional control, the regulation of NKCC1 involves protein trafficking mechanisms that ultimately control the amount of NKCC1 in the plasma membrane. Such mechanisms might represent a novel way to regulate the contribution of NKCC1 to Cl^- homeostasis. Therefore, I decided to explore potential molecular mechanisms that could control the intracellular trafficking of NKCC1.

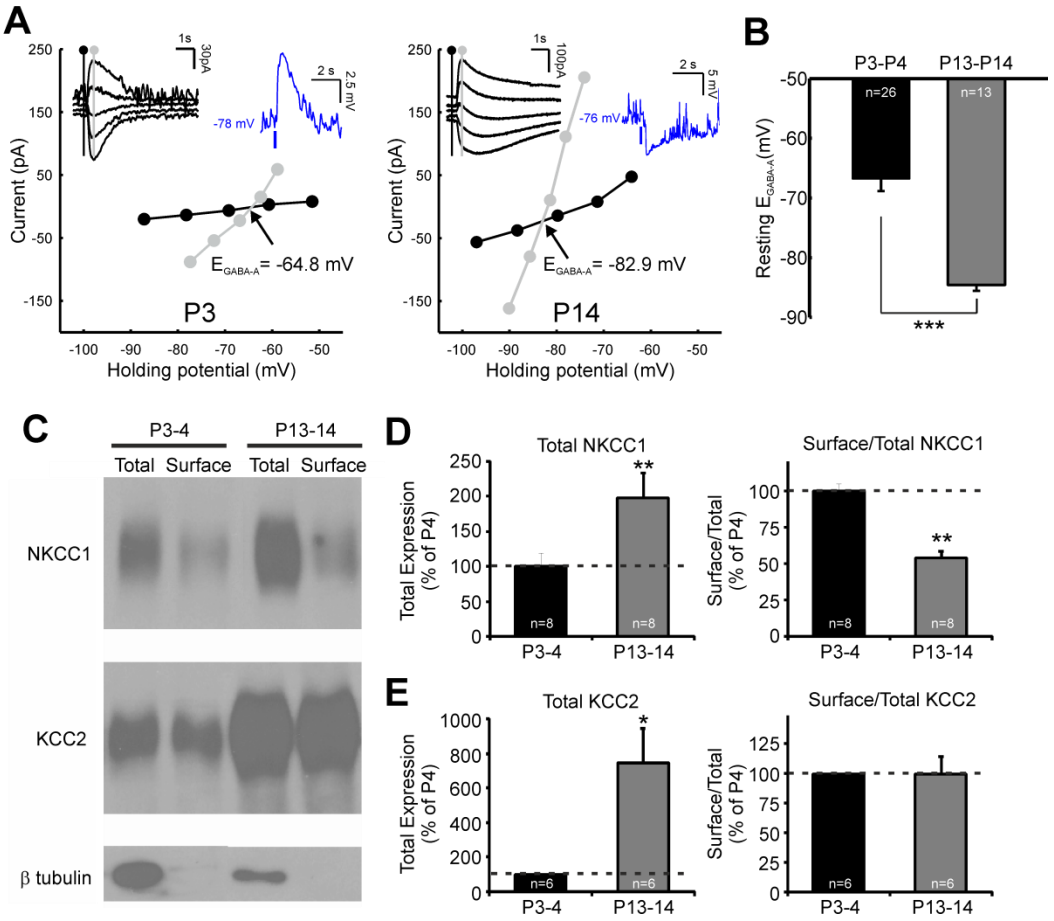


Figure 4.1 Developmental regulation of E_{GABA-A} and NKCC1 and KCC2 transporter expression in the rat hippocampus.

A, Example E_{GABA-A} measurements from gramicidin-perforated patch recordings in CA3 pyramidal neurons from rat organotypical hippocampal slices at P3 (left) and at P14 (right). Small black inserts represent $GABA_AR$ currents evoked by GABA puffs at different holding voltages (-50 to -90 mV). Holding currents (reflecting membrane current) and peak currents (reflecting membrane current plus $GABA_AR$ current) were measured at the points indicated by the vertical black and grey lines, respectively. I-V plots of the holding and peak currents were constructed and E_{GABA-A} was calculated as the voltage at which the peak current was equal to the holding current. Arrows indicate E_{GABA-A} values. Small blue inserts represent the response to $GABA_AR$ activation in current clamp recordings. ***B,*** Resting E_{GABA-A} was significantly more depolarised in cells from neonatal slices (P3-4) than in mature slices (P13-P14). ***C,*** Representative Western blots from biotinylation experiments showing 'total' and 'surface' (captured biotinylated) NKCC1, KCC2 and β-tubulin at P3-4 and P13-14, in rat organotypic hippocampal slices. ***D,*** Quantification of NKCC1 expression in terms of total protein levels (left) and the proportion of protein that is present at the membrane surface ('surface/total'; right). Data was normalised to the P3-4 tissue. Total NKCC1 expression levels showed a significant two-fold increase between P3-4 and P13-14. However, there was a significant decrease in the proportion of surface NKCC1 over the same developmental period. ***E,*** Quantification of KCC2 expression in terms of total protein levels (left) and the proportion of protein present at the membrane surface (right). Same conventions as in 'D'. There was a substantial, six-fold increase in total KCC2 protein levels between P3-4 and P13-14 and the relative proportion of KCC2 at the membrane surface remained stable. Error bars - S.E.M., * - $p < 0.05$, ** - $p < 0.01$, *** - $p < 0.001$, unpaired t-test.

4.2 A potential association between NKCC1 and the motor protein Myosin Va

The process of delivering proteins to, and removing them from, the plasma membrane requires associations with adaptor proteins, intracellular trafficking proteins and the exocytosis/endocytosis machinery. For example, the trafficking of neurotransmitter receptors (AMPARs, GlyRs and $GABA_ARs$) to, and from, the plasma membrane, involves interactions with multiple adaptor proteins and molecular motor proteins (Maas et al., 2006; Correia et al., 2008; Heisler et al., 2011). It seems likely that NKCC1 regulation at the plasma membrane will also require associations with other proteins. Nevertheless, such mechanisms have been largely unexplored.

In order to identify potential interacting proteins that might be involved in regulating NKCC1 delivery and/or function, Dr. Sarah Newey performed a proteomics screen using a combination of co-immunoprecipitation and mass spectrometry techniques to identify functionally important components of NKCC1 protein complexes. An anti-NKCC1 antibody (T4 monoclonal; DSHB) was used to isolate antibody-protein complexes from P5 rat forebrain (see Materials and Methods). Analysis of the resulting peptides by SDS-PAGE and mass spectrometry led to the identification of potential NKCC1 associated proteins, a list of which is shown in Figure 4.2A. This approach identified proteins that have previously been shown to associate with NKCC1, such as the serine/threonine protein kinase OSR1 (Piechotta et al., 2002). However, it also identified potentially associated proteins that have not been described before. One such protein was Myosin Va (Figure 4.2A). Previous studies have revealed that Myosin Va functions as a molecular motor protein that transports different cargo proteins along actin filaments and delivers them to the surface of the cell (Correia et al., 2008). It is conceivable that Myosin Va could also be involved in regulating the

delivery/function of NKCC1 at the cell surface and therefore this novel protein association was investigated with a series of experimental techniques.

To further explore the potential association between NKCC1 and Myosin Va, immunolabelling was performed in dissociated embryonic rat hippocampal neurons that had been maintained for 12 days in vitro. Consistent with the biochemical evidence for an association, immunofluorescence staining and epifluorescence imaging suggested a potential co-localisation between endogenous NKCC1 and Myosin Va in neurons, which seemed strongest in the soma, perinuclear region and dendrites (Figure 4.2B). This is consistent with previous studies that have found expression of Myosin and NKCC1 in both the soma and dendrites (Marty et al., 2002; Correia et al., 2008; Brinn et al., 2010). Nevertheless, wide field epifluorescence imaging used in my study has limited resolution for fine details, primarily due to out of focus scattered fluorescence. This limitation is reduced by confocal microscopy that images a thin focal plane, and may explain the lack of punctate appearance of Myosin Va in my images compared to studies that have used confocal imaging (Correia et al., 2008). Therefore, although wide field epifluorescence imaging is consistent with a possible co-localisation of Myosin Va and NKCC1, future studies using higher resolution imaging should further confirm this aspect.

To confirm the results from the proteomics screen, co-immunoprecipitation experiments were performed on solubilised protein lysates from rat organotypic hippocampal slices. Using the T4 monoclonal as the immunoprecipitating NKCC1 antibody, western blots of the resulting complexes revealed that Myosin Va can indeed be co-immunoprecipitated with NKCC1 (Figure 4.2C). In contrast, Myosin Va was not precipitated by an IgG control antibody. As confirmation that NKCC1 was being immunoprecipitated successfully, the same blots were stripped and re-probed with the T4 antibody, which revealed less NKCC1 in the

A

Protein Name	Mwt (kDa)	RefSeq No.	Peptides	Reference
Myosin Va	212	NP071514	27	
Myomegalin	262	NP071777	22	
Serine/threonine protein kinase OSR1	58	NP001101664	10	Piechotta et al. 2002
Internexin, alpha	56	NP062001	8	

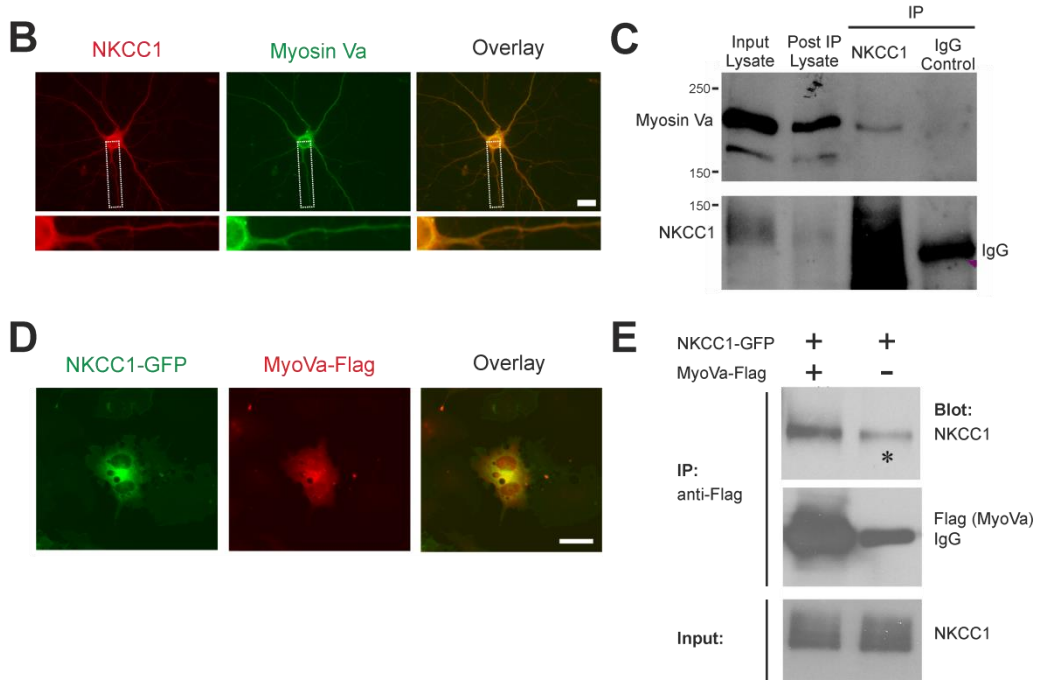


Figure 4.2 NKCC1 associates with Myosin Va in developing rat hippocampus.

A, Affinity purification and mass spectrometry was used to identify proteins associated with NKCC1 in neonatal rat hippocampus. The table shows the molecular weight, RefSeq number and unique peptide count for proteins identified by mass spectrometry. Where the identified proteins have previously been shown to associate with NKCC1, a reference is provided. ***B,*** Fluorescence imaging of dissociated embryonic hippocampal neurons at 12 DIV co-labelled with antibodies to NKCC1 (left) and Myosin Va (middle) revealed significant overlap in staining, suggesting that the proteins are co-localised. Magnifications of the areas highlighted within the white boxes are provided in the panels below. The merged image (yellow signal, right) suggests co-localisation between NKCC1 and Myosin Va. Scale bar 20 µm. ***C,*** NKCC1 and Myosin Va associate in neonatal rat hippocampus. Protein lysates from P4 rat organotypic hippocampal slices were incubated with the immunoprecipitating anti-NKCC1 antibody (lane 3) or with control IgG (lane 4). Resulting complexes were then probed for Myosin Va (top blot) or NKCC1 (bottom blot). The input lysate and post immunoprecipitation lysate are also shown (lanes 1 and 2). ***D,*** Co-localisation of NKCC1 and Myosin Va globular tail (MyoVa-Flag) in transfected COS-7 cells. Fluorescence microscope image of NKCC1-GFP (left) and immunolabelled MyoVa-Flag (middle) suggests co-localisation in the same perinuclear compartment (yellow signal, right). Scale bar 20µm. ***E,*** Association of NKCC1 and Myosin Va globular tail (MyoVa-Flag) in a heterologous cell line. Co-immunoprecipitation experiments were performed on COS-7 cells transfected with NKCC1-GFP and MyoVa-Flag (left lane) or with NKCC1-GFP and a Flag only vector as a control (right lane). Immunoprecipitation of Myosin Va using an anti-Flag antibody resulted in greater pull down of NKCC1. Immunoblots were probed with anti-NKCC1 (top and bottom blots) and anti-Flag (middle blot) antibodies.

lysate after the immunoprecipitation (IP) and a strong NKCC1 signal in the NKCC1 IP lane (Figure 4.2C).

As an independent method to test the association between NKCC1 and Myosin Va, tagged versions of the two proteins were co-expressed in COS-7 cells. NKCC1 was tagged with GFP at the C-terminus (NKCC1-GFP), while a short version of Myosin Va containing the cargo-binding domain (responsible for interacting with transported proteins) was tagged with Flag (MyoVa-Flag). Fluorescence microscopy revealed a high degree of overlap between GFP and immunostaining for the Flag epitope, indicating that NKCC1-GFP and MyoVa-Flag colocalise in the cell (Figure 4.2D). Finally, for co-immunoprecipitation experiments, NKCC1-GFP was co-transfected with either MyoVa-Flag or a Flag-only control vector in COS-7 cells. Lysates were then immunoprecipitated using an anti-Flag antibody and blots were probed for NKCC1. As illustrated in Figure 4.2E, immunoprecipitation with an anti-Flag antibody resulted in greater pull-down of NKCC1 in lysates from cells expressing MyoVa-Flag, than in control lysates from cells expressing the Flag-only construct.

Taken together, these results support a molecular association between Myosin Va and NKCC1 in hippocampal neurons. In the next series of experiments I focused on characterising the functional significance of this association.

4.3 An electrophysiological assay to measure the contribution of NKCC1 to Cl^- homeostasis

As shown earlier, NKCC1 was found to be at the cell membrane in hippocampal slices in the neonatal period (P3-P4; see Figure 4.1D). At this stage resting E_{GABA-A} values are more positive than in mature neurons, consistent with higher $[Cl^-]_i$ in neonatal neurons (Figure

4.1C). These results would suggest that NKCC1 is contributing to the depolarised E_{GABA-A} values observed in neonatal neurons. To directly test this idea, I used gramicidin-perforated patch clamp recordings to measure E_{GABA-A} in CA3 pyramidal neurons from neonatal slices (aged P3-5) under control conditions and in the presence of the NKCC1 blocker, bumetanide (10 µM). The half maximal inhibitory concentration (IC50) of bumetanide for NKCC1 has been reported to be ~4 µM (Hannaert et al., 2002), which is significantly smaller that the reported inhibitory constant of bumetanide for KCC2 (~55 µM; Payne, 1997). Therefore, at a concentration of 10 µM bumetanide can selectively block NKCC1 over KKC2.

Figure 4.3A illustrates typical E_{GABA-A} measurements under these two conditions. The mean E_{GABA-A} in control slices was -68.7 ± 1.7 mV, n = 35 and this was more positive than the mean E_{GABA-A} in slices that had been treated with the NKCC1 blocker, bumetanide (-75.4 ± 1.9 mV, n = 14, $p < 0.05$, unpaired t-test; Figure 4.3C). These results show that NKCC1 is active in neonatal CA3 pyramidal neurons and functions to increase $[Cl^-]_i$ and set E_{GABA-A} to more depolarising values. More generally, these experiments confirmed that measuring E_{GABA-A} could be used as an indication of NKCC1 contribution to Cl^- homeostasis.

To further explore this possibility, in the next set of experiments I used a within-cell design in which E_{GABA-A} was measured in the same CA3 pyramidal neuron before and after the administration of bumetanide (Figure 4.4). As illustrated in the example in Figure 4.4A, application of bumetanide shifted E_{GABA-A} to more hyperpolarising values. Moreover, this E_{GABA-A} shift was sufficient to change GABAergic signalling from depolarising to hyperpolarising (Figure 4.4B). Overall, mean E_{GABA-A} was -64.8 ± 3.9 mV under baseline conditions and bumetanide application shifted E_{GABA-A} to more negative values of -72.7 ± 3.6 mV (n = 10, $p < 0.001$, paired t-test, Figure 4.4C). These results suggest that the bumetanide-induced shift in E_{GABA-A} can be used as an assay of NKCC1 contribution to Cl^- homeostasis at the level of a single neuron. This assay has the advantage of using a within-cell design, which

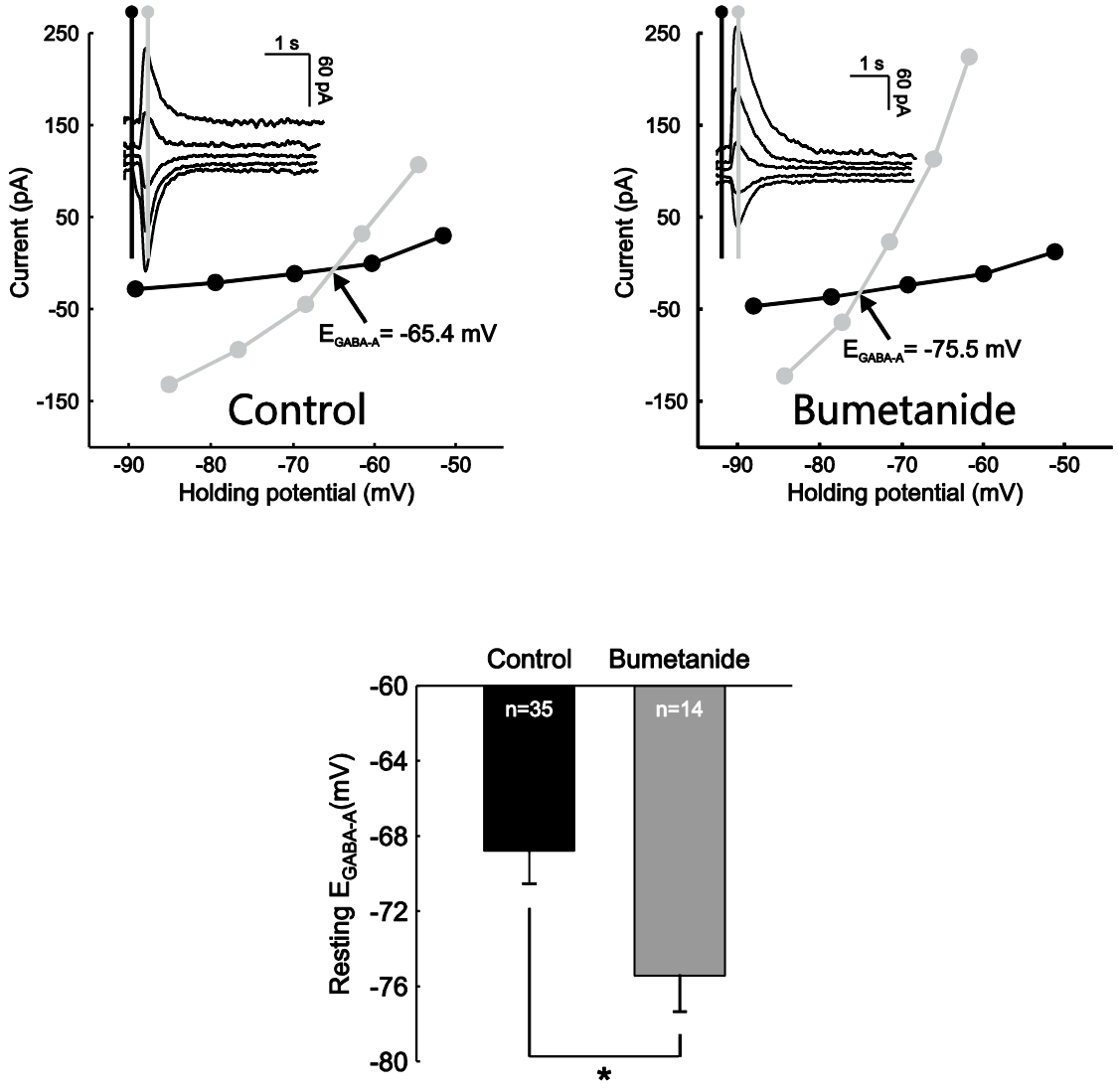


Figure 4.3 NKCC1 is active in neonatal neurons and sets E_{GABA-A} to depolarising levels.

A, Example E_{GABA-A} measurements from a CA3 pyramidal neuron from a P3 slice under control conditions (left) and from a pyramidal CA3 neuron in the presence of bumetanide (10 µM). ***B,*** Resting E_{GABA-A} was significantly more hyperpolarised in slices exposed to bumetanide (10 µM, for at least 10 min; mean E_{GABA-A} -75.4 ± 1.9 mV, n = 14, grey bar) than control slices (mean E_{GABA-A} -68.7 ± 1.7 mV, n = 35, black bar). Error bars - S.E.M., * – $p < 0.05$, unpaired t-test.

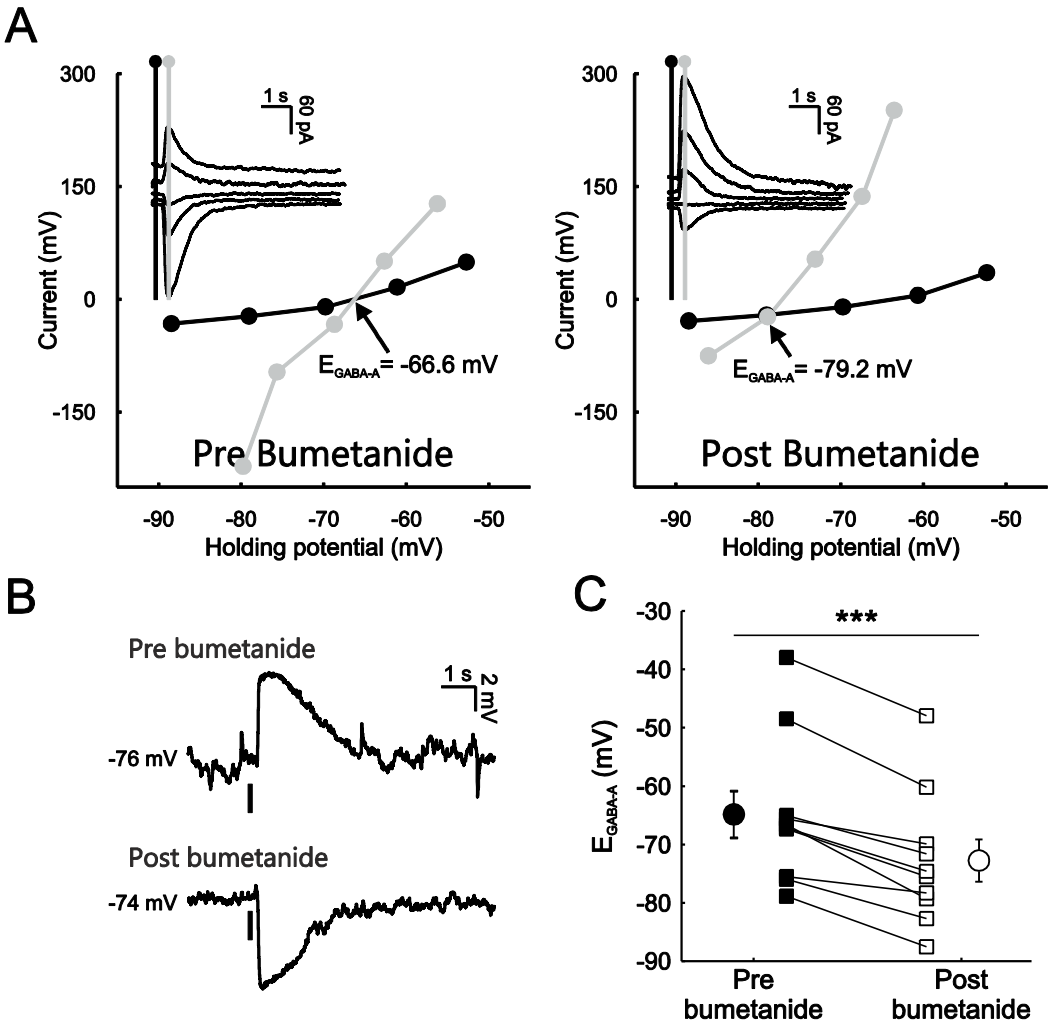


Figure 4.4 Assessing NKCC1 contribution to Cl^- homeostasis using a within-cell design.

A, Example E_{GABA-A} measurements in a CA3 pyramidal neuron in a P4 organotypic hippocampal brain slice. The data show a bumetanide-induced negative shift in E_{GABA-A} from -66.2 mV pre bumetanide (left panel), to -79.9 mV in the presence of 10 µM bumetanide (right panel). ***B,*** Current clamp recordings in the same neuron in 'A', showing that bumetanide shifted the polarity of $GABA_AR$ responses evoked by local GABA application (vertical bar) from depolarising (Pre bumetanide) to hyperpolarising (Post bumetanide). ***C,*** Population data from 10 CA3 pyramidal neurons showing a significant negative shift in E_{GABA-A} induced by bumetanide. Square symbols indicate individual measurements, circle symbols indicate population means. The bumetanide-induced E_{GABA-A} shift can therefore be used as an assay of NKCC1 contribution to Cl^- homeostasis in individual neurons. Error bars - S.E.M., *** - $p < 0.001$, $n = 10$, paired t-test.

reduces variability resulting from measurement of E_{GABA-A} across cells, and thus increases the statistical power for detecting changes in NKCC1 contribution to Cl^- homeostasis.

Having established that NKCC1 is active in the neonatal slices and having developed an electrophysiological assay for NKCC1 function, I set out to investigate the functional significance of the NKCC1-Myosin Va association.

4.4 Disrupting endogenous Myosin Va activity reduces the contribution of NKCC1 to Cl^- homeostasis

Myosin Va functions to transport different cargo proteins along actin filaments (van Diepen et al., 2009; Rudolf et al., 2011; Correia et al., 2008). Structurally, Myosin Va exists as a dimer and consists of: a) a motor domain that binds to and moves along actin filaments, b) a neck region, and c) a globular tail region that functions as a cargo-binding domain (Hirokawa et al., 2010). Thus, while the motor domain provides the movement, the cargo-binging domain links with the transported proteins. This functional dissociation between the two domains can be exploited to disrupt endogenous Myosin Va function. For example, overexpression of a short Myosin Va that contains only the cargo-binding domain (but not the motor domain) displaces endogenous Myosin from its cargos and therefore acts in a dominant-negative fashion to interfere with the normal transport function (MyoVa-DN; Brown et al., 2001; Correia et al., 2008).

To test for a potential role of Myosin Va in regulating NKCC1, I overexpresed the MyoVa-DN construct in organotypic slices using biolistic gene delivery and assessed the effects upon Cl^- homeostasis. MyoVa-DN was tagged with enhanced GFP (EGFP) allowing the visualization and identification of transfected neurons under fluorescence microscopy

(Figure 4.5A). I was thus able to use gramicidin-perforated patch clamp recordings to measure E_{GABA-A} in cells overexpressing MyoVa-DN and in control cells expressing EGFP alone. If endogenous Myosin Va function is important for regulating NKCC1, then altering Myosin Va by overexpression of MyoVa-DN would be expected to result in changes to Cl^- homeostasis. Comparing passive membrane properties of MyoVa-DN and EGFP-expressing cells revealed no difference in terms of resting membrane potential (-70.3 ± 1.3 versus -70.4 ± 1.4 mV, $p = 0.96$, unpaired t-test), membrane capacitance (86.2 ± 7.6 versus 69.4 ± 9.8 pF, $p = 0.26$, unpaired t-test) and access resistance (76.7 ± 11.5 versus 84.0 ± 4.4 MOhm, $p = 0.48$, unpaired t-test). However, MyoVa-DN cells had a higher input resistance (1074.7 ± 177.3 versus 517.4 ± 62.4 MOhm, $p < 0.05$, unpaired t-test). This may reflect a role for Myosin Va in modulating membrane conductance by influencing the function of different ionic channels. Alternatively, the lower input resistance of EGFP cells may be due to a bias towards selecting more mature cells in this condition.

As a first step towards testing for a role for Myosin in modulating Cl^- homeostasis, I measured resting E_{GABA-A} in CA3 pyramidal neurons expressing MyoVa-DN and in control neurons expressing EGFP alone. As illustrated in Figure 4.5B, resting E_{GABA-A} was significantly more hyperpolarised in cells expressing MyoVa-DN than in control cells expressing EGFP only (-70.7 ± 1.8 versus -63.3 ± 2.4 mV, $p < 0.05$, unpaired t-test). These results are consistent with a lower Cl^- concentration in neurons overexpressing MyoVa-DN. Such an effect could be explained by a reduction in the activity of the NKCC1 transporter, which functions to increase intracellular Cl^- and to shift E_{GABA-A} to more depolarised values (see Figure 4.4).

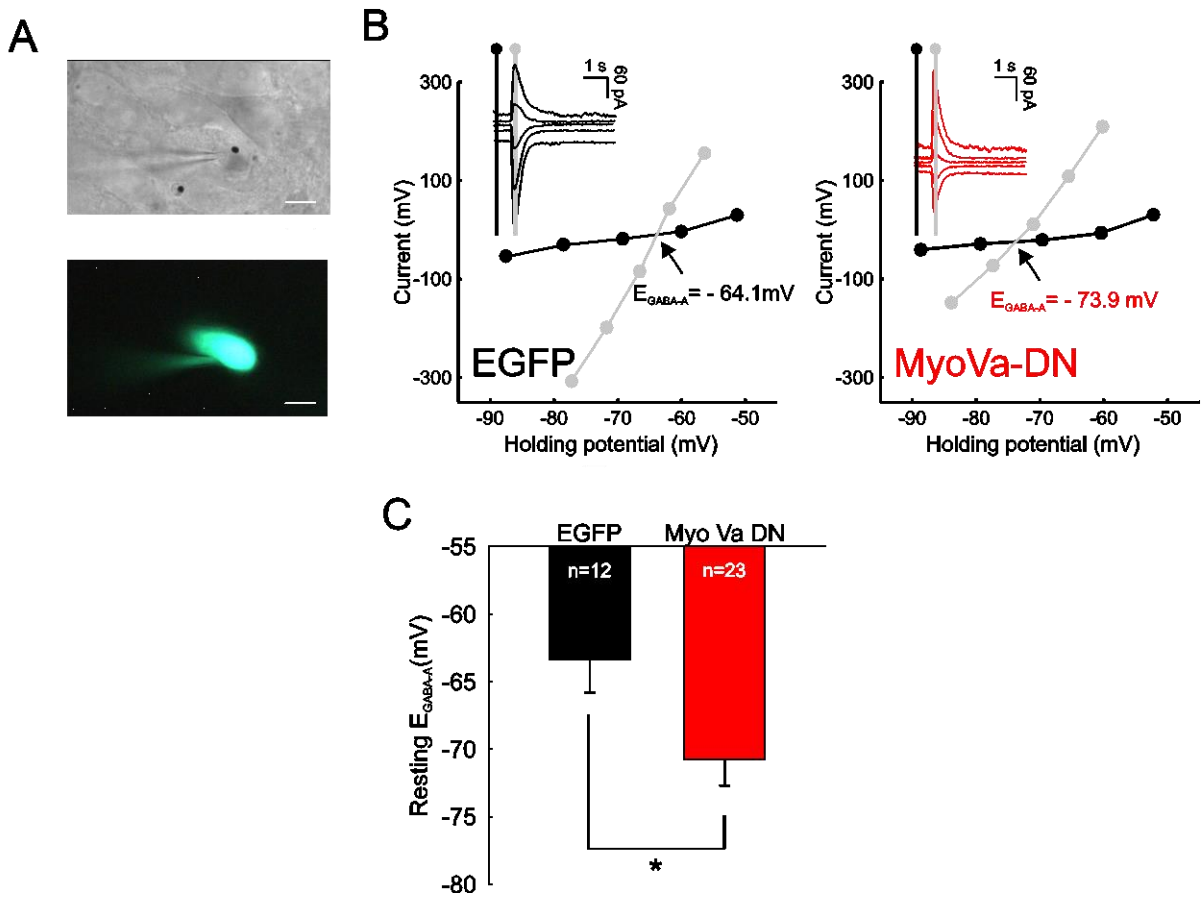


Figure 4.5 Disrupting endogenous Myosin Va shifts resting E_{GABA-A} to more negative values.

A, MyoVa-DN tagged with EGFP, or EGFP alone, were expressed in hippocampal slices using biolistic gene delivery. Fluorescence microscopy was used to identify transfected CA3 pyramidal neurons, which were then targeted for electrophysiological recordings. Images show an example CA3 pyramidal neuron expressing MyoVa-DN during gramicidin-perforated patch clamp recording under light microscopy (top) and fluorescent microscopy (bottom). Scale bar 15 µm. ***B,*** Resting E_{GABA-A} was significantly more hyperpolarised in cells expressing MyoVa-DN (red bar) than in control cells expressing EGFP only (black bar). Error bars - S.E.M., * – $p < 0.05$, unpaired t-test.

To directly test whether the effect of MyoVa-DN upon E_{GABA-A} in mediated via NKCC1, I used the within-cell bumetanide assay described above (see Figure 4.4). E_{GABA-A} was measured before and after the administration of the NKCC1 blocker bumetanide in control cells expressing EGFP, and in cells overexpressing MyoVa-DN (Figure 4.6). In control cells bumetanide induced a significant negative shift in E_{GABA-A} from -63.3 ± 2.4 mV to -72.7 ± 2.5 mV ($n = 10$, $p < 0.001$, paired t-test; Figure 4.6B). In cells overexpressing MyoVa-DN, bumetanide induced a small negative shift in E_{GABA-A} from -68.3 ± 2.5 mV to -71.5 ± 2.2 mV ($n = 14$, $p < 0.05$, paired t-test; Figure 4.6D). Consistent with a role for Myosin Va in regulating NKCC1 function, the bumetanide-induced shift in E_{GABA-A} was significantly smaller in cells overexpressing MyoVa-DN than in control cells expressing EGFP only (-3.2 ± 1.2 mV versus -9.3 ± 1.1 mV, $p < 0.01$, unpaired t-test; Figure 4.6E). These results reveal that disrupting Myosin Va activity reduces the contribution of NKCC1 to Cl^- homeostasis. They are therefore consistent with previous biochemical evidence for a molecular association between NKCC1 and Myosin Va and a role for the motor protein in regulating the Cl^- transporter protein. Given a role for Myosin Va in regulating NKCC1, a further question was whether this reflects a constitutive role for Myosin Va or whether Myosin Va could also be involved in the activity-dependent regulation of NKCC1. For instance, previous studies have reported that Myosin Va regulates the activity-dependent delivery of AMPA-receptors to synapses during LTP (Correia et al., 2008). To explore whether Myosin Va could be involved in an activity-dependent regulation of NKCC1, in the next set of experiments I focused my attention on investigating potential changes in NKCC1 function in the context of neonatal seizure activity.

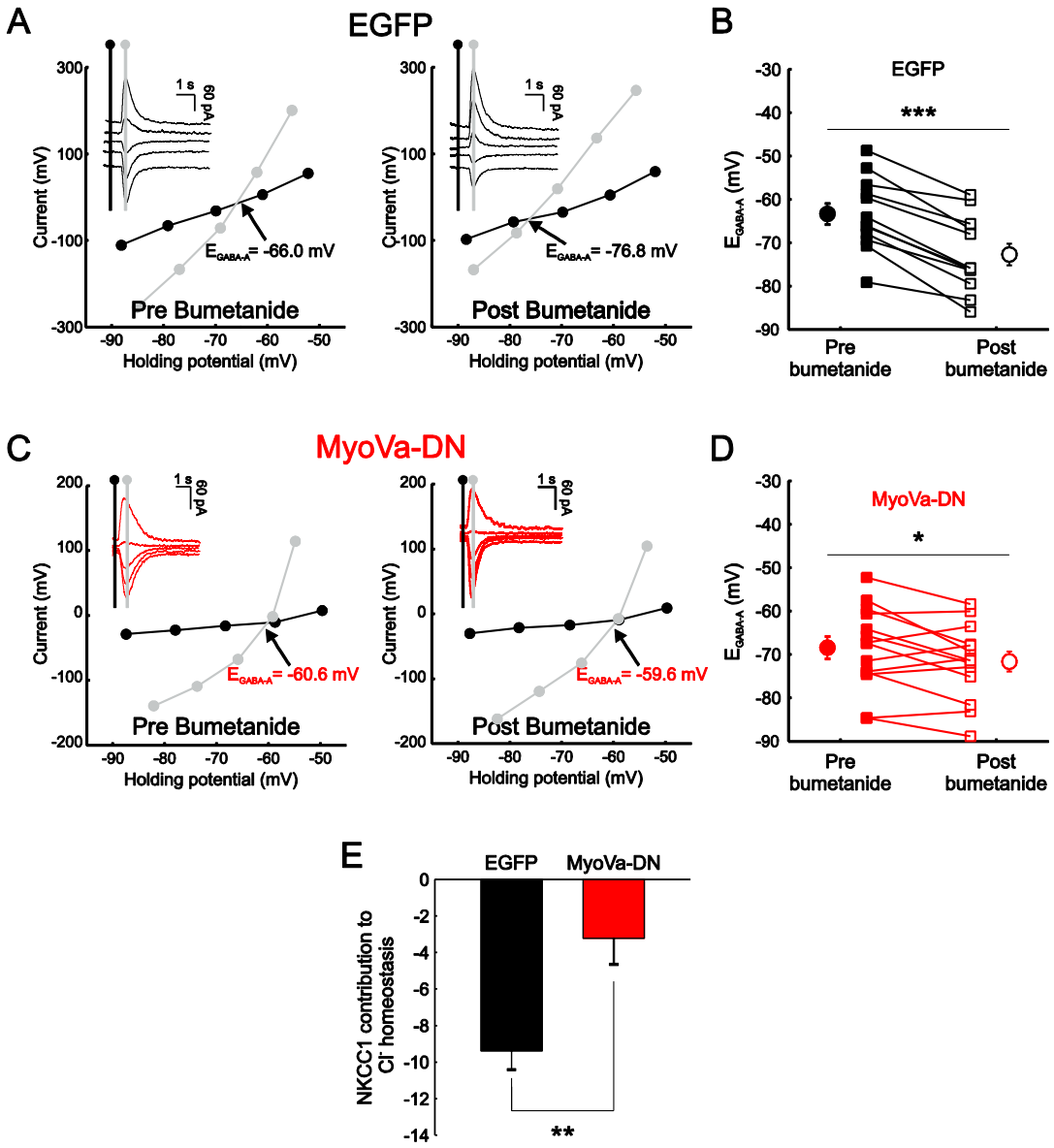


Figure 4.6 Disrupting endogenous Myosin Va function reduces NKCC1 contribution to Cl^- homeostasis.

A, Example E_{GABA-A} measurements from a control CA3 pyramidal neuron transfected with EGFP showing a bumetanide-induced negative shift in E_{GABA-A} from -66.0 mV pre bumetanide (left panel) to -79.9 mV in the presence of 10 µM bumetanide (right panel). ***B,*** Population data from 10 cells showing a significant negative shift in E_{GABA-A} induced by bumetanide in EGFP expressing cells from -63.3 ± 2.4 to -72.7 ± 2.5 mV. Square symbols represent individual measurements, circle symbols represent population means. ***C,*** Example E_{GABA-A} measurements from a CA3 pyramidal neuron expressing MyoVa-DN showing that 10 µM bumetanide did not induce a negative change in $E_{GABA-A.}$ Conventions as in 'A'. ***D,*** Population data from 14 cells showing a small overall negative shift in E_{GABA-A} induced by bumetanide in MyoVa-DN expressing cells from -68.3 ± 2.5 mV to -71.5 ± 2.2 mV. Conventions as in 'B'. ***E,*** Population data showing a significantly smaller bumetanide-induced E_{GABA-A} shift in cells expressing MyoVa-DN (red bar) compared to control cells expressing EGFP only (black bar). Error bars - S.E.M., * - $p < 0.05$, ** - $p < 0.01$, *** - $p < 0.001$.

4.5 Investigating the activity-dependent regulation of NKCC1 in the context of neonatal seizures

Previous studies have reported several activity-dependent mechanisms involved in regulating the Cl^- extruding transporter KCC2, both under normal conditions and in the context of epilepsy (Lee et al., 2011a; Puskarjov et al., 2012; Khirug et al., 2010; Fiumelli et al., 2005). Relatively less is known about whether the NKCC1 transporter can undergo similar activity-dependent modifications. It has been shown that during development, pre- and postsynaptic activity can downregulate NKCC1 activity and hyperpolarise E_{GABA-A} (Balena and Woodin, 2008). And in the context of seizure activity, there is evidence that NKCC1 activity might be enhanced such that it leads to a progressive Cl^- accumulation, a depolarising shift in E_{GABA-A} and a change in $GABA_AR$ signalling from inhibitory to excitatory (Dzhala et al., 2010). Moreover, in the epileptogenic period of post-status epilepticus, it has been reported that the expression of NKCC1 at the surface of the neurons is increased (Bragin et al., 2009). Consistent with these studies and with a pro-excitatory role for NKCC1 in epilepsy, several clinical studies have reported improvements in seizure management after NKCC1 blockade both in neonatal (Kahle et al., 2009) and adult patients (Eftekhari et al., 2012). Taken together, these studies suggest that seizure activity might lead to an increase in NKCC1 function and/or expression, which could be responsible for increasing $[Cl^-]_i$ and weakening $GABA_AR$-mediated inhibition. Nevertheless, the exact mechanisms by which seizure activity can lead to changes in NKCC1 function/expression have remained unclear. To explore these aspects, I investigated whether seizure activity in the neonatal brain can induce activity-dependent changes in NKCC1 function and whether Myosin Va plays a role in these changes.

To develop a neonatal seizure model I first tested the effect of removing extracellular Mg^{2+} upon the activity of CA3 neurons in P3-5 organotypic hippocampal slices. In contrast to the mature slices, where 0 Mg^{2+} treatment successfully triggered seizures, removal of

extracellular Mg^{2+} was not sufficient to induce seizures in neonatal hippocampal slices (Figure 4.7A, n = 3). This is likely to be due to the reduced number and strength of synaptic connections between neurons in the neonatal period, which would increase the threshold for seizure induction (Hsia et al., 1998). Another widely used model for inducing seizure-like activity is the administration of 4-aminopyridine (4-AP; Chesnut and Swann, 1988; Luhmann et al., 2000; Voskuyl and Albus, 1985), which increases excitability by blocking several K^+ currents including the delayed rectifier K^+ current (Ulbricht and Wagner, 1976) and the fast inactivating K^+ current (I_A; Segal and Barker, 1984; Gustafsson et al., 1982). I found that when 4-AP (100 µM) was applied in combination with 0 Mg^{2+}, seizures were easily triggered in all neonatal hippocampal slices (Figure 4.7). Similar to seizures in mature slices, I could distinguish two phases of seizure activity: (1) the initial ictal-like phase (also referred to as the 'tonic' phase) and (2) the after-discharge phase (also referred to as the 'clonic' phase). In order to induce long-lasting seizures, similar to status-epilepticus, the 4-AP and 0 Mg^{2+} aCSF was applied for 10 min following the start of a seizure, at which point the extracellular solution was switched back to normal aCSF. This led to the induction of long-lasting seizure-like events that had a mean duration of 1297.2 ± 71.3 s, n = 15. To investigate $GABA_AR$ signalling during the course of these neonatal seizures, $GABA_ARs$ were activated every 15 seconds by local application of GABA (100 µM) via a puffer pipette. Figure 4.7 illustrates a typical experiment in a CA3 pyramidal neuron from a P5 hippocampal slice. Consistent with more positive E_{GABA-A} values in the neonatal hippocampus, activation of $GABA_ARs$ generally gave rise to depolarising responses under baseline conditions (Figure 4.7). Nevertheless, this depolarisation was below the threshold for triggering action potentials. During the course of seizure activity, however, activation of $GABA_ARs$ gave rise to much larger depolarising events that were now able to trigger action potentials. These results are consistent with the idea that seizures lead to intracellular Cl^- accumulation, which underlies the depolarising shift

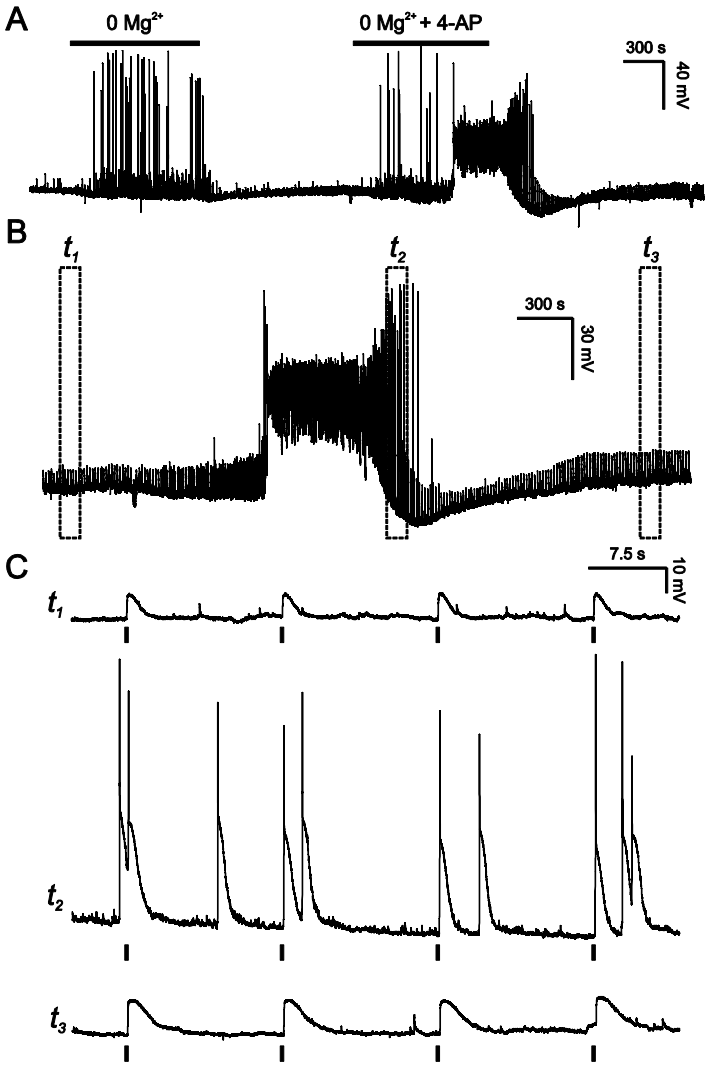


Figure 4.7 Seizures in the neonatal hippocampus lead to excitatory effects of $GABA_AR$ activation.

A, Example current clamp recording in a CA3 pyramidal neuron in a P5 hippocampal slice. Application of 0 Mg^{2+} (first horizontal black bar) increased the activity of the neuron but was not sufficient to trigger a seizure. Co-application of 0 Mg^{2+} with 4-AP (100 µM; second horizontal line) was sufficient to trigger robust seizure activity. ***B,*** Example recording during which $GABA_ARs$ were activated by local GABA application every 15 seconds. Dashed rectangles represent three different time points. ***C,*** Expanded traces from the rectangles in 'B', showing $GABA_AR$ responses before (t_1), during (t_2) and after the seizure (t_3). Vertical black bars represent the point when GABA was applied. Before the seizure, $GABA_AR$ responses were depolarising but not able to trigger action potentials (t_1). During the after-discharge period, depolarising $GABA_AR$ responses were increased in amplitude and able to trigger action potentials (t_2). Note the resemblance between evoked $GABA_AR$ responses and spontaneous after-discharges, suggesting that the latter are triggered by excitatory actions of interneurons. After the seizure, $GABA_AR$ responses continued to be depolarising, but no longer triggered action potentials (t_3). Note that the amplitude of $GABA_AR$ responses was larger in the post-seizure period (+15.0 mV) compared to the pre-seizure period (+10.4 mV), suggesting that seizure-activity could lead to long-term changes in E_{GABA-A}.

in E_{GABA-A} and renders GABAergic signalling excitatory. After the seizure end, $GABA_AR$ responses continued to be depolarising but were no longer able to trigger action potentials, consistent with a recovery of intracellular Cl^- levels in the post-seizure period (Figure 4.7B). These results show that, similar to seizures in the mature brain (see Chapter 3), seizures in the neonatal brain lead to intracellular Cl^- accumulation and an accompanying change in $GABA_AR$ signalling to excitatory.

Interestingly, the amplitude of $GABA_AR$ responses seemed to be larger in the post-seizure period compared to pre-seizure baseline values. This observation suggests that seizure activity can induce changes in Cl^- homeostasis such that post-seizure intracellular Cl^- levels remain elevated. Such effects could involve the upregulation of NKCC1 function, potentially through activity-dependent mechanisms triggered during the seizure activity. As a first step towards investigating an activity-dependent modulation in NKCC1 function, I applied the NKCC1 blocker bumetanide in the post-seizure period. As illustrated in Figure 4.8, application of bumetanide switched $GABA_AR$ signalling from depolarising to hyperpolarising. These results suggest that NKCC1 continues to be active in the post-seizure period and contributes to increasing Cl^- levels. The data presented so far suggest that after a seizure episode, depolarising $GABA_AR$ responses have increased amplitude and that NKCC1 continues to be active and to contribute to Cl^- accumulation during this period.

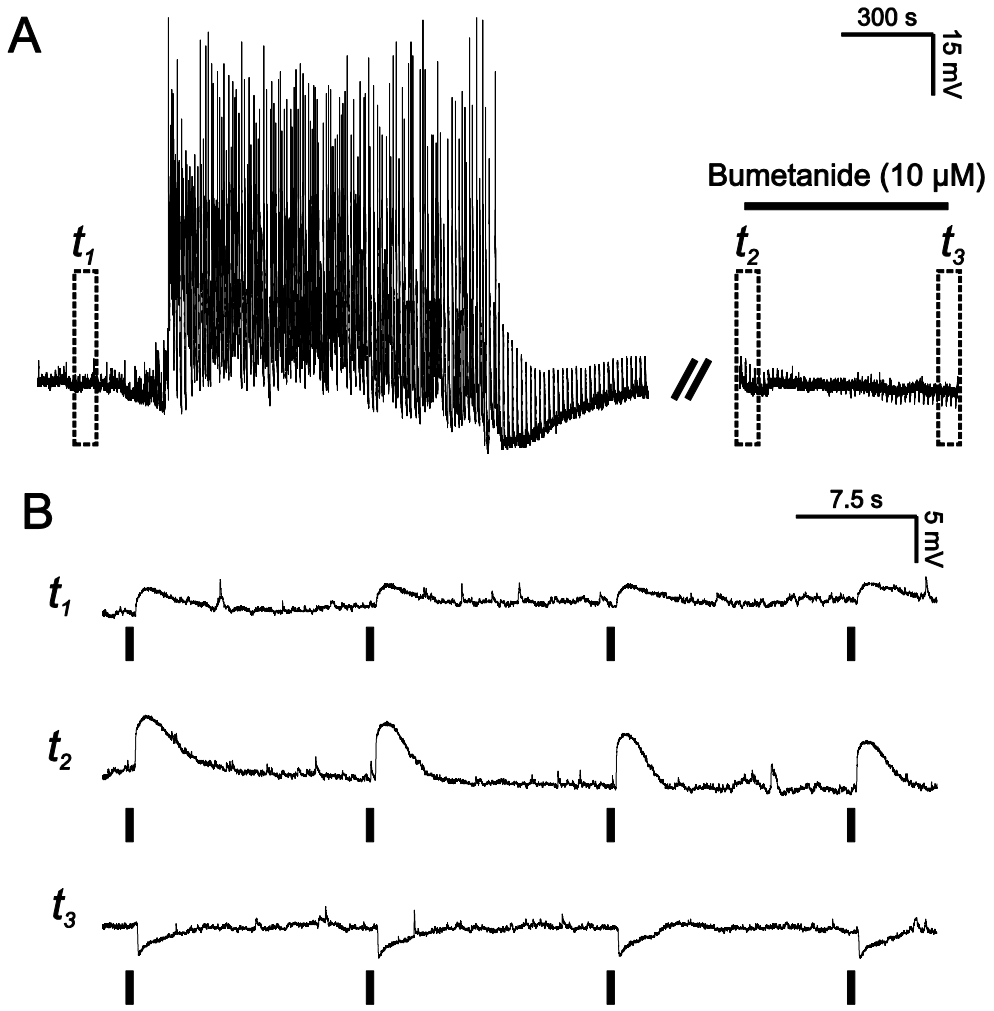


Figure 4.8 NKCC1 is active in the post-seizure period and continues to contribute to Cl^- accumulation.

A, Example seizure in a neonatal hippocampal slice in which $GABA_AR$ responses were recorded every 15 seconds. Bumetanide was applied in the post-seizure period (horizontal black bar). Dashed rectangles represent three time points: before the seizure (t_1), during the post-seizure period but before bumetanide application (t_2) and 10 min after bumetanide application (t_3). Parallel oblique bars show a 5-min interruption of the current clamp recording. ***B,*** Expanded traces from the rectangles in A, showing $GABA_AR$ responses; vertical black bars indicate when GABA (100 µM) was applied via a puffer pipette. Before the seizure $GABA_AR$ responses were depolarising (+2.9 mV; t_1). In the post-seizure period $GABA_AR$ responses continued to be depolarising and had increased amplitude (+5.7 mV; t_2). Application of bumetanide reversed the polarity of $GABA_AR$ responses from depolarising to hyperpolarising (-3.1 mV; t_3).

To quantify such seizure-induced changes in Cl^- homeostasis, I next used voltage clamp recordings to measure E_{GABA-A} before and after a single seizure episode. Figure 4.9A illustrates a typical experiment. Seizures were triggered as described earlier by exposing the slices to aCSF containing 0 Mg^{2+} and 4-AP. After 10 min of seizure activity the perfusion was switched back to normal aCSF. E_{GABA-A} was measured using voltage step protocols 10-15 min before the seizure start (Pre) and in the post-seizure period at two different time points: 10-15 min (Post1) and 25-30 min (Post2) after the washout of 0 Mg^{2+} and 4-AP. E_{GABA-A} before the start of the seizure was -71.7 ± 2.9 mV and not different from E_{GABA-A} measured shortly after the end of the seizure (Post1; -69.2 ± 2.0 mV, n = 8, $p > 0.05$, repeated measurements ANOVA with Dunnett multiple comparisons test). This suggests that shortly after the seizure end, E_{GABA-A} has fully recovered from the acute Cl^- load that occurs during the course of the seizure. Interestingly however, later in the post-seizure period (Post2), E_{GABA-A} became more positive compared to pre-seizure baseline E_{GABA-A} (-66.4 ± 3.4 mV versus -71 ± 2.9 mV, n = 8, $p < 0.01$, repeated measurements ANOVA with Dunnett multiple comparisons test; Figure 4.9B). This suggests that Cl^- homeostasis is altered later in the post-seizure period, and in a manner that is consistent with an increase in intracellular Cl^-.

One possibility for such changes is increased activity/expression of the NKCC1 transporter, which would lead to intracellular Cl^- accumulation in the post-seizure period. To directly test this hypothesis, I applied bumetanide (10 μM) to block NKCC1 throughout the whole recording period and measured E_{GABA-A} before and after seizures (Figure 4.9A and C). As illustrated in Figure 4.9, bumetanide prevented the seizure-induced changes in E_{GABA-A}. In slices exposed to bumetanide, there was no difference between pre-seizure baseline E_{GABA-A} (-78.9 ± 2.1 mV) and E_{GABA-A} measured shortly after the seizure end (Post1; -78.2 ± 3.3 mV, n = 5, $p > 0.05$) or E_{GABA-A} measured later in the post seizure period (Post2; -77.9 ± 1.9 mV, n

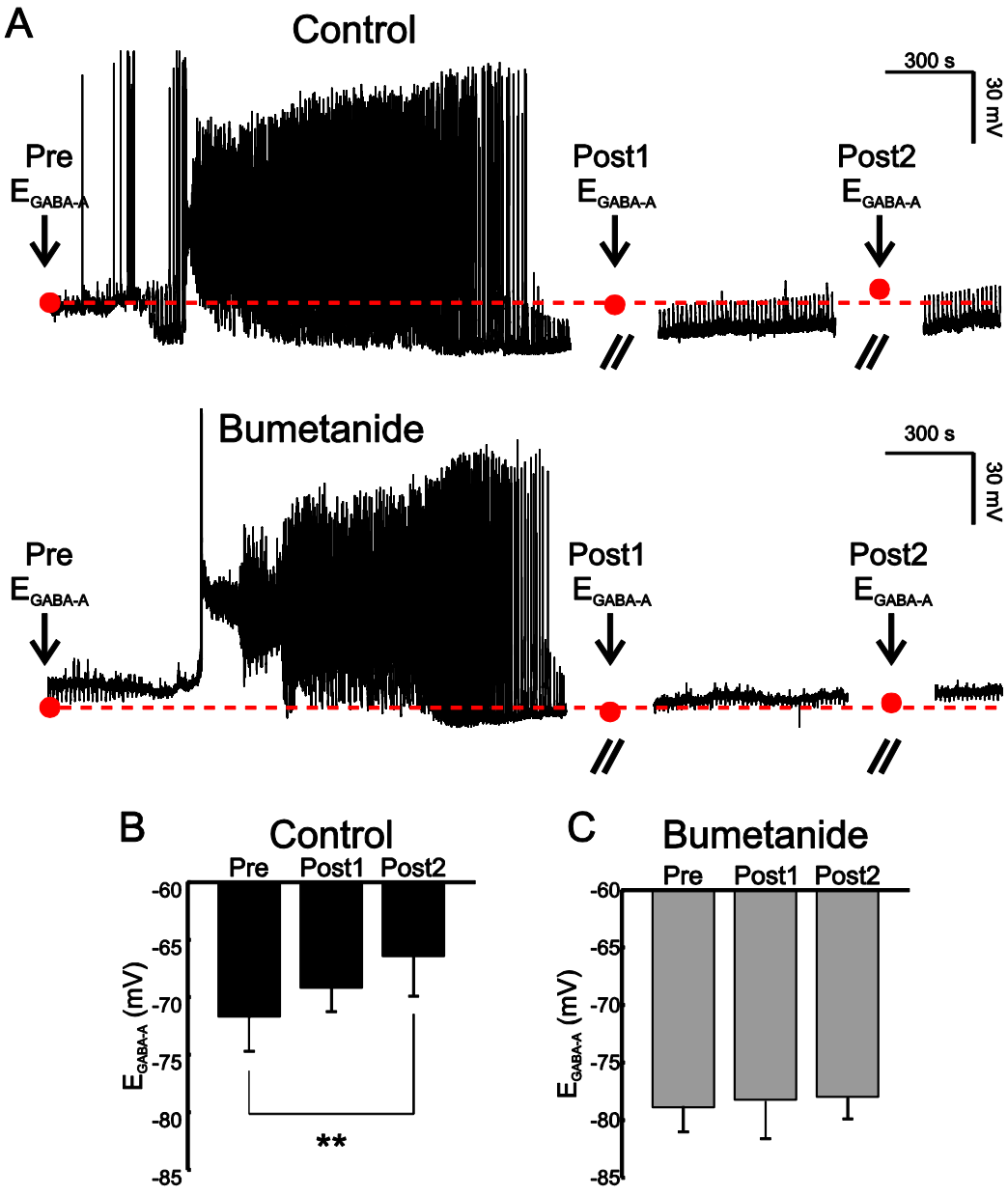


Figure 4.9 Neonatal seizure activity induces a bumetanide-dependent shift in E_{GABA-A}.

A, Example seizures recorded in neonatal slices under control conditions (top) and in the presence of 10 µM bumetanide (bottom). E_{GABA-A} was measured before the seizure ('Pre') and at two time points in the post-seizure period ('Post1' and 'Post2') by switching from current clamp to voltage clamp and using a voltage-step protocol. Arrows indicate the time points when E_{GABA-A} was measured. Red circles represent E_{GABA-A} values at (Pre, Post1 and Post2) and the dashed red line represents the baseline level of E_{GABA-A} before the seizure (Pre). Oblique black bars represent periods spent in voltage clamp mode for E_{GABA-A} measurements. ***B,*** Under control conditions (left), E_{GABA-A} was more depolarised at the Post2 time point (25-30 min from the washout of 0 Mg^{2+} and 4-AP) compared to the Pre time point (i.e. the pre-seizure baseline value). ***C,*** Blocking NKCC1 prevented the seizure-induced depolarising shift in E_{GABA-A}. Error bars - S.E.M., ** - $p < 0.01$.

= 5, p > 0.05, repeated measurements ANOVA with Dunnett multiple comparisons test, Figure 4.9C). These results suggest that the seizures induced an activity-dependent change in NKCC1 function, such that in the post-seizure period NKCC1 drove increased Cl^- accumulation and shifted E_{GABA-A} to more depolarising values. Such changes might have important functional consequences as they are predicted to increase the overall network excitability and therefore increase the susceptibility for triggering further seizure episodes.

The seizure-induced depolarising shift in E_{GABA-A} was evident towards the end of the post-seizure recording period (at Post2). Therefore this time point was used in the next set of experiments, which investigated the role of Myosin Va in seizure-induced changes in NKCC1 activity. Figure 4.10A illustrates typical recordings in untransfected neurons under control conditions, untransfected neurons under bumetanide-treated conditions, and neurons transfected with MyoVa-DN. E_{GABA-A} was measured 10-15 min before the seizure start (Pre) and in the post seizure period, 25-30 min after the washout of 0 Mg^{2+} and 4-AP (Post2). Experiments from Figure 4.9 made some of the data for the control and bumetanide-treated conditions. Consistent with earlier experiments (Fig. 4.5), there was a trend towards more negative resting E_{GABA-A} in MyoVa-DN (-74.8 ± 2.9 mV, n = 7) and bumetanide treated neurons (-77.0 ± 1.6 mV, n = 10) compared to control neurons (-71.2 ± 1.9 mV, n = 14), although this was not statistically significant (p > 0.05, ANOVA) probably due to inter-cell variability in resting $E_{GABA-A.}$ Seizure activity induced a significant depolarising shift in E_{GABA-A} in untransfected neurons under control conditions from -71.2 ± 1.9 mV to -67.2 ± 2.0 mV, n = 14, p < 0.001, paired t-test (Figure 4.10B). This shift was abolished under bumetanide-treated conditions when E_{GABA-A} remained unchanged (-77.0 ± 1.6 mV versus -76.2 ± 1.7 mV, n = 10, p = 0.25, paired t-test; Figure 4.10C). Moreover, seizure activity did not induce a significant shift in E_{GABA-A} in neurons overexpressing MyoVa-DN.

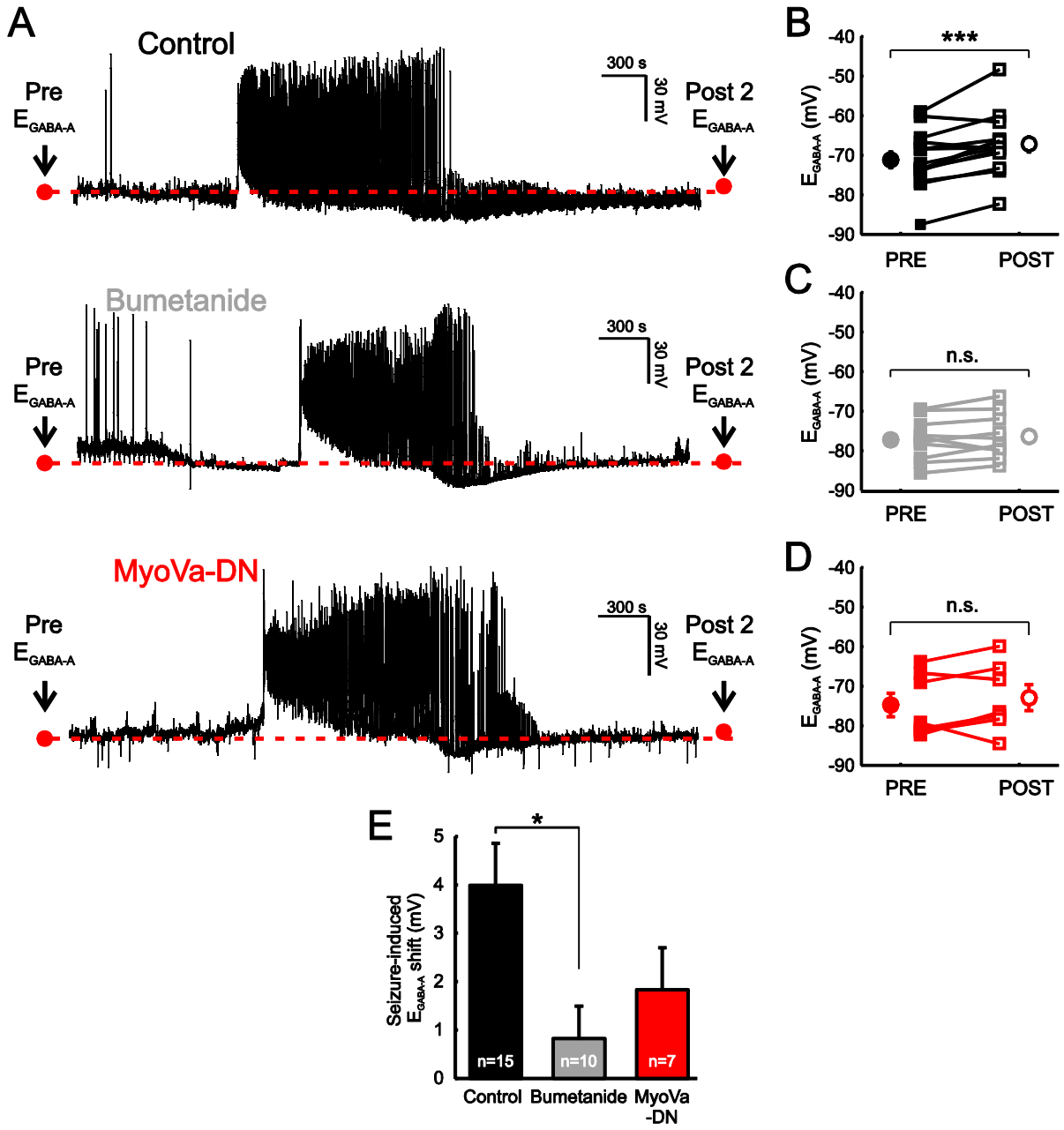


Figure 4.10 Investigating the role of Myosin Va in the seizure-induced shift in E_{GABA-A}.

A, Example recordings in CA3 pyramidal neurons under control conditions (top), under bumetanide treated conditions (middle) and in neurons expressing MyoVa-DN (bottom). E_{GABA-A} was measured before the seizure ('Pre') and in the post-seizure period ('Post2'). Red circles represent E_{GABA-A} values and the dashed red line represents baseline E_{GABA-A} before the seizure (i.e. the Pre value). ***B***, Seizures induced a significant shift in E_{GABA-A} under control conditions, square symbols represent individual experiments and circle symbols represent population means. ***C*** and ***D***, The seizure induced shift was not statistically significant in bumetanide-treated conditions (***C***) and in neurons expressing MyoVa-DN (***D***). ***E***, Seizure-induced shift in E_{GABA-A} for control untransfected cells, bumetanide treated untransected cells, and cells overexpressing MyoVa-DN. Error bars - S.E.M., * – $p < 0.05$, ANOVA with Dunnett post-hoc test.

Before the seizure E_{GABA-A} was -74.8 ± 2.9 mV and remained unchanged in the post-seizure period when E_{GABA-A} was -72.9 ± 3.2, n = 7, p = 0.25, paired t-test (Figure 4.10D). These results indicate a loss of the statistically significant effect of seizure activity upon E_{GABA-A} in both bumetanide-treated conditions and neurons expressing MyoVa-DN. However, it is important to test whether the delta E_{GABA-A} (i.e. the seizure-induced E_{GABA-A} shift) was statistically different when compared to the delta E_{GABA-A} in the control group (Nieuwenhuis et al., 2011). I therefore compared delta E_{GABA-A} between the three conditions (Figure 4.10E). The seizure-induced shift was significantly smaller in bumetanide-treated conditions compared to control conditions (0.8 ± 0.6 mV versus 3.9 ± 0.9 mV, $p < 0.05$, ANOVA, with Dunnett post-hoc test). And while there was a trend towards a smaller E_{GABA-A} shift in MyoVa-DN cells compared to control conditions, it did not reach statistical significance (1.8 ± 1.4 mV versus 3.9 ± 0.9 mV, p = 0.27, ANOVA, with Dunnett post-hoc test; Figure 4.10E). Therefore, from these data it is not possible to conclude that MyoVa-DN reduces the seizure-induced shift in E_{GABA-A}. Taken together, these results suggest that seizure activity can induce a rapid activity-dependent increase in the contribution of NKCC1 to Cl^- homeostasis in the post-seizure period. However, this increase in NKCC1 is relatively modest in amplitude for a single seizure episode and it is not possible to conclude at this stage whether this activity-dependent change requires Myosin Va.

Regarding the functional role of NKCC1 contribution to E_{GABA-A} and neonatal seizure activity I found that the time to seizure initiation was significantly higher in bumetanide-treated slices (688.7 ± 83.9 s, n = 10) compared to control slices (489.9 ± 43.1 s, n = 15, $p < 0.05$, unpaired t-test). This effect was associated with more hyperpolarised E_{GABA-A} values in neurons from bumetanide-treated slices (-76.7 ± 1.5 mV, n = 10) compared to control slices (-70.2 ± 1.8 mV, n = 15, $p < 0.05$, unpaired t-test). These results suggest that more hyperpolarised E_{GABA-A} values have a protective role and delay the initiation of a seizure

when the network is challenged with hyperexcitability conditions. However, once a seizure was triggered, seizure duration was not different between bumetanide (1245.3 ± 58.6 s, n = 10) and control groups (1297.2 ± 71.3, n = 15, p = 0.61, unpaired t-test). Taken together, these results show that blocking NKCC1 activity delays the initiation of a seizure without affecting seizure duration. Therefore, seizure-induced changes in NKCC1 contribution to Cl^- accumulation might have important consequences and may render the network more susceptible to induction of further seizure activity.

4.6 Discussion

In this Chapter I investigated the developmental regulation of E_{GABA-A} in relation to the expression of Cl^- transporter proteins in organotypic hippocampal slices. Consistent with previous studies (Rivera et al., 1999; Tyzio et al., 2007; Yamada et al., 2004), I found that E_{GABA-A} undergoes a hyperpolarising shift during the first two postnatal weeks. Over the same period, KCC2 expression levels increase substantially and the relative proportion of KCC2 at the cell surface remains constant. In contrast, the relative proportion of NKCC1 that is delivered to the cell surface is reduced. These results suggest that, in addition to transcriptional regulation, NKCC1 may be regulated via its trafficking to, and/or from, the surface of the cell. To investigate the molecular mechanisms that may underlie such a regulation of NKCC1, I searched for proteins that can associate with NKCC1. Immunoprecipitation combined with mass-spectrometry identified Myosin Va as a candidate NKCC1-associated protein. Myosin Va functions as a molecular motor protein, which transports different cargo proteins along actin filaments and delivers them to the surface of the cell (Correia et al., 2008; Rudolf et al., 2011; van Diepen et al., 2009). Co-immunoprecipitation of Myosin Va and NKCC1, in both hippocampal slices and

heterologous cells, further confirmed the mass-spectrometry experiments. Moreover, epifluorescence imaging suggested that Myosin Va and NKCC1 co-localise both in hippocampal neurons and when expressed in heterologous cells. To test the functional role of Myosin Va in regulating NKCC1, I developed an electrophysiological assay that is able to measure the contribution of NKCC1 to Cl^- homeostasis. Overexpression of a MyoVa-DN construct, which disrupts endogenous Myosin Va activity, resulted in a significant reduction in NKCC1 contribution to Cl^- homeostasis. These data provide strong evidence that the association with Myosin Va is important for NKCC1 function. To investigate a potential activity-dependent regulation of NKCC1 via Myosin Va, I developed a neonatal seizure model and found that seizures induced a positive shift in E_{GABA-A} that was evident in the post seizure period. Both bumetanide treatment and expression of MyoVa-DN abolished the statistically significant effect of seizure activity upon E_{GABA-A}. However, when directly comparing the E_{GABA-A} shift between bumetanide treatment, MyoVa-DN expression and control conditions, only bumetanide treatment was significantly different to control. Blocking NKCC1 shifted E_{GABA-A} to more hyperpolarised values and increased the time to seizure initiation, suggesting that more negative E_{GABA-A} values can have a protective role against the induction of seizure activity. In summary, in this Chapter I have revealed a novel interaction between NKCC1 and the motor protein Myosin Va which can regulate NKCC1 function. This interaction is likely to be important for regulating NKCC1 activity under basal conditions. Whether this interaction is also involved in the activity-dependent regulation of NKCC1 during seizure activity remains to be fully determined.

Previous studies in the rat hippocampus have reported that GABAergic signalling switches from depolarising to hyperpolarising during the first two postnatal weeks (Rivera et al., 1999; Tyzio et al., 2007). I found that a similar switch is present in CA3 pyramidal neurons in organotypic hippocampal slices prepared from rats. To explore the mechanisms

controlling this switch, I measured changes in the expression of NKCC1 and KCC2 transporters, which are responsible for setting the Cl^- concentration and thus E_{GABA-A}. In agreement with previous reports (Rivera et al., 1999; Rivera et al., 2005; Wang et al., 2002), total levels of KCC2 were substantially upregulated. Given that the proportion delivered to the surface of the cells was constant over development, these findings are consistent with an increase in absolute Cl^- extrusion capacity that can shift E_{GABA-A} to more negative values. Interestingly, NKCC1 expression was also upregulated over the same period, but the delivery of NKCC1 to the surface of the cell was significantly reduced. These findings suggest that a novel mechanism by which NKCC1 function might be regulated during development is via controlling its delivery to the membrane.

The delivery and recycling of proteins to and from the cell surface is regulated by interactions with adaptor proteins and with molecular motor proteins (Hirokawa et al., 2010; Heisler et al., 2011). Co-immunoprecipitatation of NKCC1 protein complexes, followed by mass spectrometry identified the motor protein Myosin Va as a candidate protein associated with NKCC1. These results were further confirmed by a series of biochemical, immunohistochemical and molecular experiments. The mass-spectrometry also identified an association with the protein kinase OSR1, which has been previously reported to interact with NKCC1 in a yeast two-hybrid assay (Piechotta et al., 2002), thereby providing further validation of the proteomics screening. In addition, mass-spectrometry revealed myomegalin and internexin alpha as two novel potential NKCC1-associated proteins. Myomegalin has recently been suggested to be involved in the trafficking of protein cargos from the Golgi apparatus to the inner segment of photoreceptor cells (Overlack et al., 2011). Internexin alpha is a member of the intermediate filaments family, which are a component of the cytoskeleton and serve scaffolding roles in axons and dendrites (Steinert et al., 1999; Pachter and Liem,

1985; Yuan et al., 2006). It remains to be determined whether these proteins are involved in regulating NKCC1 activity/trafficking at different post-translational stages.

The experiments conducted here are not able to determine if the association between Myosin Va and NKCC1 is direct, or whether it requires additional partners. Adaptor proteins such as Rab11, for example, have been reported to be part of some protein complexes transported by Myosin Va (Correia et al., 2008). To investigate this further in relation to NKCC1, it would be interesting to examine whether the expression of adaptor proteins could increase the strength of the Myosin Va-NKCC1 association in heterologous cells. Furthermore, future studies could use truncated versions of NKCC1 to identify the exact protein domain that is responsible for interacting with Myosin Va. A direct interaction between Myosin Va and NKCC1 could allow the design of specific cell permeable peptides (Bonny, 2006) that could be used to specifically modulate the function of Myosin Va in regulating NKCC1.

Consistent with a role for Myosin Va in regulating NKCC1 activity, expression of the MyoVa-DN dominant negative construct, resulted in more hyperpolarised resting E_{GABA-A} values and a reduction in NKCC1 contribution to Cl^- homeostasis. The contribution of NKCC1 was significantly reduced, but not completely abolished by MyoVa-DN. This could be due to some residual function of endogenous Myosin Va under these conditions. Alternatively, other mechanisms could contribute to NKCC1 trafficking. MyoVa-DN has been suggested to disrupt endogenous Myosin Va function by displacing Myosin Va from its cargos (Brown et al., 2001; Correia et al., 2008). Although this approach has been shown to be specific, even for different Myosin V subtypes (Brown et al., 2001; Correia et al., 2008), future studies could use alternative approaches to disrupt Myosin activity. For instance, it would be interesting to use RNA-interference technologies to downregulate endogenous Myosin Va protein levels. As an RNA-interference approach is likely to require several days

to be effective (Gavrilov and Saltzman, 2012), this would have to be considered in relation to the developmental downregulation of NKCC1when designing experiments. Alternatively, rodents expressing a non-functional mutated version of Myosin Va could be used to confirm the role of Myosin Va in regulating NKCC1 function (Takagishi and Murata, 2006).

The exact mechanisms by which Myosin Va controls the contribution of NKCC1 to Cl^- homeostasis also require further investigation. For instance, it will be important to test the hypothesis that disrupting Myosin Va results in changes in the proportion of NKCC1 at the surface of the cell. One approach to test this possibility would be to use biotinylation to quantify the proportion of surface NKCC1 under different manipulations. In order to detect an effect, this would require that the Myosin Va manipulation would affect large numbers of neurons, which could be achieved by the use of viral-mediated delivery in organotypic hippocampal slices or transgenic animals in which Myosin Va has been selectively manipulated. Alternatively, immunohistochemistry studies could be performed to detect surface NKCC1 at the level of individual neurons.

Previous studies have reported that NKCC1 activity/expression is increased in epilepsy. For instance, acute seizures in the neonatal brain are associated with NKCC1-dependent intracellular Cl^- accumulation, which renders GABAergic signalling excitatory (Dzhala et al., 2010). Furthermore, NKCC1 expression levels have been reported to increase in the epileptogenic period, following insults such as status epilepticus (Barmashenko et al., 2011; Bragin et al., 2009), and increased NKCC1 levels have also been observed in human patients with chronic refractory epilepsy (Sen et al., 2007). Nevertheless, the exact time course and the mechanisms responsible for changes in NKCC1 expression and function have been largely unexplored. Using a neonatal seizure model I found that seizure activity induced a positive shift in $E_{GABA\text{-}A}$, which was evident in the post-seizure period and dependent upon NKCC1. As a first step to testing whether Myosin Va is required for this seizure-induced

increase in NKCC1 function, I used the dominant negative MyoVa-DN construct. Disrupting protein trafficking via Myosin Va prevented the seizure-induced increase in $E_{GABA-A,}$ suggesting a role for the NKCC1-Myosin Va association in this process. However, the results were not statistically conclusive because a significant reduction was not found when comparisons were made to an untransfected control group. Future work will therefore have to address this issue. First it will be useful to increase the size of the current data set to increase the statistical power for detecting a significant difference. Second, it will be important to confirm findings using other control groups including cells transfected with EGFP only. Third it will be interesting to test whether other manipulations of Myosin Va (e.g. RNA-interference knockdown) affect seizure-induced increases in NKCC1 function.

Regarding the functional significance of changes in E_{GABA-A}, blocking NKCC1 with bumetanide hyperpolarised baseline E_{GABA-A} by approximately -7 mV and significantly increased the time to seizure initiation. These results suggest that hyperpolarised E_{GABA-A} values have a protective effect and delay the initiation of a seizure when the network is challenged with hyperexitability conditions. Interestingly, once a seizure had been triggered, bumetanide had no effect on the seizure duration. This implies that NKCC1 contribution to Cl^- accumulation is not important during the course of the seizure, when most Cl^- accumulation probably occurs via other processes such as intense $GABA_AR$ activation in combination with membrane depolarisation (Isomura et al., 2003b). In the post seizure period however, NKCC1 did contribute to a Cl^- loading effect and shifted E_{GABA-A} towards more depolarised values by approximately +4 mV. Given the relationship observed between E_{GABA-A} and seizure initiation, even a modest, persistent increase in NKCC1 activity could render the network more susceptible to further seizures. And with subsequent seizures this effect could be additive such that seizure activity could have a positive feed-back effect on the propensity to triggering new seizures. Interestingly, it was observed that the seizure-induced

shift in E_{GABA-A} was not evident immediately after the seizure end but required approximately 25 min to emerge. This suggests that there are time-dependent process underlying these effects and therefore understanding the dynamics of seizure-induced changes in E_{GABA-A} became the focus of the next Chapter.

5 Exploring the dynamics of E_{GABA-A} during neonatal seizure activity

The previous Chapter explored the role of NKCC1 in regulating Cl^- homeostasis and E_{GABA-A} in a model of neonatal seizures. Measuring E_{GABA-A} at two separate time points following a single seizure episode revealed important differences and suggested that time-dependent processes could be regulating Cl^- homeostasis in the post-seizure period. To better understand these processes, I wanted to explore the dynamics of E_{GABA-A} with respect to seizure activity in more detail. Therefore my specific aims were:

1. To develop a protocol that allows repeated E_{GABA-A} measurements concomitant with the monitoring of seizure activity.
2. To use this protocol to explore E_{GABA-A} dynamics with respect to neonatal seizure activity.

5.1 Repeated E_{GABA-A} measurements reveal interesting dynamics during neonatal seizure activity

Seizure activity was triggered as described in the previous Chapter, by switching from normal aCSF solution to a convulsant solution containing 0 Mg^{2+} and the K^+ channel blocker 4-AP (100 μM). After 10 min of seizure activity the perfusion solution was switched back to normal aCSF and this led to the termination of seizure activity in all experiments. Recordings were maintained for at least 18 min after the end of the seizure. An example seizure and post-seizure recording is illustrated in Figure 5.1A. To investigate E_{GABA-A} dynamics I developed a protocol that allowed me to repeatedly measure E_{GABA-A} and the cell's membrane potential throughout the seizure. In order to preserve the native $[Cl^-]_i$, all recordings were performed

using the gramicidin-perforated patch clamp technique. The recording mode was repeatedly switched between current clamp and voltage clamp modes every 30 seconds (Figure 5.1B). The current clamp epochs had a duration of 27.5 seconds and were used to monitor the cell's membrane potential during the seizure. The voltage clamp epochs had a duration of 2.5 seconds and were used to measure $E_{GABA\text{-}A}$. Each voltage clamp epoch was composed of 2 voltage ramps ranging from -110 to -50 mV, from a holding potential of -70 mV. The first ramp was applied under baseline conditions and the second ramp was applied during activation of $GABA_A$Rs by local application of GABA (100 µM; Figure 5.1B). This made it possible to construct I-V plots for the holding current generated by the first ramp and for the total current generated by the second ramp (reflecting the holding current plus the current through the activated $GABA_A$Rs). $E_{GABA\text{-}A}$ was calculated as the intersection of the linear fits for the holding current and the total current (Figure 5.1C). In some instances, the voltage ramps were contaminated by ongoing seizure activity, thus precluding precise $E_{GABA\text{-}A}$ measurements. These data points were excluded from further analysis. As illustrated in Figure 5.1A, this protocol allowed repeated $E_{GABA\text{-}A}$ measurements in relation to seizure activity.

To allow systematic analysis of $E_{GABA\text{-}A}$ in relation to seizure activity, the start and the end of each seizure were defined as reference points (see arrows in Figure 5.2A and B). The start of the seizure was defined as the time at which the membrane potential depolarized beyond a 'threshold' set at 40 mV above the cell's resting membrane potential. The end of the seizure was defined as the last after-discharge that crossed the 40 mV threshold that was used to define the start of the seizure. Seizure duration ranged from 1046 s to 1920 with a mean of 1418 ± 118.6 s. To account for variation in seizure duration, all $E_{GABA\text{-}A}$ measurements were aligned to the seizure start and seizure end (Figure 5.2B). This allowed $E_{GABA\text{-}A}$ to be compared between the pre-seizure period, the actual seizure

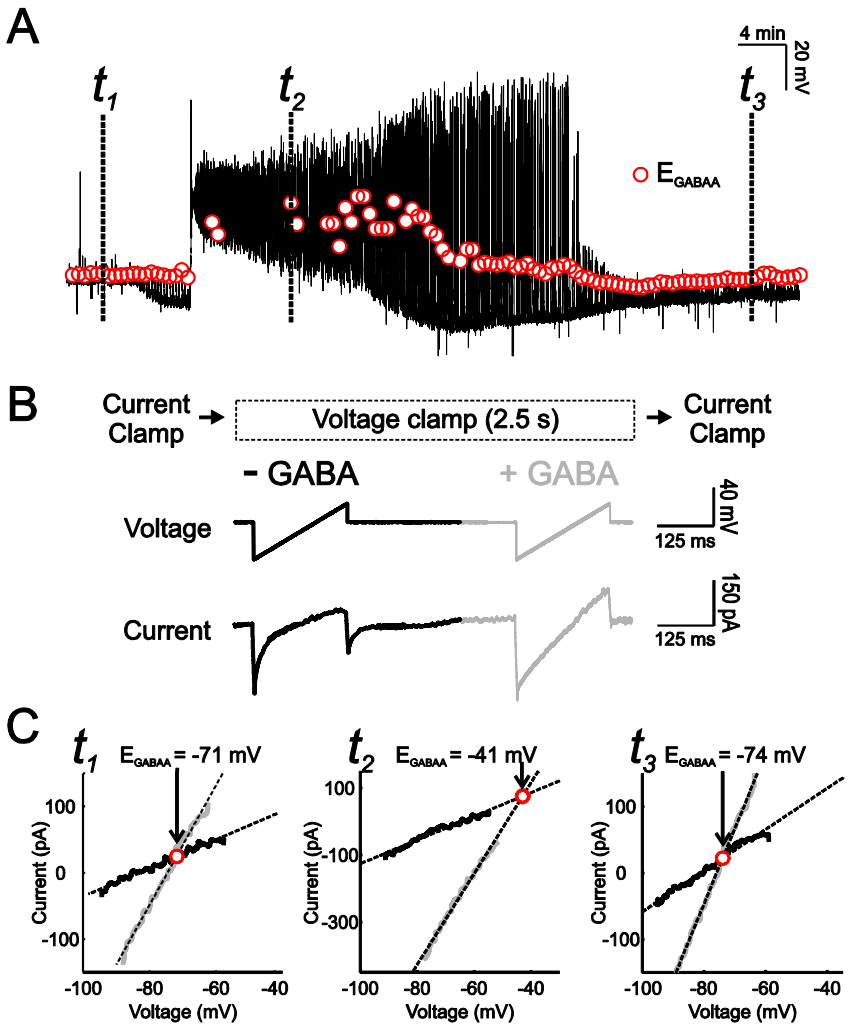


Figure 5.1 Monitoring $E_{GABA\text{-}A}$ throughout the seizure and post-seizure period.

A, Example neonatal seizure recorded from a CA3 pyramidal neuron. The cell's membrane potential and $E_{GABA\text{-}A}$ were monitored by repeatedly switching between current and voltage clamp modes. The current clamp epochs (27.5 s each) were used to describe the seizure activity (black trace). The voltage clamp epochs (2.5s each) were used to measure $E_{GABA\text{-}A}$ every 30 s (red circles). Vertical dashed lines represent example $E_{GABA\text{-}A}$ measurements before the seizure (t_1), during the seizure (t_2) and in the post-seizure period (t_3). ***B,*** $E_{GABA\text{-}A}$ was measured by applying two consecutive voltage ramps, in voltage clamp mode, the first under baseline conditions (black line; - GABA) and the second during activation of $GABA_A$Rs (grey line; + GABA). ***C,*** I-V plots for $E_{GABA\text{-}A}$ measurements for the three time points represented by the dashed lines in 'A'. $E_{GABA\text{-}A}$ was defined as the voltage at which the linear fits (dashed lines) for the holding current (generated by the first ramp; black line) and the total current (reflecting the holding current plus the current through the activated $GABA_A$Rs; grey line) intersected with one another.

period, and the post-seizure period. As illustrated in Figure 5.2B, seizure activity induced a positive shift in E_{GABA-A} from pre-seizure values of -68.8 ± 2.4 mV to -51.8 ± 2.0 mV during the first 5 min of the seizure ($n = 8$, $p < 0.01$, repeated measures ANOVA with post-hoc Dunnett multiple comparisons). This positive shift is consistent with previous studies (Isomura et al., 2003b; Isomura et al., 2008) and likely reflects intracellular Cl^- accumulation that occurs as a result of intense $GABA_AR$ activity coupled with depolarisation of the membrane potential. As seizure activity progressed from the tonic to the tonic-clonic phase, E_{GABA-A} began to recover and reached a mean value of -59.5 ± 3.7 mV during the last 5 min of seizure activity ($n = 8$, $p < 0.05$). Full recovery of E_{GABA-A} to pre-seizure values occurred in the first 2 min of the post-seizure period when E_{GABA-A} reached -69.9 ± 2.1 mV ($n = 8$, $p > 0.05$). Interestingly however, E_{GABA-A} did not stabilise at this point but instead continued to move in a hyperpolarising direction so that it exhibited an "undershoot" relative to pre-seizure values. This undershoot reached its minimum of -73.1 ± 2.6 mV at 6 min after the end of the seizure ($n = 8$, $p < 0.01$). This negative shift was transitory and E_{GABA-A} slowly moved back towards baseline values, so that it was no longer statistically different to pre-seizures values at 14 min after the end of the seizure and reached -69.7 ± 2.6 mV ($n = 8$, $p > 0.05$) by the end of the recordings, 18 min after the end of the seizure (Figure 5.2B).

These repeated E_{GABA-A} measurements revealed two important phases of E_{GABA-A} dynamics with respect to seizure activity: (1) a rapid positive shift in E_{GABA-A} that occurs during the seizure and recovers as the seizure comes to an end and; (2) a negative shift in E_{GABA-A} (the 'undershoot') during the post-seizure period; that eventually recovers towards more positive values. The transitory negative shift in E_{GABA-A} (i.e. phase '2') has not been described before and could represent a phase during which the Cl^- extruding capacity of the cell is actually enhanced, such that intracellular Cl^- levels reach levels that are lower than pre-seizure levels. This would be predicted to increase the strength of GABAergic inhibition

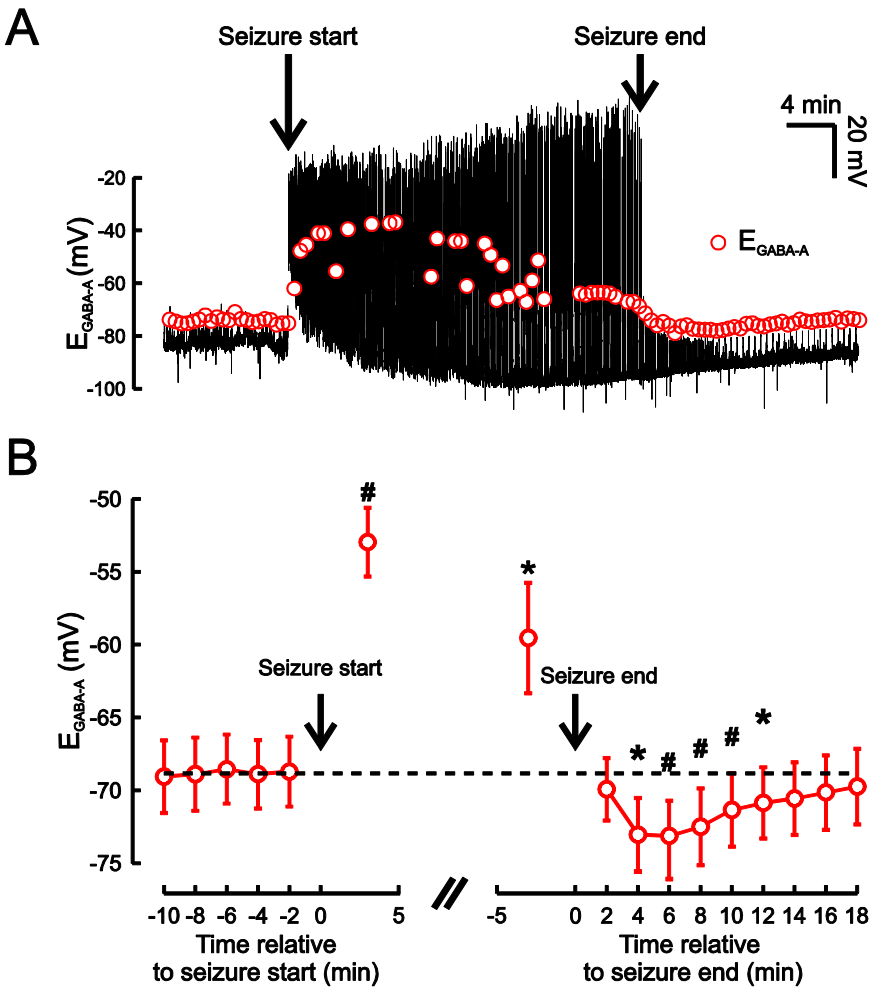


Figure 5.2 E_{GABA-A} exhibits a positive shift during neonatal seizures, which is followed by a recovery and transitory negative shift during the post-seizure period.

A, Example seizure recorded in current clamp mode (black trace) during which E_{GABA-A} measurements were made every 30 seconds (red circles). Arrows indicate the start and end of the seizure, which were used as reference points across cells. ***B,*** Mean E_{GABA-A} values plotted in relation to seizure start and end times. Seizures induced a positive shift in E_{GABA-A}, which recovered and then exhibited a transitory negative undershoot during the post-seizure period. This undershoot then gradually returned towards more positive values. The horizontal dashed line indicates the mean E_{GABA-A} before the start of the seizure; error bars - S.E.M; * - $p < 0.05$, # - $p < 0.01$, repeated ANOVA measurements with post-hoc Dunnett test for multiple comparisons.

as a result of the increased driving force for the $GABA_A$Rs and therefore could help to minimise further seizure activity. Therefore, understanding the mechanisms that underlie this undershoot in E_{GABA-A} could offer important insights into the pathophysiology of epilepsy and this was my focus for the remainder of this Chapter.

5.2 Post-seizure hyperpolarisation of the cell's membrane potential is required for the transitory negative shift in E_{GABA-A}.

Several mechanisms could account for an increased Cl^- extrusion in the post-seizure period. First, there could be an increased activity/availability of the Cl^--extruding transporter KCC2. Previous studies have reported that seizures in the neonatal brain can trigger the increase in surface availability of KCC2, which can enhance Cl^- extruding capabilities (Khirug et al., 2010). Nevertheless, these effects occur over a much longer timescale making it an unlikely candidate for the effects presented here. Second, increased Cl^- extrusion could result from the recruitment of voltage-gated ClC-2 Cl^- channels. ClC-2 Cl^- channels have been reported to be activated by high intracellular Cl^- levels and membrane hyperpolarisation, and have been shown to contribute to Cl^- clearance during intense activation of GABAergic synapses (Foldy et al., 2010). Third, increased Cl^- extrusion could occur via active $GABA_A$Rs if the cell's membrane potential is hyperpolarised relative to E_{GABA-A}, as this would set the driving force for Cl^- to move out through the receptor. Given that hyperpolarisation of the membrane potential would play an important role in clearing Cl^- through either ClC-2 channels or $GABA_A$Rs, I decided to explore the relationship between the membrane potential and changes in E_{GABA-A} in the neonatal seizures.

As shown in Chapter 3, seizures can lead to the activation of downstream K^+ channels, which generate a significant hyperpolarisation of the membrane potential in the

post-seizure period. To test whether a similar phenomenon is present during neonatal seizures and how it might influence Cl^- extrusion, I averaged the membrane potential for each epoch in current clamp (27.5 s duration) and compared this to the E_{GABA-A} measured in voltage clamp (Figure 5.3A). To account for variations in resting E_{GABA-A} and membrane potential values, all measurements were normalised to the mean of the pre-seizure values. This allowed the simultaneous monitoring of relative changes in both membrane potential and E_{GABA-A} (Δ-MP and Δ-E_{GABA-A}) in relation to seizure activity. As illustrated in Figure 5.3B, seizure activity induced a hyperpolarisation of the membrane potential in the post-seizure period. In the first 2 min post-seizure, the level of hyperpolarisation reached a value of -12.4 ± 2.4 mV relative to pre-seizure baseline ($p < 0.01$, $n = 8$, repeated measures ANOVA with post-hoc Dunnett multiple comparisons). This hyperpolarisation of the membrane potential then gradually decreased and reached a value of -5.1 ± 0.6 mV at 18 min post seizure ($p < 0.01$, $n = 8$, repeated measures ANOVA with post-hoc Dunnett multiple comparisons). These results show that seizures induce a long-lasting hyperpolarisation of the membrane potential in the post-seizure period, which could therefore contribute to the negative shift in E_{GABA-A} by stimulating Cl^- clearance via mechanisms such as ClC-2 channels and/or $GABA_A$Rs. As a first step towards investigating the relationship between the post-seizure membrane hyperpolarisation and the transitory undershoot in E_{GABA-A}, I tested whether the two parameters correlate with one another. As illustrated in Figure 5.4 there was a significant positive correlation between the level of post-seizure hyperpolarisation and the post-seizure shift in E_{GABA-A} ($r = 0.45$, $p < 0.001$, linear regression; Figure 5.4). This correlation is consistent with a role for post-seizure hyperpolarisation in modulating E_{GABA-A} changes, although it is not possible to say whether this is a causal relationship.

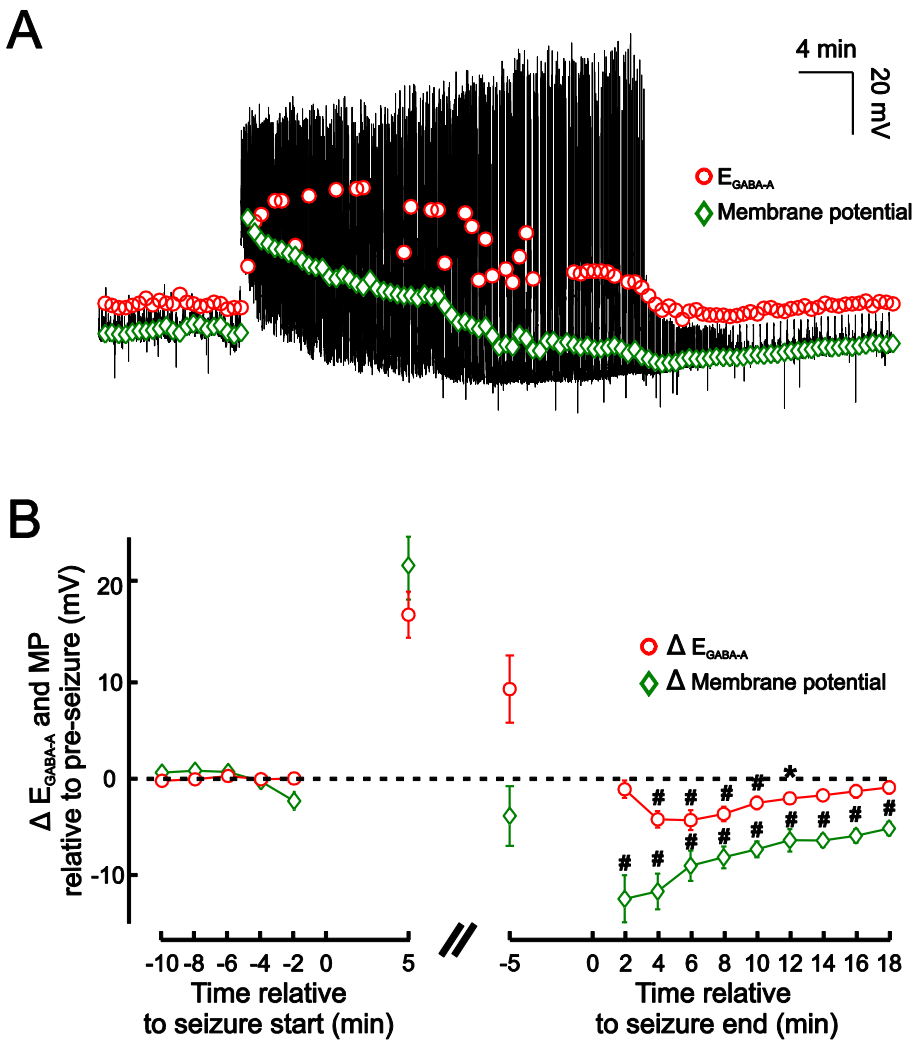


Figure 5.3 Neonatal seizures induce a post-seizure hyperpolarisation of the membrane potential that correlates with the post-seizure negative shift in E_{GABA-A}.

A, Example seizure recorded in current clamp mode (black trace) in which both E_{GABA-A} (red circles) and the membrane potential (green diamonds) were assessed every 30 seconds. ***B***, Seizures induced a long-lasting hyperpolarisation of the membrane potential in the post-seizure period. Note that this post-seizure hyperpolarisation was evident even at 18 min post-seizure. Error bars - S.E.M; * - $p < 0.05$, # - $p < 0.01$, repeated ANOVA measurements with post-hoc Dunnett test for multiple comparisons versus the pre-seizure baseline values.

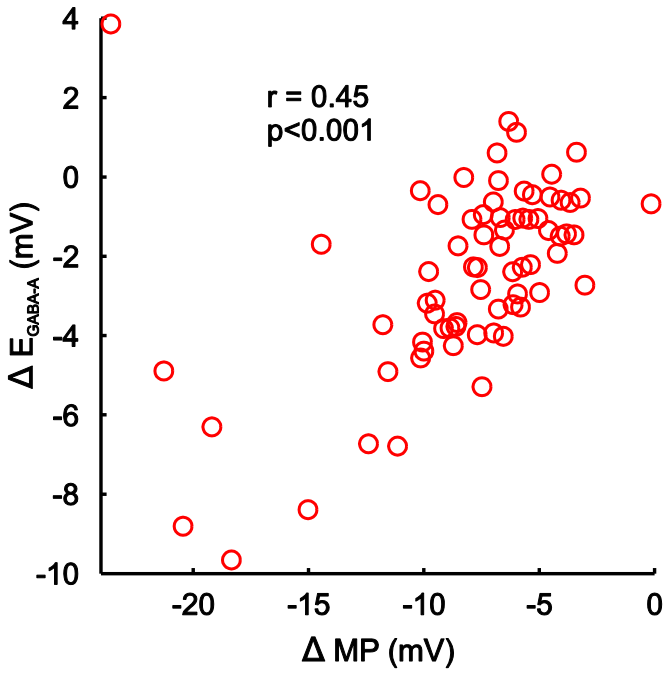


Figure 5.4 Post-seizure membrane potential hyperpolarisation correlates with the negative shift in E_{GABA-A}.

The degree of post-seizure hyperpolarisation of the membrane potential (MP) correlated strongly with the post-seizure shift in E_{GABA-A} ($r = 0.45$, $p < 0.001$, linear regression). More hyperpolarised membrane potentials were associated with more negative shifts in E_{GABA-A}. Data are from the post-seizure period of 8 CA3 pyramidal neurons.

To test directly whether post-seizure membrane hyperpolarisation contributes to the negative shift in E_{GABA-A}, I conducted a series of experiments in which I prevented CA3 pyramidal cells from experiencing the hyperpolarisation by clamping their membrane potential at -70 mV. Recordings initially alternated between current clamp and voltage clamp modes, as described above. However, 10 min after the start of the seizure the recording mode was switched to continuous voltage clamp and the holding potential was set to -70 mV. For the reminder of the experiment E_{GABA-A} continued to be measured every 30 s. As illustrated in Figure 5.5A and B, voltage clamping cells at -70 mV abolished the post-seizure negative shift in E_{GABA-A}. This effect was first detected at 8 min post-seizure (+0.4 ± 1.4 mV versus -3.6 ± 0.7 mV, $p < 0.05$, unpaired t-test) and persisted to the end of the recordings, 18 min after the end of the seizure (+4.0 ± 2.5 mV versus -0.9 ± 0.6 mV, $p < 0.05$, unpaired t-test). Across the entire post-seizure period, voltage clamped cells showed a small positive shift in E_{GABA-A} in contrast to the negative shift in E_{GABA-A} observed in the control cells (+1.4 ± 1.6 mV versus -2.4 ± 0.6 mV, $p < 0.05$, unpaired t-test; Figure 5.5C). These differences were not due to different levels of intracellular Cl^- loading during the actual seizure, as the positive shift in E_{GABA-A} during the seizure was statistically indistinguishable for voltage clamped and control cells (+13.3 ± 3.7 mV versus +14.2 ± 2.7 mV, $p = 0.84$, unpaired t-test).

In addition to preventing the negative shift in E_{GABA-A}, the voltage clamped cells revealed a trend towards an increasingly depolarised E_{GABA-A} during the post-seizure period, which reached +4.0 ± 2.5 mV by the end of the recordings ($n = 5$, slope = 0.76, r-squared = 0.13, $p < 0.05$, repeated ANOVA measures test for linear trend). This observation suggests that, concomitant with the hyperpolarisation-dependent Cl^- unloading mechanism, there could be an underlying slow, Cl^- accumulating mechanism that gradually shifts E_{GABA-A} towards more depolarised values during the post-seizure period.

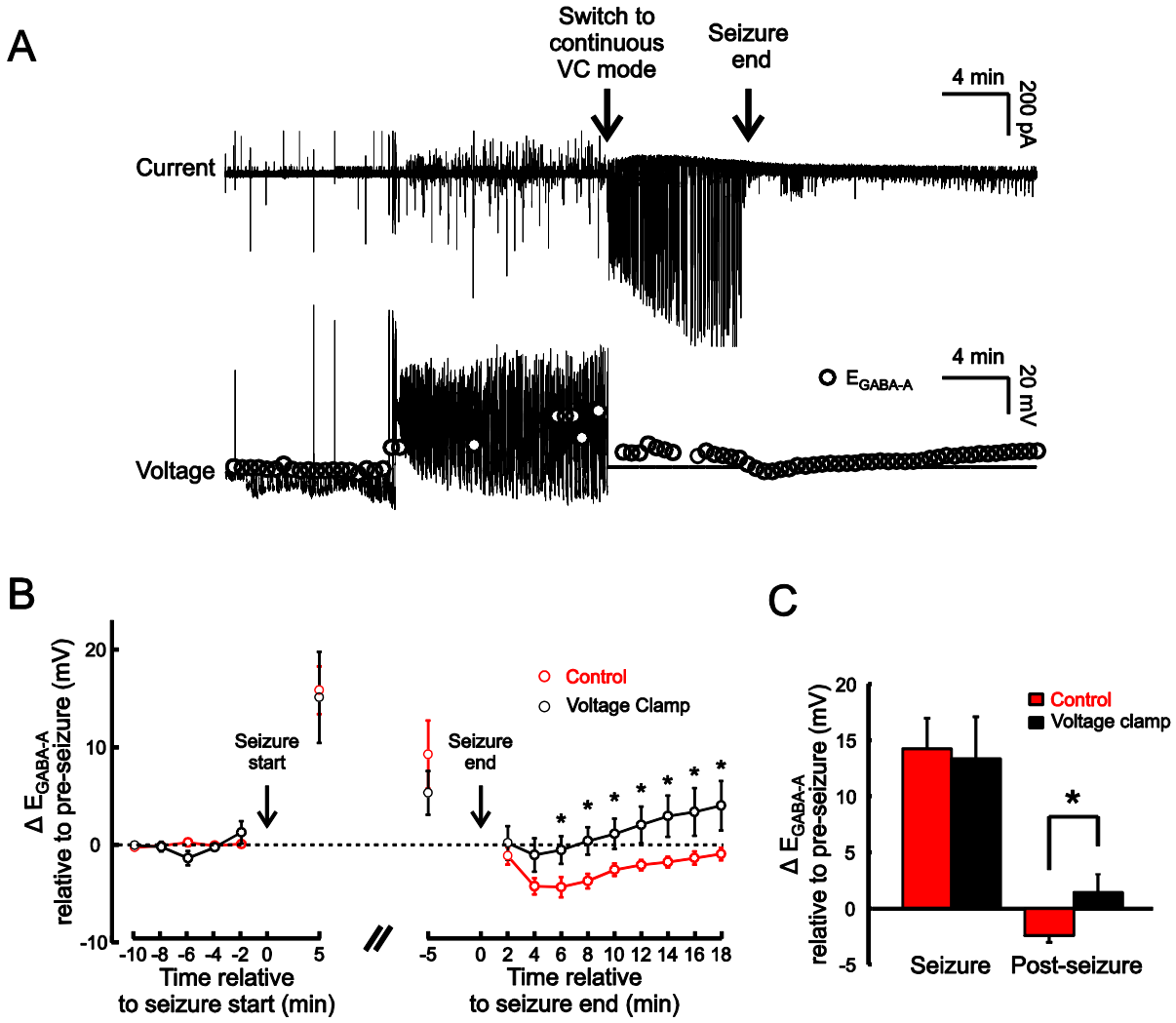


Figure 5.5 Preventing the post-seizure hyperpolarisation of the membrane potential abolishes the negative shift in E_{GABA-A}.

A, Example recording from a CA3 pyramidal neuron in which the post-seizure hyperpolarisation was prevented by voltage clamping the cell's membrane potential at -70 mV. First arrow indicates the point when the recording was switched to continuous voltage clamp mode. E_{GABA-A} continued to be assessed every 30 seconds (circles). Seizure end (second arrow) was determined from the current recordings. ***B,*** Population data showing that voltage clamping cells prevented the post-seizure negative shift in E_{GABA-A}. Dashed horizontal line represents the pre-seizure values. ***C,*** A comparable depolarising shift in E_{GABA-A} occurred during the course of the actual seizure in control and voltage clamped cells. However, across the post-seizure period voltage clamped cells did not show the negative shift in E_{GABA-A} that was shown by control cells. Error bars - S.E.M; * - $p < 0.05$, unpaired t-test.

.

The two most likely candidates to account for such an effect are Cl^- clearance via voltage-gated ClC-2 channels and/or via $GABA_A$Rs and these could be explored in future studies.

5.3 Discussion

In this Chapter I developed protocols to investigate $E_{GABA\text{-}A}$ dynamics during neonatal seizures and their post-seizure recovery periods. In agreement with previous studies, I found that $E_{GABA\text{-}A}$ shifts to more positive values during the seizure, consistent with Cl^- loading during periods of intense neuronal activity (Isomura et al., 2003b; Isomura et al., 2008). At the end of the seizure $E_{GABA\text{-}A}$ had already recovered to approximately pre-seizure values. Surprisingly, during the post-seizure period $E_{GABA\text{-}A}$ actually exhibited a transient undershoot as $E_{GABA\text{-}A}$ became more negative than before the seizure. I explored potential mechanisms that may be responsible for this effect and found that hyperpolarisation of the cell's membrane potential is both correlated with, and required for, the transient $E_{GABA\text{-}A}$ undershoot during the post-seizure recovery period. These results reveal a powerful post-seizure hyperpolarisation-dependent Cl^- unloading mechanism. Consistent with the importance of this mechanism, when the post-seizure hyperpolarisation was prevented, the undershoot in $E_{GABA\text{-}A}$ was abolished. Indeed, under these conditions $E_{GABA\text{-}A}$ showed a gradual shift towards more positive values, consistent with the concomitant presence of a slow Cl^- loading mechanism. The dynamic changes in $E_{GABA\text{-}A}$ described here could have important implications for the pathophysiology of epilepsy and may relate to the observation that repeated seizures can lead to progressive changes in Cl^- homeostasis.

Previous studies have reported both acute increases in intracellular Cl^- levels during seizures (Fujiwara-Tsukamoto et al., 2003) and long-lasting changes in Cl^- homeostasis that

are associated with chronic epilepsy (Cohen et al., 2002; Huberfeld et al., 2007). Indeed, repeated seizures have been shown to be associated with intracellular Cl^- accumulation, a progressive shift in E_{GABA-A} towards more positive values, and a shift in the operating mode of GABAergic signalling from inhibitory to excitatory (Dzhala et al., 2010; Nardou et al., 2009; Nardou et al., 2011). Nevertheless, the exact time course of these changes and the mechanisms by which seizures lead to such persistent changes in Cl^- homeostasis are not fully understood. One crucial question is what happens in the period immediately following a seizure. Using repeated E_{GABA-A} measurements I was able to address this question for single neonatal seizure episodes. My experiments revealed for the first time the presence of a transitory negative shift in E_{GABA-A} during the post-seizure period. This correlated with the hyperpolarisation of the membrane potential and was abolished when the membrane potential was clamped experimentally. The exact mechanisms by which neonatal seizures induce hyperpolarisation of the membrane potential remain to be elucidated. However, it seems feasible that, as shown in Chapter 3, seizures in the neonatal brain could trigger the release of adenosine, which results in the activation of K^+ channels that hyperpolarise the postsynaptic membrane potential (Kawamura, Jr. et al., 2010; Takigawa and Alzheimer, 2002). Indeed, consistent with this idea, ARs have been found to be expressed early in the developing hippocampus (Rivkees, 1995). In addition, Na^+ entry during sustained burst firing may increase the activation of the Na^+/K^+-ATPase pump, which could contribute to post-seizure hyperpolarisation. Future work could use pharmacological manipulations to explore the effect of blocking ARs and the Na^+/K^+-ATPase pump on post-seizure hyperpolarisation and E_{GABA-A} dynamics.

The transient E_{GABA-A} undershoot suggests the existence of a hyperpolarisation-dependent Cl^- unloading mechanism in the post-seizure period. One question that remains to be answered is what are the mechanisms by which hyperpolarisation of the postsynaptic

membrane potential leads to enhanced Cl^- clearance. The two most likely candidates for such an effect are Cl^- extrusion via voltage-gated ClC-2 channels and/or Cl^- extrusion via $GABA_A$Rs. Hyperpolarisation of the membrane potential activates the voltage-gated ClC-2 channel, which is known to be expressed in the neonatal hippocampus (Clayton et al., 1998b) and has been shown to contribute to Cl^- clearance during periods of intense GABAergic activity in the mature hippocampus (Foldy et al., 2010). To test if this mechanism plays a significant role in post-seizure Cl^- unloading, future studies could investigate $E_{GABA\text{-}A}$ dynamics in ClC-2 knock-out mice. An alternative approach could be the acute knock-down of ClC-2 in individual neurons using RNA-interference methods. This would have the advantage of avoiding the effects of ClC-2 knock-down on the whole network and any potential compensatory mechanisms (Rinke et al., 2010). The other possibility is that hyperpolarisation of the membrane potential leads to Cl^- unloading via the $GABA_A$R. This would require that $GABA_A$Rs remain active in the post seizure period. Since seizures are associated with intense activation of GABAergic synapses and the release of large amounts of GABA (Meurs et al., 2008), it is conceivable that $GABA_A$R activity does persist into the post-seizure recovery period. Indeed, tonic $GABA_A$R currents are reported to be preserved in epileptic tissue (Pavlov and Walker, 2012). To test the significance of the $GABA_A$R for Cl^- unloading, future studies could use Cl^- imaging techniques in combination with the administration of $GABA_A$R antagonists in the post-seizure period (Berglund et al., 2008).

When the post-seizure membrane potential hyperpolarisation was prevented, the negative shift in $E_{GABA\text{-}A}$ was abolished and $E_{GABA\text{-}A}$ gradually moved towards more positive values, indicating that Cl^- accumulating mechanisms might also be active in the post-seizure period. It should be noted that due to the effects of access resistance in patch clamp recordings, the voltage control of the cell would not have been ideal in these experiments and some hyperpolarisation is still likely to have occurred. This suggests that the underlying Cl^-

accumulating mechanism may be more pronounced than the data indicate and highlights that future studies are required to dissect the different contributions to Cl^- homeostasis following a seizure.

In summary, the data presented in this Chapter reveal that the interplay of Cl^- loading and unloading mechanisms control the dynamics and stability of $E_{GABA\text{-}A}$, not only during seizures, but also beyond the seizure, into the post-seizure period.

6 General Discussion

In this Chapter I will summarise the main experimental observations from my thesis, discuss methodological considerations and finish by integrating my findings with current hypotheses regarding altered GABAegic signalling in epilepsy.

6.1 Experimental findings

The aim of my thesis was to investigate the factors and processes responsible for controlling postsynaptic GABAergic signalling during seizure activity. These phenomena could prove crucial for understanding the pathophysiology of epilepsy given that during seizure activity, GABAergic inhibition fails and GABA can become an excitatory and seizure-promoting factor (Cohen et al., 2002; Dzhala et al., 2005; Dzhala et al., 2010; Fujiwara-Tsukamoto et al., 2003; Fujiwara-Tsukamoto et al., 2006; Isomura et al., 2003b; Nardou et al., 2011). In Chapter 3, I investigated the role of the neuromodulator adenosine in regulating post-seizure GABAergic signalling during epileptiform activity. I found that seizure activity leads to a transient switch in the action of $GABA_A$Rs from inhibitory to excitatory, consistent with a temporary collapse in the transmembrane gradient for Cl^- (Fujiwara-Tsukamoto et al., 2003; Isomura et al., 2003b). At the same time, seizure activity induces the release of adenosine into the extracellular space. The resulting AR activation reduces the amplitude of excitatory postsynaptic GABAergic responses during seizures and the suppression of GABAergic responses lasts beyond the period that $E_{GABA\text{-}A}$ is depolarised. These effects of endogenously released adenosine are mimicked by exogenous adenosine administration. In examining the mechanism of adenosine's effects, I established that adenosine does not change the Cl^-

homeostasis mechanisms that set $E_{GABA\text{-}A,}$ or the conductance of $GABA_A$Rs. Rather, A_1R-dependent activation of K^+ channels accounts for the suppression of depolarising and hyperpolarising GABAergic potentials via an increase in postsynaptic membrane conductance and a resulting shunting effect. This adenosine-induced suppression of depolarising and excitatory GABAergic responses might represent a novel mechanism by which adenosine exerts antiepileptic effects.

To better understand the depolarising actions of GABA during seizure activity, I turned my focus to Cl^- regulating mechanisms. In Chapter 4 I began by examining the developmental regulation of $E_{GABA\text{-}A}$ and its relation to the expression of the Cl^- transporters NKCC1 and KCC2. I found that $E_{GABA\text{-}A}$ undergoes a hyperpolarising shift during the first two post-natal weeks. In this period total KCC2 expression increases significantly and the relative proportion of KCC2 at the surface of cells remains constant. Interestingly, NKCC1 expression also increases over the same period, but its delivery to the surface of the cell is reduced. These results suggest that in addition to transcriptional control, NKCC1 could be regulated via its trafficking to the membrane. To investigate the molecular mechanisms that underlie such regulation of NKCC1 I screened for NKCC1-associated proteins. A combination of immunoprecipitation, mass spectrometry, biochemical and immunohistochemical studies all identified the motor protein Myosin Va as a candidate NKCC1-associated protein. To test the functional role of Myosin Va in regulating NKCC1 I developed an electrophysiological assay that allows the measurement of NKCC1 contribution to Cl^- homeostasis. Disrupting endogenous Myosin Va activity resulted in a significant reduction in NKCC1 contribution to Cl^- homeostasis, suggesting that Myosin Va is crucial for NKCC1 function. To investigate a potential activity-dependent regulation of NKCC1 via Myosin Va, I developed a neonatal seizure model and found that seizures induced an NKCC1-dependent positive shift in $E_{GABA\text{-}A}$ that was evident only later during the post-

seizure period. Although disrupting Myosin Va function seemed to prevent this seizure-induced shift, more studies are needed to conclusively establish Myosin Va's role in the activity-dependent regulation of NKCC1.

In Chapter 5 I conducted experiments to further explore the time-dependent processes that are responsible for modulating E_{GABA-A} during, and after, seizures. I developed a method that allows repeated E_{GABA-A} measurements, which enabled me to investigate E_{GABA-A} dynamics during seizure activity. This confirmed that E_{GABA-A} shifts to more positive values during the seizure, consistent with Cl^- loading during the period of most intense neuronal activity. By the end of the seizure, E_{GABA-A} had recovered to approximately pre-seizure values. Surprisingly however, in the post-seizure period E_{GABA-A} became more negative than pre-seizure values. This 'undershoot' in E_{GABA-A} was relatively long-lasting as it persisted for over 10 min during the post-seizure period. In exploring the mechanisms responsible for this effect, I found that post-seizure hyperpolarisation of the cell's membrane potential correlated with the E_{GABA-A} undershoot and that preventing the post-seizure hyperpolarisation abolished the E_{GABA-A} undershoot. These results therefore identify a novel post-seizure hyperpolarisation-dependent Cl^- extruding mechanism. Furthermore, when this mechanism was prevented, E_{GABA-A} showed a slow shift towards more depolarised values thus revealing the concomitant presence of a slow Cl^- loading mechanism. This further highlights the importance of the membrane hyperpolarisation mechanism in preventing potentially deleterious depolarising shifts in E_{GABA-A} during the post seizure period. Alterations in the balance of these Cl^- loading and extruding processes could render the network more or less susceptible to further seizure episodes.

6.2 Methodological considerations

6.2.1 Organotypic hippocampal slices

Experiments in my thesis were performed in organotypic hippocampal slices. This preparation has the advantage of preserving the basic features of hippocampal organisation while allowing easy access to the tissue for genetic and chronic pharmacological manipulations. Dissociated neuron cultures could also be used for genetic and pharmacological manipulations. Nevertheless, dissociated cultures do not preserve the network architecture and connectivity patterns, which are crucial for studying seizure activity. This further highlights the advantage of using organotypic slices over dissociated cultures. When compared to acute hippocampal slices, organotypic slices have been found to preserve nearly all aspects of GABAergic and glutamatergic synaptic transmission (Streit et al., 1989; De et al., 2003). Furthermore, I found that organotypic slices preserve the developmental transition in $E_{GABA\text{-}A}$ from depolarising to hyperpolarising, which has been described previously in the first two post-natal weeks using acute hippocampal slices from rat (Tyzio et al., 2007). Nevertheless, in addition to preserving the basic hippocampal architecture and synaptic transmission properties, organotypic slices also develop recurrent connectivity that can increase the overall excitability of the network (Gutierrez and Heinemann, 1999). Indeed, when kept for more than 14 days in vitro the organotypic slices develop spontaneous seizure activity (Berdichevsky et al., 2012). Similar recurrent connectivity that leads to increased excitability has also been reported in human epileptic tissue and tissue form epileptic animal models (Parent and Lowenstein, 1997; Sutula and Dudek, 2007). These aspects make the organotypic hippocampal slices an attractive in vitro model for studying the development of epilepsy (Berdichevsky et al., 2012).

6.2.2 Measuring E_{GABA-A} with gramicidin-perforated patch clamp recordings

Throughout my thesis I used gramicidin-perforated patch clamp recordings to measure E_{GABA-A}. Gramicidin forms pores in the cell's membrane that are permeable to cations, but not to Cl^- ions. This technique therefore allows electrical access to the cell without interfering with the native $[Cl^-]_i$ (Kyrozis and Reichling, 1995). Nevertheless, one potential concern is that Cl^- levels might be indirectly affected by the fact that the pores are permeable to K^+ and Na^+, which in principle could alter the ionic gradients that drive KCC2 and NKCC1 transporters (Brumback and Staley, 2008a). An alternative to gramicidin-perforated patch clamp recordings is to use cell-attached recordings to measure E_{GABA-A} from single $GABA_AR$ channel activity. However, E_{GABA-A} measurements have been shown to be very similar in studies using gramicidin-perforated recordings (Tyzio et al., 2007) or cell attached recordings (Tyzio et al., 2008), suggesting that ionic gradients are not affected. A further advantage of gramicidin is that it is compatible with the long duration recordings that are required for investigating E_{GABA-A} dynamics, whereas the cell-attached technique uses $GABA_AR$ agonists in the pipette that are likely to cause desensitisation of the receptor.

6.2.3 Seizure models

In order to study seizure-like activity I used two in vitro models in organotypic hippocampal slices: 1) the 0 Mg^{2+} model used in mature slices and 2) the 0 Mg^{2+} combined with 4-AP model used in neonatal slices. Both 0 Mg^{2+} and 4-AP increase neuronal excitability by un-blocking NMDA receptors (in the case of 0 Mg^{2+}) and by blocking K^+ currents (in the case of 4-AP). In the mature slices, 0 Mg^{2+} alone was sufficient to trigger seizures. In the neonatal slices, although 0 Mg^{2+} increased the activity of neurons, it was not sufficient to trigger seizures. This difference between the mature and neonatal slices is probably due to lower levels of glutamatergic synaptic connectivity between neurons at the neonatal stage (Hsia et

al., 1998). In addition, mature slices were kept in culture for longer than the neonatal slices, thus further increasing the potential for forming recurrent connections (Berdichevsky et al., 2012; Gutierrez and Heinemann, 1999). In spite of these differences, seizures triggered in both mature and neonatal slices showed similar electrophysiological characteristics with two distinguishable seizure phases: 1) the tonic (ictal-like) phase followed by 2) the clonic (after-discharge) phase. These two phases of seizure activity have been described in numerous studies in vitro and in vivo using different methods for triggering seizure activity, including pharmacological manipulations and electrical stimulation (Trevelyan et al., 2007a; McCormick and Contreras, 2001; Matsumoto and Marsan, 1964; Luhmann et al., 2000; Isomura et al., 2003a). This suggests that regardless of the initial precipitating factor that initiates the seizure, common electrophysiological patterns are present once a seizure has begun.

In addition to the tonic-clonic pattern of neuronal activity, seizures in mature slices (Chapter 3) reproduced another general feature of seizure activity: the release of adenosine and activation of ARs followed by hyperpolarisation of the membrane potential. Indeed, numerous studies using in vitro and in vivo animal models, and even direct measurements in the hippocampus of human epileptic patients, have revealed high levels of adenosine release during seizures (Berman et al., 2000; During and Spencer, 1992; Lopatar et al., 2011). Although not directly tested here, it is likely that seizures in neonatal slices also induced release of adenosine given that there was a pronounced hyperpolarisation of the membrane potential in the post-seizure period and that ARs are expressed at an early stage in the developing hippocampus (Rivkees, 1995).

Another characteristic finding in both neonatal and mature seizures was the depolarising shift in GABAergic signalling that occurred during the course of seizure activity and which was sufficient to render $GABA_AR$ responses excitatory. Such a change has

previously been reported both in the acute setting of a seizure (Isomura et al., 2003b; Fujiwara-Tsukamoto et al., 2003) and in the chronic epileptogenic period following an insult such as status epilepticus (Barmashenko et al., 2011; Jin et al., 2005). In addition, recordings in hippocampal slices generated from tissue that was surgically excised from adult human epileptic patients, have found that ~25 % of pyramidal neurons exhibit depolarising GABAergic responses during inter-ictal events (Cohen et al., 2002). Moreover, these depolarising responses correlate with alterations in the expression of Cl^- transporters that are responsible for Cl^- homeostasis (Huberfeld et al., 2007). Taken together, these studies suggest that alterations in Cl^- homeostasis that lead to depolarising GABAergic transmission are a key process in the pathophysiology of epilepsy. Nevertheless, Cl^- accumulation and a shift to excitatory GABAergic signalling have not yet been directly demonstrated in vivo. Repeated E_{GABA-A} measurements from Chapter 5 suggest that seizure activity as short as 30 seconds is sufficient to induce a significant depolarising shift in E_{GABA-A}. Given that in vivo single seizure episodes usually range from tens of seconds to min (reaching over 30 min in the case of status-epilepticus), it is likely that Cl^- accumulation does occur in vivo and could lead to weakened inhibition and even excitatory GABAergic signalling. This could explain why positive modulators of $GABA_A$Rs such as diazepam are effective in stopping seizures only if administered early after the start of the seizure and not after prolonged seizure activity (Walton and Treiman, 1988; Goodkin et al., 2003).

One important consideration is whether the in vitro seizure models reliably reproduce the features of seizures in humans with chronic epilepsy. Most of the evidence regarding human seizure activity comes from extracellular recordings in patients under evaluation for surgical epilepsy treatment. Recently it has been found that the pattern of seizure propagation is extremely similar between spontaneous seizures recorded in human patients and seizures triggered in brain slices exposed to 0 Mg^{2+} (Schevon et al., 2012; Trevelyan et al., 2007b;

Trevelyan et al., 2006). Work in rodent brain slices has revealed an important role for feed-forward inhibitory circuits in restraining the spread of seizure activity from the seizure focus to adjacent neuronal tissue (Trevelyan et al., 2007b; Trevelyan et al., 2006). A similar pattern has been found in human seizures where neuronal territories away from the initial seizure focus have been shown to be recruited to participate in the seizure activity, but only once the inhibitory restraint on neuronal activity has been overcome (Schevon et al., 2012). This suggests that even though in vitro seizure models may not reproduce the initial cause of a seizure, they are a reliable representation of seizure propagation from an epileptic focus into adjacent neuronal tissue.

In summary, in vitro seizure models reproduce fundamental features of seizures triggered in vivo and resemble seizures recorded in human patients. Therefore such models represent a valuable tool for studying the basic pathophysiological mechanisms underlying seizure propagation and for the development of new antiepileptic drugs aimed at restricting the spread of seizure activity. They offer important possibilities to study the cellular and molecular mechanisms that would not be accessible in in vivo preparations. However, it would seem logical that once a mechanism is described in vitro, its relevance should be confirmed using in vivo models. By this argument, an area for future research is to examine seizure-related changes in postsynaptic GABAergic transmission in the fully intact brain.

6.3 The role of adenosine in regulating postsynaptic GABAergic responses during seizures

In my thesis I have explored several mechanisms responsible for regulating the postsynaptic response to $GABA_AR$ activation. In the remaining sections I will discuss the relevance of these mechanisms for seizure activity that has been described in other studies.

In Chapter 3 I showed that GABAergic signalling during seizures switches from inhibitory to excitatory, and therefore activation of $GABA_A$Rs under these conditions is predicted to contribute to ongoing seizure activity. At the same time, seizures trigger the release of the neuromodulator adenosine, which leads to K^+ channel activation in the postsynaptic cell. This results in an increase in the cell's membrane conductance, and in doing so, creates a shunting effect that reduces the impact of depolarising GABAergic signalling. This may represent a novel mechanism by which adenosine limits seizure activity. Consistent with this idea, I found that blocking ARs increases the seizure duration primarily by increasing the number of after-discharge events. Adenosine activates both pre- and postsynaptic A_1Rs (Fredholm et al., 2005) and by doing so it influences both glutamatergic and GABAergic synaptic transmission. Activation of presynaptic A_1Rs has been shown to reduce glutamate release at excitatory synapses but not GABA release at inhibitory synapses onto pyramidal cells in the hippocampus (Thompson et al., 1992; Yoon and Rothman, 1991). This is consistent with a scenario in which adenosine mediates the shut-down of excitatory glutamatergic synaptic transmission as the seizure progresses. Meanwhile, as GABAergic transmission is maintained and becomes depolarising due to the collapse in Cl^- gradients, GABAergic synapses may become the principal driver of activity. Consistent with this view, it has recently been shown that electrical stimulation can induce prototypic seizure-like activity that is dependent solely on GABAergic transmission (Fujiwara-Tsukamoto et al., 2010). Under such conditions it is likely that the postsynaptic activation of A_1Rs and the resulting reduction in depolarising GABAergic responses plays an important role in reducing ongoing seizure activity. Nevertheless, the presynaptic reduction in glutamate release would be predicted to reduce neuronal activity in both pyramidal cells and interneurons. Therefore it seems likely that during the course of a seizure, both pre- and postsynaptic activation of A_1Rs play important seizure-limiting roles via different mechanisms: while presynaptic A_1R

activation decreases glutamate release, postsynaptic A_1R activation reduces the effects of incoming depolarising GABAergic responses.

One interesting question is whether adenosine differentially modulates different types of inhibitory synaptic inputs. More than 20 different types of interneurons have been described in the hippocampus (Klausberger and Somogyi, 2008). These have different properties, morphologies and target different compartments of the pyramidal neurons. Recently, it has been suggested that Cl^- can be differentially regulated in different subcellular compartments of pyramidal neurons. For instance, the axon initial segment has been reported to have higher Cl^- levels, which could render the inputs from axo-axonic cells depolarising (Khirug et al., 2008; Szabadics et al., 2006). In addition, CLC-2 channels have been reported to aid Cl^- extrusion at synaptic inputs formed on the pyramidal cell soma by parvalbumin-expressing basket (Foldy et al., 2010). Currently it is unclear whether spatial differences in Cl^- regulation arise during the course of seizure activity. However, it is conceivable that synaptic inputs from different interneurons may be affected differentially by seizure-induced Cl^- accumulation. Moreover, the somato-dendritic distribution of the K^+ channels, which are responsible for the adenosine-induced shunt effect, might also be important for differentially modulating different GABAergic inputs. In my study, $GABA_ARs$ were activated by local application of GABA, which does not differentiate between different types of interneuronal input. However, recent advances in the genetics of interneurons have identified specific promoters for several types of interneurons (Madisen et al., 2012). Using these promoter sequences, several mouse lines expressing Cre recombinase in specific interneuron subtypes have been generated and are now readily available (Madisen et al., 2012). Future studies could combine these mice with viral-mediated gene transfer in order to deliver optogenetic tools that would allow the specific activation/inhibition of different interneuron subtypes.

This would make it possible to address whether interneuron subtypes are differentially affected by Cl^- accumulation and by adenosine release during seizure activity.

The exact mechanism of adenosine release has not been fully elucidated but it is likely that different adenosine sources are important during normal and pathological conditions (Dale and Frenguelli, 2009). Under normal physiological conditions, ATP released from astrocytes and the extracellular degradation of ATP into adenosine has been shown to be responsible for a low basal adenosine tone (Pascual et al., 2005). Furthermore, electrical stimulation in the hippocampus has been found to increase adenosine levels via both direct release from neurons and ATP release from glial cells (Wall and Dale, 2013). During seizures however, it has recently been suggested that adenosine accumulates via direct release from neurons and that extracellular ATP degradation does not play a significant role (Lovatt et al., 2012). An important question is how the temporal and spatial distribution of adenosine release relates to the seizure dynamics. Unfortunately, current techniques for measuring adenosine concentration are somewhat limited in both time and space (During and Spencer, 1992; Lopatar et al., 2011). Nevertheless, previous studies using microdialysis in human patients with epilepsy have reported that during a seizure, adenosine is increased in both the epileptogenic hippocampus (where seizures are initiated) and in the contralateral hippocampus (During and Spencer, 1992). These results are in accordance with a widespread role for adenosine in both stopping ongoing seizure activity and in restricting the spread of seizures from an epileptic focus (Fedele et al., 2006). After the end of the seizure, adenosine persists in the extracellular space for several minutes until it is cleared or metabolized (During and Spencer, 1992; Lopatar et al., 2011). Consistent with this, I found that adenosine signalling in the post-seizure period continued to attenuate $GABA_AR$ signalling once it had returned to having a hyperpolarising effect.

In addition to epilepsy, adenosine has been found to be released in other pathological conditions such as cerebral ischemia (Dale and Frenguelli, 2009). Interestingly, this condition has also been associated with alterations in Cl^- homeostasis mechanisms (Jaenisch et al., 2010; Galeffi et al., 2004). Therefore, it seems likely that the adenosine-induced modulation of GABAergic responses described in Chapter 3 may also be relevant in the 'ischemic' brain. Indeed, activation of A_1R has been found to control both the suppression and recovery of network activity during an ischemic episode (Ilie et al., 2006; Ilie et al., 2009; Constantinescu et al., 2011). Future studies could investigate the exact timing of GABAergic signalling changes in ischemia and their relation to AR activation.

In conclusion, recordings from hippocampal pyramidal neurons have revealed that adenosine does not have a direct effect upon the presynaptic release of GABA, although GABAergic synapses in other systems do show evidence of presynaptic modulation (Han et al., 2011; Kruglikov and Rudy, 2008; Thompson et al., 1992; Yoon and Rothman, 1991). My observations extend this work by demonstrating that adenosine modulates the postsynaptic effects of GABAergic inputs during the dynamic events of a seizure. The increase in extracellular adenosine that results from intense network activity appears to be well placed to attenuate the deleterious effects of depolarising $GABA_AR$ signaling that typically emerge under the same conditions. Adenosine does this without 'shutting down' GABAergic transmission, unlike its effect upon the glutamateergic system (Thompson et al., 1993). The net effect is that synaptic inhibition is still functional during the recovery period, as activity throughout the network begins to be reinstated.

6.4 Molecular regulation of NKCC1 in the normal and epileptic neonatal brain

To better understand the potential for depolarising actions of GABA, Chapter 4 focused upon mechanisms that are directly involved in Cl^- regulation. I started by examining the developmental expression profile for the Cl^- transporters NKCC1 and KCC2. In agreement with previous studies (Yamada et al., 2004; Tyzio et al., 2007) I found that E_{GABA-A} undergoes a hyperpolarising developmental shift between the early neonatal period and the first two postnatal weeks. Consistent with an increase in Cl^- extrusion capacity that would shift E_{GABA-A} to more negative values, KCC2 expression increased substantially over this period of development and was matched by a proportional delivery of the transporter to the membrane surface. NKCC1 expression increased to a lesser extent, but importantly the rate at which NKCC1 was delivered to the surface of the cell was reduced. These results imply that in addition to transcriptional control, NKCC1's activity is regulated via its delivery to/from the surface of the cell.

The delivery and recycling of proteins at the membrane requires interactions with molecular motor proteins (Hirokawa et al., 2010; Heisler et al., 2011). For example, the trafficking of neurotransmitter receptors (such as Glutamate Rs, Glycine Rs or $GABA_A$ Rs) to and from the cell surface is regulated by adaptor proteins that interact with microtubule- and actin-based molecular transporters (Nakajima et al., 2012; Setou et al., 2002; Maas et al., 2006; Correia et al., 2008; Heisler et al., 2011). Although it seems likely that similar interactions control the delivery of Cl^- transporters to the surface of the cell, this possibility has been largely unexplored to date. Using a combination of immunoprecipitation, mass spectrometry, biochemical and immunohistochemical experiments I identified the molecular motor protein Myosin Va as a candidate NKCC1-associated protein. Myosin Va is an actin-based molecular motor, which has been previously found to mediate delivery of different

cargos to the surface of the cells including AMPA receptors (Correia et al., 2008) and intracellular signalling molecules such as phosphatase and tensin homolog (PTEN; van Diepen et al., 2009).

In testing the functional significance of the NKCC1-Myosin Va association, I found that disrupting Myosin Va with a dominant negative construct resulted in more negative resting E_{GABA-A} values and a decrease in NKCC1 contribution to Cl^- homeostasis. These results indicate that Myosin Va is involved in regulating NKCC1 function. However, the exact mechanism by which Myosin Va regulates NKCC1 remains to be explored in future studies. One possibility is that Myosin Va delivers NKCC1 to the plasma membrane and that disrupting Myosin Va results in less NKCC1 protein at the surface. To test this hypothesis, future studies could use biotinylation experiments or immunohistochemical techniques to quantify the proportion of NKCC1 at the surface of cells. Alternatively, Myosin Va could be involved in delivering another protein that could regulate the activity or membrane stability of NKCC1. For instance, NKCC1 activity is regulated via phosphorylation (Rinehart et al., 2011; Delpire and Austin, 2010) and Myosin Va has been previously shown to interact with and regulate the activity of the phosphatase PTEN (van Diepen et al., 2009). It is conceivable that Myosin Va might deliver other kinases/phosphatases to the membrane where they can exert regulatory actions upon NKCC1. Furthermore, it has recently been suggested that Myosin Va is developmentally regulated such that higher levels of Myosin Va are present in developing hippocampal neurons and then decrease with age (Brinn et al., 2010). It is therefore tempting to speculate that the developmental reduction in NKCC1 delivery to the membrane is related to the developmental downregulation in Myosin Va levels.

To test the significance of Myosin Va regulation of NKCC1 in the context of neonatal seizures, I developed an assay to investigate seizure-induced changes in Cl^- homeostasis. I found that seizures induced a NKCC1-dependent depolarising shift that was evident

approximately 30 min after the seizure. Interestingly, cells in which Myosin Va activity was disrupted did not exhibit a statistically significant seizure-induced shift in $E_{GABA-A.}$ However, when the seizure-induced E_{GABA-A} shift was compared between untransfected control cells, untransfected cells in the presence of bumetanide and cells expressing dominant negative Myosin Va, only the control and bumetanide group showed a statistically significant difference. The cells in which Myosin Va was disrupted showed a non-significant trend towards a reduced E_{GABA-A} shift compared to control cells. Therefore at this stage, it is not possible to conclude whether Myosin Va contributes to the seizure-induced shift in E_{GABA-A} and future studies are needed to fully establish a role for Myosin Va during seizure activity. The seizure-induced shift in E_{GABA-A} was relatively modest, with an amplitude of approximately +4 mV. This may have made it difficult to detect a statistically significant effect upon the seizure-induced shift in NKCC1, especially as the Myosin Va manipulation I used did not fully abolish NKCC1 activity under baseline conditions. Future studies could investigate whether the contribution of NKCC1 to the seizure-induced E_{GABA-A} shift is increased with repeated seizure activity. This may make it easier to detect a role for Myosin Va in the activity-dependent regulation of the transporter. Nevertheless, taken together, the results in Chapter 4 are consistent with Myosin Va being important for regulating NKCC1 contribution to Cl^- homeostasis.

Mutations in the human Myosin Va gene have been associated with Griscelli type I or Elejalde syndrome, which is characterised by hypopigmentation of the skin and hair and severe neurological abnormalities including mental retardation and epilepsy (Hurvitz et al., 1993; Griscelli et al., 1978; Pastural et al., 1997). Mutations in the Myosin Va gene in mouse and rat reproduce the clinical symptoms of the human disorder (Takagishi and Murata, 2006; Mercer et al., 1991). It would therefore be interesting to use these genetic models in order to test whether NKCC1 function is reduced, as predicted by the results presented in Chapter 4.

Previous studies have suggested that disruption of NKCC1 function can also lead to altered neuronal circuit development (Wang and Kriegstein, 2011). In addition, knock-out of NKCC1 has been associated with compensatory increases in intrinsic excitability of neurons (Sipila et al., 2009). It remains to be investigated whether such alterations could account for some of the clinical findings in Griscelli syndrome, such as mental retardation and seizures.

In conclusion, previous studies have reported increased NKCC1 activity during both acute seizures and chronic epilepsy (Barmashenko et al., 2011; Dzhala et al., 2010; Li et al., 2008; Sen et al., 2007); however the mechanisms responsible for this effect have been largely unexplored. Here I described a novel molecular association between NKCC1 and Myosin Va and showed that endogenous Myosin Va function is crucial for regulating NKCC1 contribution to Cl^- homeostasis. The exact mechanism of this regulation, and the relevance for epilepsy and for human conditions caused by Myosin Va mutations remain to be explored.

6.5 A chloride unloading mechanism in the post-seizure period

It was observed that the NKCC1-dependent shift in E_{GABA-A} described in Chapter 4 was not evident immediately after the end of the seizure but only after approximately 30 min. In Chapter 5 I further explored the time-dependent processes responsible for modulating E_{GABA-A} during and after a neonatal seizure. I first developed a method that allowed repeated E_{GABA-A} measurements and the investigation of E_{GABA-A} dynamics in relation to seizure activity. Consistent with previous studies (Dzhala et al., 2010; Fujiwara-Tsukamoto et al., 2003; Fujiwara-Tsukamoto et al., 2006; Li et al., 2008; Sen et al., 2007) and with Cl^- accumulation during intense neuronal activity, I found that seizure activity induced a positive shift in E_{GABA-A} that can account for the excitatory responses to $GABA_AR$ activation. Early after the

end of the seizure, E_{GABA-A} recovered to pre-seizure levels but then surprisingly continued to move towards more hyperpolarised values during the post-seizure period. This 'undershoot' in E_{GABA-A} was long-lasting (over 10 min) and correlated with the degree of post-seizure hyperpolarisation of the cell's membrane potential. Furthermore, the undershoot in E_{GABA-A} was abolished when post-seizure hyperpolarisation was prevented by voltage clamping the cell's membrane potential. These results are consistent with a hyperpolarisation-dependent increase in Cl^- extrusion capacity, which aids E_{GABA-A} recovery and boosts the strength of GABAergic inhibition in the post-seizure period. The exact mechanism by which hyperpolarisation of the membrane potential enhances Cl^- clearance in the post-seizure period remains to be investigated. The two most likely candidates for such an effect are Cl^- extrusion via voltage-gated ClC-2 channels and/or Cl^- extrusion via active $GABA_A$Rs that are experiencing an outward driving force for Cl^-. As outlined in Chapter 5, future studies should investigate the contribution of these processes to Cl^- unloading during the post-seizure period.

The hyperpolarisation-dependent Cl^- unloading mechanism described here might have important consequences for the pathophysiology of seizures. Recovery from the seizure-induced Cl^- load and a negative shift in E_{GABA-A} are predicted to increase the strength of GABAergic inhibition in the post-seizure period. This might serve as a preventive mechanism against the induction of multiple seizures. Consistent with this idea, mutations in ClC-2 channels that would reduce the ability of neurons to remove intracellular Cl^- under intense neuronal activity have been associated with human epileptic syndromes (Everett et al., 2007; D'Agostino et al., 2004). It will therefore be interesting to test whether modulating the hyperpolarisation-dependent Cl^- unloading does affect the probability for inducing repeated seizure episodes. Future experiments could alter the degree of membrane hyperpolarisation in the network by manipulating either the adenosine system or K^+ channels and then assess the probability of repeated seizures. Equally important will be to test whether

repeated seizures by themselves can induce alterations in the post-seizure hyperpolarisation-dependent Cl^- unloading mechanism. If repeated seizures do reduce the degree of post-seizure hyperpolarisation, this could result in a positive feed-back for inducing further seizure activity.

The hyperpolarisation-dependent Cl^- unloading mechanism also has implications for the interpretation of experimental data. For instance, if an experimental protocol involves manipulating a cell's membrane potential, this could influence the balance between the cell's Cl^- loading and unloading processes. This is relevant in Chapter 4 for example, where a step protocol was used to estimate E_{GABA-A} and cells were maintained in voltage clamp at -70 mV mode when E_{GABA-A} was measured in the post-seizure period. One would predict that this protocol would effectively disrupt the hyperpolarisation-dependent Cl^- unloading mechanism and, indeed, the post-seizure undershoot in E_{GABA-A} was not observed under these conditions (see Figure 4.9). Future studies into E_{GABA-A} changes should therefore consider the impact of factors that might influence the membrane potential during recordings.

6.6 The role of NKCC1 in neonatal seizure activity

Previous studies have suggested that NKCC1 plays a pro-excitatory role in the context of neonatal seizures by promoting depolarising GABAergic signalling (Dzhala et al., 2005; Dzhala et al., 2008; Dzhala et al., 2010; Nardou et al., 2009; Nardou et al., 2011). Consistent with this view, I found that blocking NKCC1 with bumetanide shifted E_{GABA-A} to more hyperpolarised values and significantly increased the time to seizure initiation. These results suggest that negative E_{GABA-A} values have a protective effect and delay the initiation of a seizure when the network is challenged by hyperexitability conditions (such as occurs during exposure to 0 Mg^{2+} and 4-AP). However, once a seizure was triggered, blocking NKCC1 had

no effect on seizure duration. This suggests that over the course of a seizure, most Cl^- accumulation occurs via alternative mechanisms such as the combined effect of intense $GABA_AR$ activation and increased driving force on the $GABA_AR$ as a result of membrane depolarisation.

During the post-seizure period however, NKCC1 continued to be active and ultimately contributed to a net Cl^- accumulation that shifted E_{GABA-A} to more depolarised values. Although relatively modest in amplitude (approximately + 4 mV), this long-term increase in NKCC1 contribution to E_{GABA-A} could render the network more susceptible to future seizure episodes. Indeed, one would predict this given that NKCC1 activity was associated with shorter times to seizure initiation. Furthermore, the increased activity of NKCC1 could be a cumulative effect in neonatal tissue that would become more pronounced with repeated seizure episodes.

In conclusion, previous animal studies have found a pro-excitatory role for NKCC1 during acute seizures (Dzhala et al., 2005; Dzhala et al., 2010; Nardou et al., 2011) and increased NKCC1 expression in the period preceding the development of epilepsy (Barmashenko et al., 2011; Bragin et al., 2009). These findings are corroborated by studies in humans where NKCC1 expression has been found to be increased in hippocampal tissue from epileptic patients (Sen et al., 2007). Furthermore, blocking NKCC1 has been reported to improve seizure management in both neonatal (Kahle et al., 2009) and adult epileptic patients (Eftekhari et al., 2012). My results further extend these findings by showing that: 1) blocking NKCC1 increases the time to seizure initiation and; 2) seizures induce a delayed, activity-dependent increase in NKCC1 function that can contribute to Cl^- accumulation during the post-seizure period.

6.7 Concluding remarks

Epileptic seizure activity induces a transient intracellular Cl^- accumulation that leads to a depolarising shift in E_{GABA-A}, which is evident in both neonatal and mature brain tissue. Under these conditions, it is likely that GABAergic synapses switch to being excitatory and contribute to ongoing neuronal activity rather than exerting their normal inhibitory role. I found that adenosine release during seizures acts to reduce the deleterious effects of excitatory GABA by reducing postsynaptic depolarising $GABA_AR$ responses. In investigating Cl^- handling mechanisms in the context of neonatal seizures I identified a novel molecular association between the Cl^--intruding transporter NKCC1 and the molecular motor protein Myosin Va. Myosin Va was shown to regulate NKCC1's contribution to Cl^- homeostasis and this may be important for seizure-induced NKCC1-dependent shifts in E_{GABA-A}. In addition, I identified a post-seizure hyperpolarisation-dependent Cl^- unloading mechanism that aids E_{GABA-A} recovery and shifts E_{GABA-A} to more negative values. This mechanism would be expected to augment GABAergic inhibition in the period immediately after the seizure and could provide a protective role against further seizure episodes. This work extends our understanding of seizure-related activity and suggests new mechanisms that could be relevant for the development of rational antiepileptic treatments.

Bibliography

Abdelmalik PA, Burnham WM, Carlen PL (2005) Increased seizure susceptibility of the hippocampus compared with the neocortex of the immature mouse brain in vitro. Epilepsia 46:356-366.

Achilles K, Okabe A, Ikeda M, Shimizu-Okabe C, Yamada J, Fukuda A, Luhmann HJ, Kilb W (2007) Kinetic properties of Cl uptake mediated by Na+-dependent K+-2Cl cotransport in immature rat neocortical neurons. J Neurosci 27:8616-8627.

Acton BA, Mahadevan V, Mercado A, Uvarov P, Ding Y, Pressey J, Airaksinen MS, Mount DB, Woodin MA (2012) Hyperpolarizing GABAergic transmission requires the KCC2 C-terminal ISO domain. J Neurosci 32:8746-8751.

Akerman CJ, Cline HT (2006) Depolarizing GABAergic conductances regulate the balance of excitation to inhibition in the developing retinotectal circuit in vivo. J Neurosci 26:5117-5130.

Alger BE, Nicoll RA (1979) GABA-mediated biphasic inhibitory responses in hippocampus. Nature 281:315-317.

Alger BE, Nicoll RA (1982) Feed-forward dendritic inhibition in rat hippocampal pyramidal cells studied in vitro. J Physiol 328:105-123.

Ali AB, Bannister AP, Thomson AM (1999) IPSPs elicited in CA1 pyramidal cells by putative basket cells in slices of adult rat hippocampus. Eur J Neurosci 11:1741-1753.

Ali AB, Deuchars J, Pawelzik H, Thomson AM (1998) CA1 pyramidal to basket and bistratified cell EPSPs: dual intracellular recordings in rat hippocampal slices. J Physiol 507 (Pt 1):201-217.

Amaral DG, Witter MP (1989) The three-dimensional organization of the hippocampal formation: a review of anatomical data. Neuroscience 31:571-591.

Andersen P, Bliss TV, Skrede KK (1971) Lamellar organization of hippocampal pathways. Exp Brain Res 13:222-238.

Anderson WW, Lewis DV, Swartzwelder HS, Wilson WA (1986) Magnesium-free medium activates seizure-like events in the rat hippocampal slice. Brain Res 398:215-219.

Antonucci F, Alpar A, Kacza J, Caleo M, Verderio C, Giani A, Martens H, Chaudhry FA, Allegra M, Grosche J, Michalski D, Erck C, Hoffmann A, Harkany T, Matteoli M, Hartig W (2012) Cracking down on inhibition: selective removal of GABAergic interneurons from hippocampal networks. J Neurosci 32:1989-2001.

Avoli M, D'Antuono M, Louvel J, Kohling R, Biagini G, Pumain R, D'Arcangelo G, Tancredi V (2002) Network and pharmacological mechanisms leading to epileptiform synchronization in the limbic system in vitro. Prog Neurobiol 68:167-207.

Balena T, Woodin MA (2008) Coincident pre- and postsynaptic activity downregulates NKCC1 to hyperpolarize E(Cl) during development. Eur J Neurosci 27:2402-2412.

Barmashenko G, Hefft S, Aertsen A, Kirschstein T, Kohling R (2011) Positive shifts of the GABAA receptor reversal potential due to altered chloride homeostasis is widespread after status epilepticus. Epilepsia 52:1570-1578.

Ben-Ari Y (2002) Excitatory actions of gaba during development: the nature of the nurture. Nat Rev Neurosci 3:728-739.

Ben-Ari Y, Cherubini E, Corradetti R, Gaiarsa JL (1989) Giant synaptic potentials in immature rat CA3 hippocampal neurones. J Physiol 416:303-325.

Ben-Ari Y, Gaiarsa JL, Tyzio R, Khazipov R (2007) GABA: a pioneer transmitter that excites immature neurons and generates primitive oscillations. Physiol Rev 87:1215-1284.

Ben-Ari Y, Khalilov I, Kahle KT, Cherubini E (2012) The GABA excitatory/inhibitory shift in brain maturation and neurological disorders. Neuroscientist 18:467-486.

Ben-Ari Y, Tyzio R, Nehlig A (2011) Excitatory action of GABA on immature neurons is not due to absence of ketone bodies metabolites or other energy substrates. Epilepsia 52:1544-1558.

Benkwitz C, Banks MI, Pearce RA (2004) Influence of GABAA receptor gamma2 splice variants on receptor kinetics and isoflurane modulation. Anesthesiology 101:924-936.

Berdichevsky Y, Dzhala V, Mail M, Staley KJ (2012) Interictal spikes, seizures and ictal cell death are not necessary for post-traumatic epileptogenesis in vitro. Neurobiol Dis 45:774-785.

Berezovskii VK, Nassi JJ, Born RT (2011) Segregation of feedforward and feedback projections in mouse visual cortex. J Comp Neurol 519:3672-3683.

Berglund K, Schleich W, Wang H, Feng G, Hall WC, Kuner T, Augustine GJ (2008) Imaging synaptic inhibition throughout the brain via genetically targeted Clomeleon. Brain Cell Biol 36:101-118.

Berman RF, Fredholm BB, Aden U, O'Connor WT (2000) Evidence for increased dorsal hippocampal adenosine release and metabolism during pharmacologically induced seizures in rats. Brain Res 872:44-53.

Blaesse P, Airaksinen MS, Rivera C, Kaila K (2009) Cation-chloride cotransporters and neuronal function. Neuron 61:820-838.

Blasco-Ibanez JM, Freund TF (1995) Synaptic input of horizontal interneurons in stratum oriens of the hippocampal CA1 subfield: structural basis of feed-back activation. Eur J Neurosci 7:2170-2180.

Boison D (2006) Adenosine kinase, epilepsy and stroke: mechanisms and therapies. Trends Pharmacol Sci 27:652-658.

Boison D (2009) Adenosine augmentation therapies (AATs) for epilepsy: prospect of cell and gene therapies. Epilepsy Res 85:131-141.

Boison D (2013) Adenosine kinase: exploitation for therapeutic gain. Pharmacol Rev 65:906-943.

Boison D, Stewart KA (2009) Therapeutic epilepsy research: from pharmacological rationale to focal adenosine augmentation. Biochem Pharmacol 78:1428-1437.

Bonny C (2006) Blocking stress signaling pathways with cell permeable peptides. Adv Exp Med Biol 588:133-143.

Booth D, Evans DJ (2004) Anticonvulsants for neonates with seizures. Cochrane Database Syst RevCD004218.

Bormann J, Hamill OP, Sakmann B (1987) Mechanism of anion permeation through channels gated by glycine and gamma-aminobutyric acid in mouse cultured spinal neurones. J Physiol 385:243-286.

Bos R, Vinay L (2012) Glucose is an adequate energy substrate for the depolarizing action of GABA and glycine in the neonatal rat spinal cord in vitro. J Neurophysiol 107:3107-3115.

Bragin DE, Sanderson JL, Peterson S, Connor JA, Muller WS (2009) Development of epileptiform excitability in the deep entorhinal cortex after status epilepticus. Eur J Neurosci 30:611-624.

Brinn LS, Pereira LJ, Larson RE, Martins AR (2010) Differential patterns of myosin Va expression during the ontogenesis of the rat hippocampus. Braz J Med Biol Res 43:890-898.

Brown EN, Lydic R, Schiff ND (2010) General anesthesia, sleep, and coma. N Engl J Med 363:2638-2650.

Brown JR, Simonetta KR, Sandberg LA, Stafford P, Langford GM (2001) Recombinant globular tail fragment of myosin-V blocks vesicle transport in squid nerve cell extracts. Biol Bull 201:240-241.

Brumback AC, Staley KJ (2008a) Thermodynamic regulation of NKCC1-mediated Cl- cotransport underlies plasticity of GABA(A) signaling in neonatal neurons. J Neurosci 28:1301-1312.

Brumback AC, Staley KJ (2008b) Thermodynamic regulation of NKCC1-mediated Cl- cotransport underlies plasticity of GABA(A) signaling in neonatal neurons. J Neurosci 28:1301-1312.

Buckby LE, Jensen TP, Smith PJ, Empson RM (2006) Network stability through homeostatic scaling of excitatory and inhibitory synapses following inactivity in CA3 of rat organotypic hippocampal slice cultures. Mol Cell Neurosci 31:805-816.

Buhl EH, Han ZS, Lorinczi Z, Stezhka VV, Karnup SV, Somogyi P (1994) Physiological properties of anatomically identified axo-axonic cells in the rat hippocampus. J Neurophysiol 71:1289-1307.

Burgess N, Maguire EA, O'Keefe J (2002) The human hippocampus and spatial and episodic memory. Neuron 35:625-641.

Burrone J, O'Byrne M, Murthy VN (2002) Multiple forms of synaptic plasticity triggered by selective suppression of activity in individual neurons. Nature 420:414-418.

Buzsaki G (1984) Feed-forward inhibition in the hippocampal formation. Prog Neurobiol 22:131-153.

Buzsaki G (2005) Theta rhythm of navigation: link between path integration and landmark navigation, episodic and semantic memory. Hippocampus 15:827-840.

Chancey JH, Adlaf EW, Sapp MC, Pugh PC, Wadiche JI, Overstreet-Wadiche LS (2013) GABA depolarization is required for experience-dependent synapse unsilencing in adult-born neurons. J Neurosci 33:6614-6622.

Chervin RD, Pierce PA, Connors BW (1988) Periodicity and directionality in the propagation of epileptiform discharges across neocortex. J Neurophysiol 60:1695-1713.

Chesnut TJ, Swann JW (1988) Epileptiform activity induced by 4-aminopyridine in immature hippocampus. Epilepsy Res 2:187-195.

Clark BD, Kurth-Nelson ZL, Newman EA (2009) Adenosine-evoked hyperpolarization of retinal ganglion cells is mediated by G-protein-coupled inwardly rectifying K+ and small conductance Ca2+-activated K+ channel activation. J Neurosci 29:11237-11245.

Clayton GH, Owens GC, Wolff JS, Smith RL (1998a) Ontogeny of cation-Cl- cotransporter expression in rat neocortex. Brain Res Dev Brain Res 109:281-292.

Clayton GH, Staley KJ, Wilcox CL, Owens GC, Smith RL (1998b) Developmental expression of C1C-2 in the rat nervous system. Brain Res Dev Brain Res 108:307-318.

Cohen I, Navarro V, Clemenceau S, Baulac M, Miles R (2002) On the origin of interictal activity in human temporal lobe epilepsy in vitro. Science 298:1418-1421.

Constantinescu AO, Ilie A, Ciocan D, Zagrean AM, Zagrean L, Moldovan M (2011) Endogenous adenosine A1 receptor activation underlies the transient post-ischemic rhythmic delta EEG activity. Clin Neurophysiol 122:1117-1126.

Correia SS, Bassani S, Brown TC, Lise MF, Backos DS, El-Husseini A, Passafaro M, Esteban JA (2008) Motor protein-dependent transport of AMPA receptors into spines during long-term potentiation. Nat Neurosci 11:457-466.

Cossart R (2011) The maturation of cortical interneuron diversity: how multiple developmental journeys shape the emergence of proper network function. Curr Opin Neurobiol 21:160-168.

D'Agostino D, Bertelli M, Gallo S, Cecchin S, Albiero E, Garofalo PG, Gambardella A, St Hilaire JM, Kwiecinski H, Andermann E, Pandolfo M (2004) Mutations and polymorphisms of the CLCN2 gene in idiopathic epilepsy. Neurology 63:1500-1502.

Dale N, Frenguelli BG (2009) Release of adenosine and ATP during ischemia and epilepsy. Curr Neuropharmacol 7:160-179.

Davidson DL, Barbeau A (1975) Locomotor activity and seizures induced by picrotoxin in the fastigeal nucleus of the rat. Exp Neurol 49:622-627.

De SA, Griesinger CB, Edwards FA (2003) Development of rat CA1 neurones in acute versus organotypic slices: role of experience in synaptic morphology and activity. J Physiol 550:135-147.

Delpire E, Austin TM (2010) Kinase regulation of Na+-K+-2Cl- cotransport in primary afferent neurons. J Physiol 588:3365-3373.

Desai NS, Rutherford LC, Turrigiano GG (1999) Plasticity in the intrinsic excitability of cortical pyramidal neurons. Nat Neurosci 2:515-520.

Dinocourt C, Petanjek Z, Freund TF, Ben-Ari Y, Esclapez M (2003) Loss of interneurons innervating pyramidal cell dendrites and axon initial segments in the CA1 region of the hippocampus following pilocarpine-induced seizures. J Comp Neurol 459:407-425.

Dunwiddie TV (1999) Adenosine and suppression of seizures. Adv Neurol 79:1001-1010.

Dunwiddie TV, Masino SA (2001) The role and regulation of adenosine in the central nervous system. Annu Rev Neurosci 24:31-55.

During MJ, Spencer DD (1992) Adenosine: a potential mediator of seizure arrest and postictal refractoriness. Ann Neurol 32:618-624.

Dzhala VI, Brumback AC, Staley KJ (2008) Bumetanide enhances phenobarbital efficacy in a neonatal seizure model. Ann Neurol 63:222-235.

Dzhala VI, Kuchibhotla KV, Glykys JC, Kahle KT, Swiercz WB, Feng G, Kuner T, Augustine GJ, Bacskai BJ, Staley KJ (2010) Progressive NKCC1-dependent neuronal chloride accumulation during neonatal seizures. J Neurosci 30:11745-11761.

Dzhala VI, Staley KJ (2003) Excitatory actions of endogenously released GABA contribute to initiation of ictal epileptiform activity in the developing hippocampus. J Neurosci 23:1840-1846.

Dzhala VI, Talos DM, Sdrulla DA, Brumback AC, Mathews GC, Benke TA, Delpire E, Jensen FE, Staley KJ (2005) NKCC1 transporter facilitates seizures in the developing brain. Nat Med 11:1205-1213.

Ebihara S, Shirato K, Harata N, Akaike N (1995) Gramicidin-perforated patch recording: GABA response in mammalian neurones with intact intracellular chloride. J Physiol 484 (Pt 1):77-86.

Eftekhari S, Mehvari HJ, Najafi ZM, Hashemi Fesharaki SS, Gharakhani M, Mostafavi H, Joghataei MT, Beladimoghadam N, Rahimian E, Hadjighassem MR (2012) Bumetanide reduces seizure frequency in patients with temporal lobe epilepsy. Epilepsia.

Elfant D, Pal BZ, Emptage N, Capogna M (2008) Specific inhibitory synapses shift the balance from feedforward to feedback inhibition of hippocampal CA1 pyramidal cells. Eur J Neurosci 27:104-113.

Empson RM, Heinemann U (1995) The perforant path projection to hippocampal area CA1 in the rat hippocampal-entorhinal cortex combined slice. J Physiol 484 (Pt 3):707-720.

Etherington LA, Frenguelli BG (2004) Endogenous adenosine modulates epileptiform activity in rat hippocampus in a receptor subtype-dependent manner. Eur J Neurosci 19:2539-2550.

Etherington LA, Patterson GE, Meechan L, Boison D, Irving AJ, Dale N, Frenguelli BG (2009) Astrocytic adenosine kinase regulates basal synaptic adenosine levels and seizure activity but not activity-dependent adenosine release in the hippocampus. Neuropharmacology 56:429-437.

Everett K, et al. (2007) Linkage and mutational analysis of CLCN2 in childhood absence epilepsy. Epilepsy Res 75:145-153.

Farrant M, Kaila K (2007) The cellular, molecular and ionic basis of GABA(A) receptor signalling. Prog Brain Res 160:59-87.

Farrant M, Nusser Z (2005) Variations on an inhibitory theme: phasic and tonic activation of GABA(A) receptors. Nat Rev Neurosci 6:215-229.

Fedele DE, Li T, Lan JQ, Fredholm BB, Boison D (2006) Adenosine A1 receptors are crucial in keeping an epileptic focus localized. Exp Neurol 200:184-190.

Fino E, Yuste R (2011) Dense inhibitory connectivity in neocortex. Neuron 69:1188-1203.

Fishell G, Rudy B (2011) Mechanisms of inhibition within the telencephalon: "where the wild things are". Annu Rev Neurosci 34:535-567.

Fiumelli H, Cancedda L, Poo MM (2005) Modulation of GABAergic transmission by activity via postsynaptic Ca2+-dependent regulation of KCC2 function. Neuron 48:773-786.

Foldy C, Lee SH, Morgan RJ, Soltesz I (2010) Regulation of fast-spiking basket cell synapses by the chloride channel ClC-2. Nat Neurosci 13:1047-1049.

Fredholm BB, Chen JF, Cunha RA, Svenningsson P, Vaugeois JM (2005) Adenosine and brain function. Int Rev Neurobiol 63:191-270.

Fredholm BB, IJzerman AP, Jacobson KA, Klotz KN, Linden J (2001) International Union of Pharmacology. XXV. Nomenclature and classification of adenosine receptors. Pharmacol Rev 53:527-552.

Freund TF, Katona I (2007) Perisomatic inhibition. Neuron 56:33-42.

Fuentealba P, Begum R, Capogna M, Jinno S, Marton LF, Csicsvari J, Thomson A, Somogyi P, Klausberger T (2008) Ivy cells: a population of nitric-oxide-producing, slow-spiking GABAergic neurons and their involvement in hippocampal network activity. Neuron 57:917-929.

Fujiwara-Tsukamoto Y, Isomura Y, Imanishi M, Ninomiya T, Tsukada M, Yanagawa Y, Fukai T, Takada M (2010) Prototypic seizure activity driven by mature hippocampal fast-spiking interneurons. J Neurosci 30:13679-13689.

Fujiwara-Tsukamoto Y, Isomura Y, Nambu A, Takada M (2003) Excitatory GABA input directly drives seizure-like rhythmic synchronization in mature hippocampal CA1 pyramidal cells. Neuroscience 119:265-275.

Fujiwara-Tsukamoto Y, Isomura Y, Takada M (2006) Comparable GABAergic mechanisms of hippocampal seizurelike activity in posttetanic and low-Mg2+ conditions. J Neurophysiol 95:2013-2019.

Galeffi F, Sah R, Pond BB, George A, Schwartz-Bloom RD (2004) Changes in intracellular chloride after oxygen-glucose deprivation of the adult hippocampal slice: effect of diazepam. J Neurosci 24:4478-4488.

Gassmann M, Bettler B (2012) Regulation of neuronal GABA(B) receptor functions by subunit composition. Nat Rev Neurosci 13:380-394.

Gavrilov K, Saltzman WM (2012) Therapeutic siRNA: principles, challenges, and strategies. Yale J Biol Med 85:187-200.

Glickfeld LL, Scanziani M (2006) Distinct timing in the activity of cannabinoid-sensitive and cannabinoid-insensitive basket cells. Nat Neurosci 9:807-815.

Glykys J, Mann EO, Mody I (2008) Which GABA(A) receptor subunits are necessary for tonic inhibition in the hippocampus? J Neurosci 28:1421-1426.

Glykys J, Peng Z, Chandra D, Homanics GE, Houser CR, Mody I (2007) A new naturally occurring GABA(A) receptor subunit partnership with high sensitivity to ethanol. Nat Neurosci 10:40-48.

Gogolla N, Leblanc JJ, Quast KB, Sudhof TC, Fagiolini M, Hensch TK (2009) Common circuit defect of excitatory-inhibitory balance in mouse models of autism. J Neurodev Disord 1:172-181.

Gonchar Y, Burkhalter A (2003) Distinct GABAergic targets of feedforward and feedback connections between lower and higher areas of rat visual cortex. J Neurosci 23:10904-10912.

Gonzalez-Islas C, Chub N, Garcia-Bereguiain MA, Wenner P (2010) GABAergic synaptic scaling in embryonic motoneurons is mediated by a shift in the chloride reversal potential. J Neurosci 30:13016-13020.

Goodkin HP, Liu X, Holmes GL (2003) Diazepam terminates brief but not prolonged seizures in young, naive rats. Epilepsia 44:1109-1112.

Goold CP, Nicoll RA (2010) Single-cell optogenetic excitation drives homeostatic synaptic depression. Neuron 68:512-528.

Griscelli C, Durandy A, Guy-Grand D, Daguillard F, Herzog C, Prunieras M (1978) A syndrome associating partial albinism and immunodeficiency. Am J Med 65:691-702.

Grubb MS, Burrone J (2010) Activity-dependent relocation of the axon initial segment fine-tunes neuronal excitability. Nature 465:1070-1074.

Gruenthal M, Armstrong DR, Ault B, Nadler JV (1986) Comparison of seizures and brain lesions produced by intracerebroventricular kainic acid and bicuculline methiodide. Exp Neurol 93:621-630.

Gulledge AT, Stuart GJ (2003) Excitatory actions of GABA in the cortex. Neuron 37:299-309.

Gundlfinger A, Bischofberger J, Johenning FW, Torvinen M, Schmitz D, Breustedt J (2007) Adenosine modulates transmission at the hippocampal mossy fibre synapse via direct inhibition of presynaptic calcium channels. J Physiol 582:263-277.

Gustafsson B, Galvan M, Grafe P, Wigstrom H (1982) A transient outward current in a mammalian central neurone blocked by 4-aminopyridine. Nature 299:252-254.

Gutierrez R, Armand V, Schuchmann S, Heinemann U (1999) Epileptiform activity induced by low Mg2+ in cultured rat hippocampal slices. Brain Res 815:294-303.

Gutierrez R, Heinemann U (1999) Synaptic reorganization in explanted cultures of rat hippocampus. Brain Res 815:304-316.

Guttinger M, Fedele D, Koch P, Padrun V, Pralong WF, Brustle O, Boison D (2005a) Suppression of kindled seizures by paracrine adenosine release from stem cell-derived brain implants. Epilepsia 46:1162-1169.

Guttinger M, Padrun V, Pralong WF, Boison D (2005b) Seizure suppression and lack of adenosine A1 receptor desensitization after focal long-term delivery of adenosine by encapsulated myoblasts. Exp Neurol 193:53-64.

Haider B, Duque A, Hasenstaub AR, McCormick DA (2006) Neocortical network activity in vivo is generated through a dynamic balance of excitation and inhibition. J Neurosci 26:4535-4545.

Halasy K, Buhl EH, Lorinczi Z, Tamas G, Somogyi P (1996) Synaptic target selectivity and input of GABAergic basket and bistratified interneurons in the CA1 area of the rat hippocampus. Hippocampus 6:306-329.

Han TH, Jang SH, Lee SY, Ryu PD (2011) Adenosine reduces GABAergic IPSC frequency via presynaptic A receptors in hypothalamic paraventricular neurons projecting to rostral ventrolateral medulla. Neurosci Lett 490:63-67.

Hannaert P, Alvarez-Guerra M, Pirot D, Nazaret C, Garay RP (2002) Rat NKCC2/NKCC1 cotransporter selectivity for loop diuretic drugs. Naunyn Schmiedebergs Arch Pharmacol 365:193-199.

Heisler FF, Loebrich S, Pechmann Y, Maier N, Zivkovic AR, Tokito M, Hausrat TJ, Schweizer M, Bahring R, Holzbaur EL, Schmitz D, Kneussel M (2011) Muskelin regulates actin filament- and microtubule-based GABA(A) receptor transport in neurons. Neuron 70:66-81.

Hendry SH, Schwark HD, Jones EG, Yan J (1987) Numbers and proportions of GABA-immunoreactive neurons in different areas of monkey cerebral cortex. J Neurosci 7:1503-1519.

Hennou S, Khalilov I, Diabira D, Ben-Ari Y, Gozlan H (2002) Early sequential formation of functional GABA(A) and glutamatergic synapses on CA1 interneurons of the rat foetal hippocampus. Eur J Neurosci 16:197-208.

Higashima M, Kinoshita H, Yamaguchi N, Koshino Y (1996) Activation of GABAergic function necessary for afterdischarge generation in rat hippocampal slices. Neurosci Lett 207:101-104.

Higashima M, Ohno K, Kinoshita H, Koshino Y (2000) Involvement of GABA(A) and GABA(B) receptors in afterdischarge generation in rat hippocampal slices. Brain Res 865:186-193.

Hirokawa N, Niwa S, Tanaka Y (2010) Molecular motors in neurons: transport mechanisms and roles in brain function, development, and disease. Neuron 68:610-638.

Hirsch JC, Agassandian C, Merchan-Perez A, Ben-Ari Y, DeFelipe J, Esclapez M, Bernard C (1999) Deficit of quantal release of GABA in experimental models of temporal lobe epilepsy. Nat Neurosci 2:499-500.

Holmes GL, Khazipov R, Ben-Ari Y (2002) New concepts in neonatal seizures. Neuroreport 13:A3-A8.

Holmgren CD, Mukhtarov M, Malkov AE, Popova IY, Bregestovski P, Zilberter Y (2010) Energy substrate availability as a determinant of neuronal resting potential, GABA signaling and spontaneous network activity in the neonatal cortex in vitro. J Neurochem 112:900-912.

Hosseinzadeh H, Stone TW (1998) Tolbutamide blocks postsynaptic but not presynaptic effects of adenosine on hippocampal CA1 neurones. J Neural Transm 105:161-172.

Hsia AY, Malenka RC, Nicoll RA (1998) Development of excitatory circuitry in the hippocampus. J Neurophysiol 79:2013-2024.

Huberfeld G, Wittner L, Clemenceau S, Baulac M, Kaila K, Miles R, Rivera C (2007) Perturbed chloride homeostasis and GABAergic signaling in human temporal lobe epilepsy. J Neurosci 27:9866-9873.

Hubner CA, Lorke DE, Hermans-Borgmeyer I (2001a) Expression of the Na-K-2Cl-cotransporter NKCC1 during mouse development. Mech Dev 102:267-269.

Hubner CA, Stein V, Hermans-Borgmeyer I, Meyer T, Ballanyi K, Jentsch TJ (2001b) Disruption of KCC2 reveals an essential role of K-Cl cotransport already in early synaptic inhibition. Neuron 30:515-524.

Hurvitz H, Gillis R, Klaus S, Klar A, Gross-Kieselstein F, Okon E (1993) A kindred with Griscelli disease: spectrum of neurological involvement. Eur J Pediatr 152:402-405.

Ilie A, Ciocan D, Constantinescu AO, Zagrean AM, Nita DA, Zagrean L, Moldovan M (2009) Endogenous activation of adenosine A1 receptors promotes post-ischemic electrocortical burst suppression. Neuroscience 159:1070-1078.

Ilie A, Ciocan D, Zagrean AM, Nita DA, Zagrean L, Moldovan M (2006) Endogenous activation of adenosine A(1) receptors accelerates ischemic suppression of spontaneous electrocortical activity. J Neurophysiol 96:2809-2814.

Ilie A, Raimondo JV, Akerman CJ (2012) Adenosine release during seizures attenuates GABAA receptor-mediated depolarization. J Neurosci 32:5321-5332.

Isaacson JS, Scanziani M (2011) How inhibition shapes cortical activity. Neuron 72:231-243.

Isaev D, Isaeva E, Khazipov R, Holmes GL (2005) Anticonvulsant action of GABA in the high potassium-low magnesium model of ictogenesis in the neonatal rat hippocampus in vivo and in vitro. J Neurophysiol 94:2987-2992.

Isaev D, Isaeva E, Khazipov R, Holmes GL (2007) Shunting and hyperpolarizing GABAergic inhibition in the high-potassium model of ictogenesis in the developing rat hippocampus. Hippocampus 17:210-219.

Isaev D, Ivanchick G, Khmyz V, Isaeva E, Savrasova A, Krishtal O, Holmes GL, Maximyuk O (2012) Surface charge impact in low-magnesium model of seizure in rat hippocampus. J Neurophysiol 107:417-423.

Isomura Y, Fujiwara-Tsukamoto Y, Takada M (2003a) Glutamatergic propagation of GABAergic seizure-like afterdischarge in the hippocampus in vitro. J Neurophysiol 90:2746-2751.

Isomura Y, Fujiwara-Tsukamoto Y, Takada M (2008) A network mechanism underlying hippocampal seizure-like synchronous oscillations. Neurosci Res 61:227-233.

Isomura Y, Sugimoto M, Fujiwara-Tsukamoto Y, Yamamoto-Muraki S, Yamada J, Fukuda A (2003b) Synaptically activated Cl- accumulation responsible for depolarizing GABAergic responses in mature hippocampal neurons. J Neurophysiol 90:2752-2756.

Jaenisch N, Witte OW, Frahm C (2010) Downregulation of potassium chloride cotransporter KCC2 after transient focal cerebral ischemia. Stroke 41:e151-e159.

Jin X, Huguenard JR, Prince DA (2005) Impaired Cl- extrusion in layer V pyramidal neurons of chronically injured epileptogenic neocortex. J Neurophysiol 93:2117-2126.

Jonzon B, Fredholm BB (1985) Release of purines, noradrenaline, and GABA from rat hippocampal slices by field stimulation. J Neurochem 44:217-224.

Kahle KT, Barnett SM, Sassower KC, Staley KJ (2009) Decreased seizure activity in a human neonate treated with bumetanide, an inhibitor of the Na(+)-K(+)-2Cl(-) cotransporter NKCC1. J Child Neurol 24:572-576.

Kahle KT, Rinehart J, de Los HP, Louvi A, Meade P, Vazquez N, Hebert SC, Gamba G, Gimenez I, Lifton RP (2005) WNK3 modulates transport of Cl- in and out of cells: implications for control of cell volume and neuronal excitability. Proc Natl Acad Sci U S A 102:16783-16788.

Kahle KT, Rinehart J, Lifton RP (2010) Phosphoregulation of the Na-K-2Cl and K-Cl cotransporters by the WNK kinases. Biochim Biophys Acta 1802:1150-1158.

Kahle KT, Staley KJ, Nahed BV, Gamba G, Hebert SC, Lifton RP, Mount DB (2008) Roles of the cation-chloride cotransporters in neurological disease. Nat Clin Pract Neurol 4:490-503.

Kaila K, Lamsa K, Smirnov S, Taira T, Voipio J (1997) Long-lasting GABA-mediated depolarization evoked by high-frequency stimulation in pyramidal neurons of rat hippocampal slice is attributable to a network-driven, bicarbonate-dependent K+ transient. J Neurosci 17:7662-7672.

Kaila K, Pasternack M, Saarikoski J, Voipio J (1989) Influence of GABA-gated bicarbonate conductance on potential, current and intracellular chloride in crayfish muscle fibres. J Physiol 416:161-181.

Kaila K, Voipio J, Paalasmaa P, Pasternack M, Deisz RA (1993) The role of bicarbonate in GABAA receptor-mediated IPSPs of rat neocortical neurones. J Physiol 464:273-289.

Kakazu Y, Uchida S, Nakagawa T, Akaike N, Nabekura J (2000) Reversibility and cation selectivity of the K(+)-Cl(-) cotransport in rat central neurons. J Neurophysiol 84:281-288.

Kapfer C, Glickfeld LL, Atallah BV, Scanziani M (2007) Supralinear increase of recurrent inhibition during sparse activity in the somatosensory cortex. Nat Neurosci 10:743-753.

Karayannis T, Elfant D, Huerta-Ocampo I, Teki S, Scott RS, Rusakov DA, Jones MV, Capogna M (2010) Slow GABA transient and receptor desensitization shape synaptic responses evoked by hippocampal neurogliaform cells. J Neurosci 30:9898-9909.

Kawamura M, Jr., Ruskin DN, Masino SA (2010) Metabolic Autocrine Regulation of Neurons Involves Cooperation among Pannexin Hemichannels, Adenosine Receptors, and KATP Channels. J Neurosci 30:3886-3895.

Khakhalin AS, Aizenman CD (2012) GABAergic transmission and chloride equilibrium potential are not modulated by pyruvate in the developing optic tectum of Xenopus laevis tadpoles. PLoS One 7:e34446.

Khalilov I, Holmes GL, Ben-Ari Y (2003) In vitro formation of a secondary epileptogenic mirror focus by interhippocampal propagation of seizures. Nat Neurosci 6:1079-1085.

Khalilov I, Le Van QM, Gozlan H, Ben-Ari Y (2005) Epileptogenic actions of GABA and fast oscillations in the developing hippocampus. Neuron 48:787-796.

Khazipov R, Esclapez M, Caillard O, Bernard C, Khalilov I, Tyzio R, Hirsch J, Dzhala V, Berger B, Ben-Ari Y (2001) Early development of neuronal activity in the primate hippocampus in utero. J Neurosci 21:9770-9781.

Khazipov R, Khalilov I, Tyzio R, Morozova E, Ben-Ari Y, Holmes GL (2004) Developmental changes in GABAergic actions and seizure susceptibility in the rat hippocampus. Eur J Neurosci 19:590-600.

Khirug S, Ahmad F, Puskarjov M, Afzalov R, Kaila K, Blaesse P (2010) A single seizure episode leads to rapid functional activation of KCC2 in the neonatal rat hippocampus. J Neurosci 30:12028-12035.

Khirug S, Yamada J, Afzalov R, Voipio J, Khiroug L, Kaila K (2008) GABAergic depolarization of the axon initial segment in cortical principal neurons is caused by the Na-K-2Cl cotransporter NKCC1. J Neurosci 28:4635-4639.

Kirmse K, Witte OW, Holthoff K (2010) GABA depolarizes immature neocortical neurons in the presence of the ketone body ss-hydroxybutyrate. J Neurosci 30:16002-16007.

Kitamura A, Ishibashi H, Watanabe M, Takatsuru Y, Brodwick M, Nabekura J (2008) Sustained depolarizing shift of the GABA reversal potential by glutamate receptor activation in hippocampal neurons. Neuroscience Research 62:270-277.

Klausberger T, Marton LF, Baude A, Roberts JD, Magill PJ, Somogyi P (2004) Spike timing of dendrite-targeting bistratified cells during hippocampal network oscillations in vivo. Nat Neurosci 7:41-47.

Klausberger T, Somogyi P (2008) Neuronal diversity and temporal dynamics: the unity of hippocampal circuit operations. Science 321:53-57.

Kohling R, Vreugdenhil M, Bracci E, Jefferys JG (2000) Ictal epileptiform activity is facilitated by hippocampal GABAA receptor-mediated oscillations. J Neurosci 20:6820-6829.

Kruglikov I, Rudy B (2008) Perisomatic GABA release and thalamocortical integration onto neocortical excitatory cells are regulated by neuromodulators. Neuron 58:911-924.

Kullmann DM (2011) Interneuron networks in the hippocampus. Curr Opin Neurobiol 21:709-716.

Kyrozis A, Reichling DB (1995) Perforated-patch recording with gramicidin avoids artifactual changes in intracellular chloride concentration. J Neurosci Methods 57:27-35.

Lamsa K, Palva JM, Ruusuvuori E, Kaila K, Taira T (2000) Synaptic GABA(A) activation inhibits AMPA-kainate receptor-mediated bursting in the newborn (P0-P2) rat hippocampus. J Neurophysiol 83:359-366.

Lamsa K, Taira T (2003) Use-dependent shift from inhibitory to excitatory GABAA receptor action in SP-O interneurons in the rat hippocampal CA3 area. J Neurophysiol 90:1983-1995.

Lanska MJ, Lanska DJ (1996) Neonatal seizures in the United States: results of the National Hospital Discharge Survey, 1980-1991. Neuroepidemiology 15:117-125.

Lee HH, Deeb TZ, Walker JA, Davies PA, Moss SJ (2011a) NMDA receptor activity downregulates KCC2 resulting in depolarizing GABAA receptor-mediated currents. Nat Neurosci 14:736-743.

Lee HHC, Deeb TZ, Walker JA, Davies PA, Moss SJ (2011b) NMDA receptor activity downregulates KCC2 resulting in depolarizing GABA(A) receptor-mediated currents. Nature Neuroscience 14:736-U390.

Lee HHC, Jurd R, Moss SJ (2010) Tyrosine phosphorylation regulates the membrane trafficking of the potassium chloride co-transporter KCC2. Molecular and Cellular Neuroscience 45:173-179.

Lee HHC, Walker JA, Williams JR, Goodier RJ, Payne JA, Moss SJ (2007) Direct protein kinase C-dependent phosphorylation regulates the cell surface stability and activity of the potassium chloride cotransporter KCC2. Journal of Biological Chemistry 282:29777-29784.

Li T, Ren G, Kaplan DL, Boison D (2009) Human mesenchymal stem cell grafts engineered to release adenosine reduce chronic seizures in a mouse model of CA3-selective epileptogenesis. Epilepsy Res 84:238-241.

Li T, Steinbeck JA, Lusardi T, Koch P, Lan JQ, Wilz A, Segschneider M, Simon RP, Brustle O, Boison D (2007) Suppression of kindling epileptogenesis by adenosine releasing stem cell-derived brain implants. Brain 130:1276-1288.

Li X, Zhou J, Chen Z, Chen S, Zhu F, Zhou L (2008) Long-term expressional changes of Na+ -K+ -Cl- co-transporter 1 (NKCC1) and K+ -Cl- co-transporter 2 (KCC2) in CA1 region of hippocampus following lithium-pilocarpine induced status epilepticus (PISE). Brain Res 1221:141-146.

Lillis KP, Kramer MA, Mertz J, Staley KJ, White JA (2012) Pyramidal cells accumulate chloride at seizure onset. Neurobiol Dis 47:358-366.

Lindskog M, Li L, Groth RD, Poburko D, Thiagarajan TC, Han X, Tsien RW (2010) Postsynaptic GluA1 enables acute retrograde enhancement of presynaptic function to coordinate adaptation to synaptic inactivity. Proc Natl Acad Sci U S A 107:21806-21811.

Lopatar J, Dale N, Frenguelli BG (2011) Minor contribution of ATP P2 receptors to electrically-evoked electrographic seizure activity in hippocampal slices: Evidence from purine biosensors and P2 receptor agonists and antagonists. Neuropharmacology 61:25-34.

Lovatt D, Xu Q, Liu W, Takano T, Smith NA, Schnermann J, Tieu K, Nedergaard M (2012) Neuronal adenosine release, and not astrocytic ATP release, mediates feedback inhibition of excitatory activity. Proc Natl Acad Sci U S A 109:6265-6270.

Lovett-Barron M, Turi GF, Kaifosh P, Lee PH, Bolze F, Sun XH, Nicoud JF, Zemelman BV, Sternson SM, Losonczy A (2012) Regulation of neuronal input transformations by tunable dendritic inhibition. Nat Neurosci 15:423.

Lu J, Karadsheh M, Delpire E (1999) Developmental regulation of the neuronal-specific isoform of K-Cl cotransporter KCC2 in postnatal rat brains. J Neurobiol 39:558-568.

Lu T, Trussell LO (2001) Mixed excitatory and inhibitory GABA-mediated transmission in chick cochlear nucleus. J Physiol 535:125-131.

Luciano D (1993) Partial seizures of frontal and temporal origin. Neurol Clin 11:805-822.

Luhmann HJ, Dzhala VI, Ben-Ari Y (2000) Generation and propagation of 4-AP-induced epileptiform activity in neonatal intact limbic structures in vitro. Eur J Neurosci 12:2757-2768.

Luhmann HJ, Prince DA (1991) Postnatal maturation of the GABAergic system in rat neocortex. J Neurophysiol 65:247-263.

Maas C, Tagnaouti N, Loebrich S, Behrend B, Lappe-Siefke C, Kneussel M (2006) Neuronal cotransport of glycine receptor and the scaffold protein gephyrin. J Cell Biol 172:441-451.

Maccaferri G, Roberts JD, Szucs P, Cottingham CA, Somogyi P (2000) Cell surface domain specific postsynaptic currents evoked by identified GABAergic neurones in rat hippocampus in vitro. J Physiol 524 Pt 1:91-116.

Madisen L, et al. (2012) A toolbox of Cre-dependent optogenetic transgenic mice for light-induced activation and silencing. Nat Neurosci 15:793-802.

Malmgren K, Thom M (2012) Hippocampal sclerosis--origins and imaging. Epilepsia 53 Suppl 4:19-33.

Marin O (2012) Interneuron dysfunction in psychiatric disorders. Nat Rev Neurosci 13:107-120.

Martin JL, Sloviter RS (2001) Focal inhibitory interneuron loss and principal cell hyperexcitability in the rat hippocampus after microinjection of a neurotoxic conjugate of saporin and a peptidase-resistant analog of Substance P. J Comp Neurol 436:127-152.

Marty S, Wehrle R, Alvarez-Leefmans FJ, Gasnier B, Sotelo C (2002) Postnatal maturation of Na+, K+, 2Cl- cotransporter expression and inhibitory synaptogenesis in the rat hippocampus: an immunocytochemical analysis. Eur J Neurosci 15:233-245.

MATSUMOTO H, MARSAN CA (1964) CORTICAL CELLULAR PHENOMENA IN EXPERIMENTAL EPILEPSY: ICTAL MANIFESTATIONS. Exp Neurol 9:305-326.

McCormick DA, Contreras D (2001) On the cellular and network bases of epileptic seizures. Annu Rev Physiol 63:815-846.

Mercado A, Mount DB, Gamba G (2004) Electroneutral cation-chloride cotransporters in the central nervous system. Neurochem Res 29:17-25.

Mercer JA, Seperack PK, Strobel MC, Copeland NG, Jenkins NA (1991) Novel myosin heavy chain encoded by murine dilute coat colour locus. Nature 349:709-713.

Meurs A, Clinckers R, Ebinger G, Michotte Y, Smolders I (2008) Seizure activity and changes in hippocampal extracellular glutamate, GABA, dopamine and serotonin. Epilepsy Res 78:50-59.

Miles R, Blaesse P, Huberfeld G, Wittner L, Kaila K (2012) Chloride homeostasis and GABA signaling in temporal lobe epilepsy.

Mody I, Lambert JD, Heinemann U (1987) Low extracellular magnesium induces epileptiform activity and spreading depression in rat hippocampal slices. J Neurophysiol 57:869-888.

Moser EI, Kropff E, Moser MB (2008) Place cells, grid cells, and the brain's spatial representation system. Annu Rev Neurosci 31:69-89.

Nakajima K, Miyazaki H, Niisato N, Marunaka Y (2007) Essential role of NKCC1 in NGF-induced neurite outgrowth. Biochem Biophys Res Commun 359:604-610.

Nakajima K, Yin X, Takei Y, Seog DH, Homma N, Hirokawa N (2012) Molecular Motor KIF5A Is Essential for GABA(A) Receptor Transport, and KIF5A Deletion Causes Epilepsy. Neuron 76:945-961.

Nakashiba T, Buhl DL, McHugh TJ, Tonegawa S (2009) Hippocampal CA3 output is crucial for ripple-associated reactivation and consolidation of memory. Neuron 62:781-787.

Nakashiba T, Young JZ, McHugh TJ, Buhl DL, Tonegawa S (2008) Transgenic inhibition of synaptic transmission reveals role of CA3 output in hippocampal learning. Science 319:1260-1264.

Nardou R, Ben-Ari Y, Khalilov I (2009) Bumetanide, an NKCC1 antagonist, does not prevent formation of epileptogenic focus but blocks epileptic focus seizures in immature rat hippocampus. J Neurophysiol 101:2878-2888.

Nardou R, Yamamoto S, Chazal G, Bhar A, Ferrand N, Dulac O, Ben-Ari Y, Khalilov I (2011) Neuronal chloride accumulation and excitatory GABA underlie aggravation of neonatal epileptiform activities by phenobarbital. Brain 134:987-1002.

Nieuwenhuis S, Forstmann BU, Wagenmakers EJ (2011) Erroneous analyses of interactions in neuroscience: a problem of significance. Nat Neurosci 14:1105-1107.

Nusser Z, Sieghart W, Benke D, Fritschy JM, Somogyi P (1996) Differential synaptic localization of two major gamma-aminobutyric acid type A receptor alpha subunits on hippocampal pyramidal cells. Proc Natl Acad Sci U S A 93:11939-11944.

Okabe A, Ohno K, Toyoda H, Yokokura M, Sato K, Fukuda A (2002) Amygdala kindling induces upregulation of mRNA for NKCC1, a Na(+), K(+)-2Cl(-) cotransporter, in the rat piriform cortex. Neurosci Res 44:225-229.

Okun M, Lampl I (2008) Instantaneous correlation of excitation and inhibition during ongoing and sensory-evoked activities. Nat Neurosci 11:535-537.

Olah S, Fule M, Komlosi G, Varga C, Baldi R, Barzo P, Tamas G (2009) Regulation of cortical microcircuits by unitary GABA-mediated volume transmission. Nature 461:1278-1281.

Overlack N, Kilic D, Bauss K, Marker T, Kremer H, van WE, Wolfrum U (2011) Direct interaction of the Usher syndrome 1G protein SANS and myomegalin in the retina. Biochim Biophys Acta 1813:1883-1892.

Overstreet WL, Bromberg DA, Bensen AL, Westbrook GL (2005) GABAergic signaling to newborn neurons in dentate gyrus. J Neurophysiol 94:4528-4532.

Owens DF, Boyce LH, Davis MB, Kriegstein AR (1996) Excitatory GABA responses in embryonic and neonatal cortical slices demonstrated by gramicidin perforated-patch recordings and calcium imaging. J Neurosci 16:6414-6423.

Pachter JS, Liem RK (1985) alpha-Internexin, a 66-kD intermediate filament-binding protein from mammalian central nervous tissues. J Cell Biol 101:1316-1322.

Packer AM, Yuste R (2011) Dense, unspecific connectivity of neocortical parvalbumin-positive interneurons: a canonical microcircuit for inhibition? J Neurosci 31:13260-13271.

Palma E, Amici M, Sobrero F, Spinelli G, Di AS, Ragozzino D, Mascia A, Scoppetta C, Esposito V, Miledi R, Eusebi F (2006) Anomalous levels of Cl- transporters in the hippocampal subiculum from temporal lobe epilepsy patients make GABA excitatory. Proc Natl Acad Sci U S A 103:8465-8468.

Parent JM, Lowenstein DH (1997) Mossy fiber reorganization in the epileptic hippocampus. Curr Opin Neurol 10:103-109.

Pascual O, Casper KB, Kubera C, Zhang J, Revilla-Sanchez R, Sul JY, Takano H, Moss SJ, McCarthy K, Haydon PG (2005) Astrocytic purinergic signaling coordinates synaptic networks. Science 310:113-116.

Pastural E, Barrat FJ, Dufourcq-Lagelouse R, Certain S, Sanal O, Jabado N, Seger R, Griscelli C, Fischer A, de Saint BG (1997) Griscelli disease maps to chromosome 15q21 and is associated with mutations in the myosin-Va gene. Nat Genet 16:289-292.

Pathak HR, Weissinger F, Terunuma M, Carlson GC, Hsu FC, Moss SJ, Coulter DA (2007) Disrupted dentate granule cell chloride regulation enhances synaptic excitability during development of temporal lobe epilepsy. J Neurosci 27:14012-14022.

Pavlov I, Walker MC (2012) Tonic GABA(A) receptor-mediated signalling in temporal lobe epilepsy. Neuropharmacology.

Payne JA (1997) Functional characterization of the neuronal-specific K-Cl cotransporter: implications for [K+]o regulation. Am J Physiol 273:C1516-C1525.

Payne JA, Stevenson TJ, Donaldson LF (1996) Molecular characterization of a putative K-Cl cotransporter in rat brain. A neuronal-specific isoform. J Biol Chem 271:16245-16252.

Pearson T, Damian K, Lynas RE, Frenguelli BG (2006) Sustained elevation of extracellular adenosine and activation of A1 receptors underlie the post-ischaemic inhibition of neuronal function in rat hippocampus in vitro. J Neurochem 97:1357-1368.

Pfeffer CK, Stein V, Keating DJ, Maier H, Rinke I, Rudhard Y, Hentschke M, Rune GM, Jentsch TJ, Hubner CA (2009) NKCC1-dependent GABAergic excitation drives synaptic network maturation during early hippocampal development. J Neurosci 29:3419-3430.

Piechotta K, Lu J, Delpire E (2002) Cation chloride cotransporters interact with the stress-related kinases Ste20-related proline-alanine-rich kinase (SPAK) and oxidative stress response 1 (OSR1). J Biol Chem 277:50812-50819.

Pouille F, Scanziani M (2001) Enforcement of temporal fidelity in pyramidal cells by somatic feed-forward inhibition. Science 293:1159-1163.

Pratt KG, Aizenman CD (2007) Homeostatic regulation of intrinsic excitability and synaptic transmission in a developing visual circuit. J Neurosci 27:8268-8277.

Price CJ, Scott R, Rusakov DA, Capogna M (2008) GABA(B) receptor modulation of feedforward inhibition through hippocampal neurogliaform cells. J Neurosci 28:6974-6982.

Puskarjov M, Ahmad F, Kaila K, Blaesse P (2012) Activity-dependent cleavage of the K-Cl cotransporter KCC2 mediated by calcium-activated protease calpain. J Neurosci 32:11356-11364.

Racine RJ (1975) Modification of seizure activity by electrical stimulation: cortical areas. Electroencephalogr Clin Neurophysiol 38:1-12.

Raimondo JV, Markram H, Akerman CJ (2012) Short-term ionic plasticity at GABAergic synapses. Front Synaptic Neurosci 4:5.

Rheims S, Holmgren CD, Chazal G, Mulder J, Harkany T, Zilberter T, Zilberter Y (2009) GABA action in immature neocortical neurons directly depends on the availability of ketone bodies. J Neurochem 110:1330-1338.

Rinehart J, Vazquez N, Kahle KT, Hodson CA, Ring AM, Gulcicek EE, Louvi A, Bobadilla NA, Gamba G, Lifton RP (2011) WNK2 kinase is a novel regulator of essential neuronal cation-chloride cotransporters. J Biol Chem 286:30171-30180.

Rinke I, Artmann J, Stein V (2010) ClC-2 voltage-gated channels constitute part of the background conductance and assist chloride extrusion. J Neurosci 30:4776-4786.

Rivera C, Voipio J, Kaila K (2005) Two developmental switches in GABAergic signalling: the K+-Cl- cotransporter KCC2 and carbonic anhydrase CAVII. J Physiol 562:27-36.

Rivera C, Voipio J, Payne JA, Ruusuvuori E, Lahtinen H, Lamsa K, Pirvola U, Saarma M, Kaila K (1999) The K+/Cl- co-transporter KCC2 renders GABA hyperpolarizing during neuronal maturation. Nature 397:251-255.

Rivera C, Voipio J, Thomas-Crusells J, Li H, Emri Z, Sipila S, Payne JA, Minichiello L, Saarma M, Kaila K (2004) Mechanism of activity-dependent downregulation of the neuron-specific K-Cl cotransporter KCC2. J Neurosci 24:4683-4691.

Rivkees SA (1995) The ontogeny of cardiac and neural A1 adenosine receptor expression in rats. Brain Res Dev Brain Res 89:202-213.

Rohrbough J, Spitzer NC (1996) Regulation of intracellular Cl- levels by Na(+)-dependent Cl- cotransport distinguishes depolarizing from hyperpolarizing GABAA receptor-mediated responses in spinal neurons. J Neurosci 16:82-91.

Ronen GM, Buckley D, Penney S, Streiner DL (2007) Long-term prognosis in children with neonatal seizures: a population-based study. Neurology 69:1816-1822.

Roseti C, Martinello K, Fucile S, Piccari V, Mascia A, Di GG, Quarato PP, Manfredi M, Esposito V, Cantore G, Arcella A, Simonato M, Fredholm BB, Limatola C, Miledi R, Eusebi F (2008) Adenosine receptor antagonists alter the stability of human epileptic GABAA receptors. Proc Natl Acad Sci U S A 105:15118-15123.

Roseti C, Palma E, Martinello K, Fucile S, Morace R, Esposito V, Cantore G, Arcella A, Giangaspero F, Aronica E, Mascia A, Di GG, Quarato PP, Manfredi M, Cristalli G, Lambertucci C, Marucci G, Volpini R, Limatola C, Eusebi F (2009) Blockage of A2A and A3 adenosine receptors decreases the desensitization of human GABA(A) receptors microtransplanted to Xenopus oocytes. Proc Natl Acad Sci U S A 106:15927-15931.

Rudolf R, Bittins CM, Gerdes HH (2011) The role of myosin V in exocytosis and synaptic plasticity. J Neurochem 116:177-191.

Russell JM (2000) Sodium-potassium-chloride cotransport. Physiol Rev 80:211-276.

Ruusuvuori E, Kirilkin I, Pandya N, Kaila K (2010) Spontaneous network events driven by depolarizing GABA action in neonatal hippocampal slices are not attributable to deficient mitochondrial energy metabolism. J Neurosci 30:15638-15642.

Scanziani M, Capogna M, Gahwiler BH, Thompson SM (1992) Presynaptic inhibition of miniature excitatory synaptic currents by baclofen and adenosine in the hippocampus. Neuron 9:919-927.

Schevon CA, Weiss SA, McKhann G, Jr., Goodman RR, Yuste R, Emerson RG, Trevelyan AJ (2012) Evidence of an inhibitory restraint of seizure activity in humans. Nat Commun 3:1060.

Scoville WB, Milner B (1957) Loss of recent memory after bilateral hippocampal lesions. J Neurol Neurosurg Psychiatry 20:11-21.

Segal M, Barker JL (1984) Rat hippocampal neurons in culture: potassium conductances. J Neurophysiol 51:1409-1433.

Sen A, Martinian L, Nikolic M, Walker MC, Thom M, Sisodiya SM (2007) Increased NKCC1 expression in refractory human epilepsy. Epilepsy Res 74:220-227.

Setou M, Seog DH, Tanaka Y, Kanai Y, Takei Y, Kawagishi M, Hirokawa N (2002) Glutamate-receptor-interacting protein GRIP1 directly steers kinesin to dendrites. Nature 417:83-87.

Shepherd GM (2004) The Synaptic Organisation of the Brain. Oxford University Press.

Shimizu-Okabe C, Okabe A, Kilb W, Sato K, Luhmann HJ, Fukuda A (2007) Changes in the expression of cation-Cl- cotransporters, NKCC1 and KCC2, during cortical malformation induced by neonatal freeze-lesion. Neurosci Res 59:288-295.

Sipila ST, Huttu K, Soltesz I, Voipio J, Kaila K (2005) Depolarizing GABA acts on intrinsically bursting pyramidal neurons to drive giant depolarizing potentials in the immature hippocampus. J Neurosci 25:5280-5289.

Sipila ST, Huttu K, Yamada J, Afzalov R, Voipio J, Blaesse P, Kaila K (2009) Compensatory enhancement of intrinsic spiking upon NKCC1 disruption in neonatal hippocampus. J Neurosci 29:6982-6988.

Sloviter RS (1991) Feedforward and feedback inhibition of hippocampal principal cell activity evoked by perforant path stimulation: GABA-mediated mechanisms that regulate excitability in vivo. Hippocampus 1:31-40.

Somogyi P, Freund TF, Cowey A (1982) The axo-axonic interneuron in the cerebral cortex of the rat, cat and monkey. Neuroscience 7:2577-2607.

Staley KJ, Mody I (1992) Shunting of excitatory input to dentate gyrus granule cells by a depolarizing GABAA receptor-mediated postsynaptic conductance. J Neurophysiol 68:197-212.

Staley KJ, Proctor WR (1999) Modulation of mammalian dendritic GABA(A) receptor function by the kinetics of Cl- and HCO3- transport. J Physiol 519 Pt 3:693-712.

Staley KJ, Soldo BL, Proctor WR (1995) Ionic mechanisms of neuronal excitation by inhibitory GABAA receptors. Science 269:977-981.

Stanton PK, Jones RS, Mody I, Heinemann U (1987) Epileptiform activity induced by lowering extracellular [Mg2+] in combined hippocampal-entorhinal cortex slices: modulation by receptors for norepinephrine and N-methyl-D-aspartate. Epilepsy Res 1:53-62.

Stein V, Hermans-Borgmeyer I, Jentsch TJ, Hubner CA (2004) Expression of the KCl cotransporter KCC2 parallels neuronal maturation and the emergence of low intracellular chloride. J Comp Neurol 468:57-64.

Steinert PM, Marekov LN, Parry DA (1999) Molecular parameters of type IV alpha-internexin and type IV-type III alpha-internexin-vimentin copolymer intermediate filaments. J Biol Chem 274:1657-1666.

Stil A, Liabeuf S, Jean-Xavier C, Brocard C, Viemari JC, Vinay L (2009) Developmental up-regulation of the potassium-chloride cotransporter type 2 in the rat lumbar spinal cord. Neuroscience 164:809-821.

Stoppini L, Buchs PA, Muller D (1991) A simple method for organotypic cultures of nervous tissue. J Neurosci Methods 37:173-182.

Streit P, Thompson SM, Gahwiler BH (1989) Anatomical and Physiological Properties of GABAergic Neurotransmission in Organotypic Slice Cultures of Rat Hippocampus. Eur J Neurosci 1:603-615.

Suh J, Rivest AJ, Nakashiba T, Tominaga T, Tonegawa S (2011) Entorhinal cortex layer III input to the hippocampus is crucial for temporal association memory. Science 334:1415-1420.

Sutula TP, Dudek FE (2007) Unmasking recurrent excitation generated by mossy fiber sprouting in the epileptic dentate gyrus: an emergent property of a complex system. Prog Brain Res 163:541-563.

Suzuki N, Bekkers JM (2012) Microcircuits mediating feedforward and feedback synaptic inhibition in the piriform cortex. J Neurosci 32:919-931.

Szabadics J, Varga C, Molnar G, Olah S, Barzo P, Tamas G (2006) Excitatory effect of GABAergic axo-axonic cells in cortical microcircuits. Science 311:233-235.

Szybala C, Pritchard EM, Lusardi TA, Li T, Wilz A, Kaplan DL, Boison D (2009) Antiepileptic effects of silk-polymer based adenosine release in kindled rats. Exp Neurol 219:126-135.

Takagishi Y, Murata Y (2006) Myosin Va mutation in rats is an animal model for the human hereditary neurological disease, Griscelli syndrome type 1. Ann N Y Acad Sci 1086:66-80.

Takigawa T, Alzheimer C (2002) Phasic and tonic attenuation of EPSPs by inward rectifier K+ channels in rat hippocampal pyramidal cells. J Physiol 539:67-75.

Terunuma M, Xu J, Vithlani M, Sieghart W, Kittler J, Pangalos M, Haydon PG, Coulter DA, Moss SJ (2008) Deficits in phosphorylation of GABA(A) receptors by intimately associated protein kinase C activity underlie compromised synaptic inhibition during status epilepticus. J Neurosci 28:376-384.

Thiagarajan TC, Lindskog M, Tsien RW (2005) Adaptation to synaptic inactivity in hippocampal neurons. Neuron 47:725-737.

Thompson SM, Capogna M, Scanziani M (1993) Presynaptic inhibition in the hippocampus. Trends Neurosci 16:222-227.

Thompson SM, Gahwiler BH (1989) Activity-dependent disinhibition. I. Repetitive stimulation reduces IPSP driving force and conductance in the hippocampus in vitro. J Neurophysiol 61:501-511.

Thompson SM, Haas HL, Gahwiler BH (1992) Comparison of the actions of adenosine at pre- and postsynaptic receptors in the rat hippocampus in vitro. J Physiol 451:347-363.

Torborg CL, Nakashiba T, Tonegawa S, McBain CJ (2010) Control of CA3 output by feedforward inhibition despite developmental changes in the excitation-inhibition balance. J Neurosci 30:15628-15637.

Traub RD, Jefferys JG, Whittington MA (1994) Enhanced NMDA conductance can account for epileptiform activity induced by low Mg2+ in the rat hippocampal slice. J Physiol 478 Pt 3:379-393.

Treiman DM (2001) GABAergic mechanisms in epilepsy. Epilepsia 42 Suppl 3:8-12.

Trevelyan AJ, Baldeweg T, van DW, Yuste R, Whittington M (2007a) The source of afterdischarge activity in neocortical tonic-clonic epilepsy. J Neurosci 27:13513-13519.

Trevelyan AJ, Sussillo D, Watson BO, Yuste R (2006) Modular propagation of epileptiform activity: evidence for an inhibitory veto in neocortex. J Neurosci 26:12447-12455.

Trevelyan AJ, Sussillo D, Yuste R (2007b) Feedforward inhibition contributes to the control of epileptiform propagation speed. J Neurosci 27:3383-3387.

Turner DA (1990) Feed-forward inhibitory potentials and excitatory interactions in guinea-pig hippocampal pyramidal cells. J Physiol 422:333-350.

Turrigiano GG (2008) The self-tuning neuron: synaptic scaling of excitatory synapses. Cell 135:422-435.

Turrigiano GG, Leslie KR, Desai NS, Rutherford LC, Nelson SB (1998) Activity-dependent scaling of quantal amplitude in neocortical neurons. Nature 391:892-896.

Tyzio R, Holmes GL, Ben-Ari Y, Khazipov R (2007) Timing of the developmental switch in GABA(A) mediated signaling from excitation to inhibition in CA3 rat hippocampus using gramicidin perforated patch and extracellular recordings. Epilepsia 48 Suppl 5:96-105.

Tyzio R, Minlebaev M, Rheims S, Ivanov A, Jorquera I, Holmes GL, Zilberter Y, Ben-Ari Y, Khazipov R (2008) Postnatal changes in somatic gamma-aminobutyric acid signalling in the rat hippocampus. Eur J Neurosci 27:2515-2528.

Tyzio R, Represa A, Jorquera I, Ben-Ari Y, Gozlan H, Aniksztejn L (1999) The establishment of GABAergic and glutamatergic synapses on CA1 pyramidal neurons is

sequential and correlates with the development of the apical dendrite. J Neurosci 19:10372-10382.

Ulbricht W, Wagner HH (1976) Block of potassium channels of the nodal membrane by 4-aminopyridine and its partial removal on depolarization. Pflugers Arch 367:77-87.

Vajda FJ (2007) Pharmacotherapy of epilepsy: new armamentarium, new issues. J Clin Neurosci 14:813-823.

Valeeva G, Abdullin A, Tyzio R, Skorinkin A, Nikolski E, Ben-Ari Y, Khazipov R (2010) Temporal coding at the immature depolarizing GABAergic synapse. Front Cell Neurosci 4.

van Diepen MT, Parsons M, Downes CP, Leslie NR, Hindges R, Eickholt BJ (2009) MyosinV controls PTEN function and neuronal cell size. Nat Cell Biol 11:1191-1196.

Velazquez JL, Carlen PL (1999) Synchronization of GABAergic interneuronal networks during seizure-like activity in the rat horizontal hippocampal slice. Eur J Neurosci 11:4110-4118.

Verret L, Mann EO, Hang GB, Barth AM, Cobos I, Ho K, Devidze N, Masliah E, Kreitzer AC, Mody I, Mucke L, Palop JJ (2012) Inhibitory interneuron deficit links altered network activity and cognitive dysfunction in Alzheimer model. Cell 149:708-721.

Vitari AC, Thastrup J, Rafiqi FH, Deak M, Morrice NA, Karlsson HK, Alessi DR (2006) Functional interactions of the SPAK/OSR1 kinases with their upstream activator WNK1 and downstream substrate NKCC1. Biochem J 397:223-231.

Voskuyl RA, Albus H (1985) Spontaneous epileptiform discharges in hippocampal slices induced by 4-aminopyridine. Brain Res 342:54-66.

Waddell J, Kim J, Alger BE, McCarthy MM (2011) The depolarizing action of GABA in cultured hippocampal neurons is not due to the absence of ketone bodies. PLoS One 6:e23020.

Wall MJ, Dale N (2013) Neuronal transporter and astrocytic ATP exocytosis underlie activity-dependent adenosine release in the hippocampus. J Physiol.

Walton NY, Treiman DM (1988) Response of status epilepticus induced by lithium and pilocarpine to treatment with diazepam. Exp Neurol 101:267-275.

Wang C, Shimizu-Okabe C, Watanabe K, Okabe A, Matsuzaki H, Ogawa T, Mori N, Fukuda A, Sato K (2002) Developmental changes in KCC1, KCC2, and NKCC1 mRNA expressions in the rat brain. Brain Res Dev Brain Res 139:59-66.

Wang DD, Kriegstein AR (2008) GABA regulates excitatory synapse formation in the neocortex via NMDA receptor activation. J Neurosci 28:5547-5558.

Wang DD, Kriegstein AR (2011) Blocking early GABA depolarization with bumetanide results in permanent alterations in cortical circuits and sensorimotor gating deficits. Cereb Cortex 21:574-587.

Wang W, Gong N, Xu TL (2006) Downregulation of KCC2 following LTP-contributes to EPSP-spike potentiation in rat hippocampus. Biochemical and Biophysical Research Communications 343:1209-1215.

White TD, MacDonald WF (1990) Neural release of ATP and adenosine. Ann N Y Acad Sci 603:287-298.

Wilent WB, Contreras D (2004) Synaptic responses to whisker deflections in rat barrel cortex as a function of cortical layer and stimulus intensity. J Neurosci 24:3985-3998.

Wilent WB, Contreras D (2005) Dynamics of excitation and inhibition underlying stimulus selectivity in rat somatosensory cortex. Nat Neurosci 8:1364-1370.

Woo NS, Lu J, England R, McClellan R, Dufour S, Mount DB, Deutch AY, Lovinger DM, Delpire E (2002) Hyperexcitability and epilepsy associated with disruption of the mouse neuronal-specific K-Cl cotransporter gene. Hippocampus 12:258-268.

Woodin MA, Ganguly K, Poo MM (2003) Coincident pre- and postsynaptic activity modifies GABAergic synapses by postsynaptic changes in Cl- transporter activity. Neuron 39:807-820.

Woods G, Zito K (2008) Preparation of gene gun bullets and biolistic transfection of neurons in slice culture. J Vis Exp.

World Health Organisation (2013) WHO.Epilepsy Facts.http://www.who.int/mediacentre/factsheets/fs999/en/index.html,Last accessed 01.01.2013.

Wright R, Raimondo JV, Akerman CJ (2011) Spatial and temporal dynamics in the ionic driving force for GABA(A) receptors. Neural Plast 2011:728395.

Wu LG, Saggau P (1994) Adenosine inhibits evoked synaptic transmission primarily by reducing presynaptic calcium influx in area CA1 of hippocampus. Neuron 12:1139-1148.

Yamada J, Okabe A, Toyoda H, Kilb W, Luhmann HJ, Fukuda A (2004) Cl- uptake promoting depolarizing GABA actions in immature rat neocortical neurones is mediated by NKCC1. J Physiol 557:829-841.

Yawo H, Chuhma N (1993) Preferential inhibition of omega-conotoxin-sensitive presynaptic Ca2+ channels by adenosine autoreceptors. Nature 365:256-258.

Yeckel MF, Berger TW (1990) Feedforward excitation of the hippocampus by afferents from the entorhinal cortex: redefinition of the role of the trisynaptic pathway. Proc Natl Acad Sci U S A 87:5832-5836.

Yoon KW, Rothman SM (1991) Adenosine inhibits excitatory but not inhibitory synaptic transmission in the hippocampus. J Neurosci 11:1375-1380.

Yoshimura Y, Callaway EM (2005) Fine-scale specificity of cortical networks depends on inhibitory cell type and connectivity. Nat Neurosci 8:1552-1559.

Yuan A, Rao MV, Sasaki T, Chen Y, Kumar A, Veeranna, Liem RK, Eyer J, Peterson AC, Julien JP, Nixon RA (2006) Alpha-internexin is structurally and functionally associated with the neurofilament triplet proteins in the mature CNS. J Neurosci 26:10006-10019.

Zhang JM, Wang HK, Ye CQ, Ge W, Chen Y, Jiang ZL, Wu CP, Poo MM, Duan S (2003) ATP released by astrocytes mediates glutamatergic activity-dependent heterosynaptic suppression. Neuron 40:971-982.

Zsiros V, Aradi I, Maccaferri G (2007) Propagation of postsynaptic currents and potentials via gap junctions in GABAergic networks of the rat hippocampus. J Physiol 578:527-544.